

Westinghouse Non-Proprietary Class 3



# Master Curve Strategies for RPV Assessment

WCAP - 15075

Westinghouse Energy Systems



9811240260 981118  
PDR ADDCK 05000305  
P PDR

rec'd w/WR 11/18/98

9811240248

50305

ATTACHMENT 4

Letter from Mark L. Marchi (WPSC)

To

Document Control Desk (NRC)

Dated

November 18, 1998

Proposed Amendment 157

WCAP-15075  
Master Curve Strategies for RPV Assessment

# Master Curve Strategies for RPV Assessment

R. G. Lott and M. T. Kirk  
Westinghouse Science and Technology Center

C. C. Kim  
Westinghouse Energy Center

September 1998

Approved: C. H. Boyd  
Chuck Boyd, Manager  
Engineering and Materials Technology

---


Westinghouse Electric Company  
Energy Systems  
P.O. Box 355  
Pittsburgh, PA 15230-0355

©1998 Westinghouse Electric Company  
All Rights Reserved

---

PREFACE

This report has been technically reviewed and verified by:

  
\_\_\_\_\_  
W. L. Server

## FORWARD

This report along with four other companion documents have been prepared by Westinghouse Electric Corporation and ATI Consulting to assess and document the integrity of the Kewaunee Nuclear Power Plant (KNPP) reactor vessel relative to the requirements of 10 CFR 50.60, 10 CFR 50.61, Appendices G and H to 10 CFR Part 50, (which encompass pressurized thermal shock (PTS) and upper shelf energy (USE) evaluations), and any potential impact on low temperature overpressure (LTOP) limits or pressure-temperature limits. These reports: (1) summarize the KNPP weld metal (1P3571) surveillance capsule test results performed to date (WCAP-15074); (2) document supplemental surveillance capsule fracture toughness testing results for the KNPP weld metal both in the unirradiated and irradiated condition (WCAP-14279, Rev. 1); (3) introduce and apply a new methodology, based on the Master Curve Approach, for assessing the integrity of the KNPP reactor vessel (WCAP-15075); (4) include various PTS evaluations for KNPP conducted in accordance with the methodology given in 10 CFR 50.61 and the Master Curve Approach (WCAP-14280, Rev. 1); and (5) present heatup and cooldown curves corresponding to end of plant life fluence (WCAP-14278, Rev. 1). The heatup and cooldown limit curves presented in WCAP-14278, Rev. 1 are derived using ASME Code Case N-588. These five documents support a new proposed amendment to modify the KNPP Technical Specification limits for heatup, cooldown, and low temperature overpressure protection. The current Technical Specification heatup and cooldown limit curves will expire at 20 EFPY which is scheduled to occur in spring of 1999. The engineering evaluations incorporate all known data pertinent to the analysis of structural integrity of the KNPP reactor vessel and therefore meet and exceed the intent of NRC regulation and expectations.

Background for much of this work is linked to ongoing efforts by the NRC staff to generically resolve concerns raised during their review of reactor vessel integrity for the Yankee Rowe Nuclear Power Station. As part of this effort, the NRC staff issued Generic Letter 92-01, Revision 1 and Generic Letter 92-01, Revision 1, Supplement 1. These generic communiqué seek to obtain certain information that will permit the NRC staff to independently assess and ensure that licensees are in compliance with requirements regarding reactor pressure vessel integrity.

During review of the responses to Generic Letter 92-01, Revision 1 and Generic Letter 92-01, Revision 1, Supplement 1 the NRC discovered inconsistencies within the industry concerning the methodology used to assess reactor pressure vessel integrity including:

1. Large variability in the reported chemistries, i.e., copper and nickel contents, for welds fabricated from the same heat of weld wire.
2. Different initial properties ( $RT_{NDT}$ ) for welds fabricated from the same heat and weld wire.
3. Different transition temperature shifts for welds fabricated from the same heat and weld wire.
4. Operation with irradiation temperature less than 525°F.

5. Different approaches for determining fluence of the limiting material.

In response to this discovery, to provide assurance that all plants will maintain adequate protection against PTS events, the practice of the NRC staff has been to require that evaluations be performed using conservative inputs. This increase in conservatism seems to apply equally to all areas of assessment of reactor vessel integrity. When best estimate values have been used by utilities for the chemical composition of the reactor vessel, it appears that the NRC staff may require the use of increased margin terms to account for potential variability in chemistries. Furthermore, through the process of issuing RAIs, the NRC staff has requested that evaluations be performed using generic values for initial properties and a corresponding higher margin value from either 28°F to 56°F (if the initial  $RT_{NDT}$  is measured) or 44°F to 66°F (if the generic  $RT_{NDT}$  is used). Other recent changes include the mandatory use of the ratio procedure, if applicable; a 1°F penalty for each degree Fahrenheit when the irradiation temperature is less than 525°F; and other penalties on the projected fluence of the limiting reactor vessel beltline material at end of license. Collectively, this practice of requiring multiple conservative inputs in a layered fashion for assessment of reactor vessel integrity has the effect that a reactor vessel would be predicted to reach the PTS screening criteria at an earlier date than that given by the PTS assessment methodology given in 10 CFR 50.61. A situation of applying too much conservatism can create the illusion that a reactor vessel is unsafe to operate when in fact it may possess sufficient fracture toughness. If too much conservatism is applied the overall affect can be a decrease in safety because of unnecessary changes made to plant operations and design for the sole reason of addressing a conservative but erroneous PTS evaluation.

At about the same time Generic Letter 92-01, Revision 1, Supplement 1 was being issued, the NRC staff became aware of ABB-CE proprietary data that could affect the PTS assessment of the KNPP reactor vessel. Subsequently, ABB-CE provided KNPP a summary of the data for its evaluation in a letter dated April 6, 1995. The NRC staff met with the KNPP staff on April 13, 1995 to discuss the effect that the ABB-CE data and its plant specific surveillance data would have on their PTS assessment. Prior to this meeting, the NRC staff verbally expressed concern to KNPP management that the KNPP reactor vessel may reach the PTS screening criteria before the end of their license. The KNPP staff presented its plant specific surveillance program results and some new information related to the reactor vessel chemistry variability. Based upon using best estimate input parameters, the KNPP staff showed that the KNPP reactor vessel will not reach the PTS screening criteria before the end of their license. Recognizing that the NRC staff was still concerned about the possibility of the KNPP reactor vessel reaching the PTS screening criteria prior to end of license, the KNPP staff remained steadfast in their use of best estimate input parameters for assessment of reactor vessel integrity. At the same time KNPP committed resources to develop industry programs that would facilitate implementation of the applicable requirements specified in the 1992 Edition of Appendix G to 10 CFR 50 should it become necessary: supplemental fracture toughness tests of the beltline material after exposure to neutron irradiation; perform analysis that demonstrates the existence of equivalent margins of safety for continued operation, and thermal annealing. At the conclusion of the April 13, 1995 meeting, the KNPP staff described their future plans to ensure compliance with the requirements for reactor vessel integrity. These plans included participation with industry groups to create programs and a data base detailing the chemical composition of reactor vessel beltline materials; demonstration of the feasibility for annealing of

a PWR reactor vessel of US design; and direct measurement of fracture toughness from irradiated surveillance capsule specimens.

In a NRC internal memorandum (dated May 6, 1995 from Jack R. Strosnider, Chief - Materials and Chemical Engineering Branch, Division of Engineering to Ashok C. Thadani, Associate Director for Technical Assessment, Office of Nuclear Reactor Regulation) released following the April 13, 1995 meeting, the NRC staff wrote that they had not completed their review of the new information on the KNPP reactor vessel. The NRC staff noted that the new chemistry data could significantly change the KNPP PTS evaluation. However, based on conservative evaluations, the NRC staff concluded that the KNPP reactor vessel will not reach the PTS screening criteria in the near future. During this same time period, WPSC submitted a proposed amendment to the NRC to modify KNPP Technical Specification limits relating to heatup, cooldown, and low temperature overpressure protection (LTOP). The NRC issued two requests for additional information regarding this proposed amendment, dealing with surveillance capsule fluence and material properties, and then requested that WPSC withdraw it from the docket pending resolution of Generic Letter 92-01, Revision 1, Supplement 1 activities.

While the NRC was performing a detailed review of licensee responses to Generic Letter 92-01, Revision 1, each of the PWR NSSS Owners Groups developed and implemented programs dealing with measurement of fracture toughness for reactor vessel materials. WPSC has funded both the WOG and ABB-CE/RVWG to measure the fracture toughness of two 1P3571 archive weld metals (utilizing different coils of weld wire) using the Master Curve Approach. The WOG and ABB-CE/RVWG have obtained unirradiated  $T_0$  values for weld metal 1P3571 in accordance with ASTM E1921-97. The WOG has also obtained the fracture toughness for 1P3571 weld metal from unirradiated 1/2T-CT specimens. Furthermore, the WOG has generated irradiated  $T_0$  values for the two of 1P3571 weldments reconstituted from surveillance capsule specimens from the KNPP and Maine Yankee reactor vessels that were irradiated to  $3.36 \times 10^{19}$  n/cm<sup>2</sup> and  $6.11 \times 10^{19}$  n/cm<sup>2</sup>, respectively. The ASME B&PVC is currently working under the direction of the PVRC to develop recommendations and guidelines for the use of  $T_0$  values in lieu of  $RT_{NDT}$  values for assessment of reactor vessel integrity. The results of the supplemental fracture toughness testing for both the unirradiated and irradiated 1P3571 weld metal, along with application of the results, has been presented to the PVRC and ASME.

WPSC concluded that it is prudent to report the results of the recently completed fracture toughness testing of the EOL and beyond EOL irradiated 1P3571 weld metal along with the values derived for the various PTS evaluations given by the methodology described in 10 CFR 50.61. The results of the irradiated fracture toughness testing will serve as a means of assuring adequate conservatism is incorporated into the integrity assessment of the KNPP reactor vessel. Furthermore, since the fracture toughness transition shift is larger and more accurate than the Charpy transition shift, it is felt that continued use of the Charpy results could be inappropriate. The KNPP has volunteered to be a lead plant on behalf of the WOG for application of the Master Curve Approach. NRC feedback obtained on this application of the Master Curve Method will be considered, as appropriate, by the WOG. The fracture toughness results along with the methodology presented in WCAP-15075 indicate that the KNPP 1P3571

weld metal will continue to conservatively provide adequate fracture toughness up to and beyond extended end-of-life fluence.



---

 TABLE OF CONTENTS

LIST OF TABLES.....	v
LIST OF FIGURES.....	vii
ABSTRACT .....	ix
1.0 INTRODUCTION.....	1-1
2.0 RATIONALE AND OBJECTIVE.....	2-1
3.0 SCOPE OF REPORT .....	3-1
4.0 EXISTING ASSESSMENT STRATEGY .....	4-1
4.1 HISTORICAL DEVELOPMENT LEADING TO CURRENT REQUIREMENTS .....	4-1
4.2 LINEAR ELASTIC FRACTURE MECHANICS.....	4-2
4.2.1 Technical Basis .....	4-2
5.0 TECHNICAL ADVANCES SINCE 1973.....	5-1
5.1 ELASTIC-PLASTIC FRACTURE MECHANICS.....	5-1
5.2 CLEAVAGE FRACTURE MICRO-MECHANISMS.....	5-2
5.2.1 Micro-Mechanical Models for Cleavage Fracture.....	5-3
5.2.2 Predictive Application of a RKR-like Model .....	5-3
5.2.3 Stochastic Effects and the "Master Curve" .....	5-5
5.3 CLEAVAGE FRACTURE TOUGHNESS DATA .....	5-9
5.3.1 Weibull Description of Fracture Toughness Data .....	5-10
5.3.2 Weakest Link Size Scaling of Fracture Toughness Data.....	5-10
5.3.3 The Universality of the Master Curve Shape .....	5-11
5.3.4 Effect of Test Variables on $T_0$ Determination Bias and Accuracy .....	5-14
5.3.5 Applications Test of the Master Curve .....	5-16
5.4 SUMMARY: AN EMPIRICAL BASIS FOR THE MASTER CURVE .....	5-17
6.0 PROPOSAL FOR A NEW MEANS OF EVALUATING RPV INTEGRITY .....	6-1
6.1 BACKGROUND .....	6-1
6.2 THE ASME AND PVRC APPROACH TO MASTER CURVE IMPLEMENTATION .....	6-1
6.3 APPROACH TO DYNAMIC AND ARREST TOUGHNESS.....	6-3
6.4 OVERVIEW OF APPROACH FOR KEWAUNEE.....	6-3

---

6.5	ESTIMATING THE KIC REFERENCE TEMPERATURE ( $RT_{T_0}$ ) FROM $T_0$ .....	6-4
6.5.1	Implicit Size Effects in the $K_{IC}$ Curve.....	6-4
6.5.2	Functional Equivalence of $RT_{T_0}$ to $RT_{NDT}$ as an Index Temperature for the $K_{IC}$ Curve .....	6-6
6.6	IMPLICIT MARGINS.....	6-8
6.7	MARGIN TERMS IN THE DETERMINATION OF REFERENCE TEMPERATURES .....	6-10
6.8	SUMMARY .....	6-10
7.0	EVALUATION OF THE KEWAUNEE VESSEL .....	7-1
7.1	SUMMARY OF CURRENT APPROACH BASED ON CHARPY TESTING.....	7-1
7.2	ALTERNATIVE APPROACHES BASED ON FRACTURE TOUGHNESS TESTING .....	7-3
7.2.1	Structure of Alternative Approaches .....	7-4
7.2.2	Values of $T_0$ Used in these Evaluations.....	7-4
7.2.3	Verification of $RT_{T_0}$ for Kewaunee Weld 1P3571 .....	7-5
7.2.4	Alternative Measurements of Initial Reference Temperature (Paths 5a & 5b) .....	7-5
7.2.5	Direct Measurements of Irradiated Fracture Toughness (Path 6).....	7-7
7.2.5	Determination of Fracture Toughness Shift (Path 7) .....	7-7
7.2.7	Heat to Heat Uncertainty (Surrogate Materials) .....	7-8
7.3	CALCULATIONS FOR EXTENDED OPERATION.....	7-9
7.4	COMPARISON OF METHODS.....	7-10
7.5	RECOMMENDATION FOR ART VALUES .....	7-11
8.0	SUMMARY AND CONCLUSIONS .....	8-1
9.0	REFERENCES.....	9-1

---

**LIST OF TABLES**

Table 5-1	The number of valid fracture toughness specimens required by ASTM E1921-97. ....	5-20
Table 5-2	Values used to adjust ASTM E1921-97 $T_0$ estimates to account for the effects of finite sample size. ....	5-20
Table 5-3	Master Curve coefficients from ASTM E1921-97. ....	5-21
Table 5-4	Count of ASTM E1921-97 valid specimens in the fracture toughness database .....	5-22
Table 5-5	Count of all specimens in the fracture toughness database .....	5-24
Table 5-6	Strength and composition of steels in the fracture toughness database .....	5-26
Table 5-7	$T_0$ Weibull slope values calculated from the fracture toughness database .....	5-28
Table 5-8	Empirical assessment of the validity of the weakest link prediction of the statistical size effect on fracture toughness data.....	5-31
Table 5-9	Empirical assessment of the validity of a universal shape for the Master Curve .....	5-33
Table 5-10	Statistical assessment of the effects of deformation and test temperature on ASTM E1921-97 $T_0$ values .....	5-35
Table 7-1	ART determination for the Kewaunee weld and vessel .....	7-12
Table 7-2	Summary of Kewaunee and Maine Yankee weld $T_0$ data.....	7-13
Table 7-3	ART determination for the Kewaunee weld and vessel (5.06x10 <sup>19</sup> n/cm <sup>2</sup> version).....	7-14

## LIST OF FIGURES

Figure 2-1	Schematic transition curve for an RPV steel .....	2-3
Figure 4-1	A comparison of material independent LEFM size requirements (the E399 (2.5) curve) and LEFM size requirements specific to RPV steels (the E399 (1.0) curve) .....	4-5
Figure 4-2	A perspective on the variation of fracture toughness with specimen thickness motivated by an understanding of LEFM.....	4-6
Figure 5-1	Schematic illustration of the differences between LEFM and EPFM.....	5-36
Figure 5-2	A comparison of material independent LEFM size requirements (the E399 (2.5) curve) and a conservative EPFM size requirement (the E1737 (M=200) curve) .....	5-37
Figure 5-3	A comparison of material independent LEFM size requirements (the E399 (2.5) curve) and an EPFM size requirements specific to RPV steels (the M=50 curve) .....	5-38
Figure 5-4	Probability distribution function for carbide sizes (left), and variation of the probability of cleavage failure with increasing applied- $J$ (right) .....	5-39
Figure 5-5	Comparison of the amount of quasi-static fracture toughness data that was available to support the $K_{Ic}$ curve vs. the amount of data available today .....	5-40
Figure 5-6	Variation of ultimate tensile strength with yield strength for steels in the fracture toughness database (filled and open symbols) compared with those characteristic of the operating nuclear fleet (light plusses and crosses) .....	5-41
Figure 5-7(a)	Best-fit Weibull slope vs. sample size for un-irradiated RPV steels .....	5-42
Figure 5-7(b)	Best-fit Weibull slope vs. sample size for non-RPV steels.....	5-43
Figure 5-7(c)	Best-fit Weibull slope vs. sample size for irradiated RPV steels .....	5-44
Figure 5-8(a)	Measured $K_{Ic}$ vs. specimen size for an un-irradiated RPV steel .....	5-45
Figure 5-8(b)	Measured $K_{Ic}$ vs. specimen size for an irradiated RPV steel.....	5-46
Figure 5-9(a)	1T equivalent $K_{Ic}$ vs. specimen size for an un-irradiated RPV steel.....	5-47
Figure 5-9(b)	1T equivalent $K_{Ic}$ vs. Specimen size for an irradiated RPV steel.....	5-48
Figure 5-10	Schematic illustration of the goodness-of-fit test applied to the Master Curve shape .....	5-49
Figure 5-11	A comparison of $K_{Ic}$ residuals for all available data (left) and for only ASTM valid data (right) illustrating the bias introduced by the ASTM censoring procedure.....	5-50
Figure 5-12	Aggregated fracture toughness data (ASTM valid only) for un-irradiated RPV steels .....	5-51

Figure 5-13	Aggregated fracture toughness data (ASTM valid only) for irradiated RPV steels. ....	5-52
Figure 5-14	Statistical significance of slope and intercept values fit to $K_{Ic}$ residuals over various temperature ranges for unirradiated (top) and irradiated (bottom) steels. ....	5-53
Figure 5-15	Slope (top) and intercept (bottom) values fit to $K_{Ic}$ residuals over various temperature ranges for un-irradiated and irradiated steels.....	5-54
Figure 5-16(a)	The influence of test temperature on the difference between ASTM and maximum likelihood estimates of $T_0$ .....	5-55
Figure 5-16(b)	The influence of specimen deformation before fracture on the difference between ASTM and maximum likelihood estimates of $T_0$ .....	5-56
Figure 5-17	Comparison of maximum likelihood (vertical axis) and ASTM E1921 (horizontal axis) estimates of $T_0$ .....	5-57
Figure 5-18	Comparison of maximum likelihood (vertical axis) and ASTM E1921 (horizontal axis) estimates of $T_0$ (ASTM estimate increased by $\beta/N^{0.5}$ to account for measurement uncertainty) .....	5-58
Figure 5-19	Schematic illustration of what the Master curve may be called upon to do in nuclear RPV applications.....	5-59
Figure 5-20(a)	As-measured precracked CVN $K_{Ic}$ data for both un-irradiated and irradiated RPV steels compared with Master Curve predictions. ....	5-60
Figure 5-20(b)	As-measured 1/2T $K_{Ic}$ data for both un-irradiated and irradiated RPV steels compared with Master Curve predictions.....	5-61
Figure 5-20(c)	As-measured 1T $K_{Ic}$ data for both un-irradiated and irradiated RPV steels compared with Master Curve predictions.....	5-62
Figure 5-20(d)	As-measured 2T $K_{Ic}$ data for both un-irradiated and irradiated RPV steels compared with Master Curve predictions.....	5-63
Figure 5-20(e)	As-measured 4T $K_{Ic}$ data for both un-irradiated and irradiated RPV steels compared with Master Curve predictions.....	5-64
Figure 5-20(f)	As-measured 6T $K_{Ic}$ data for both un-irradiated and irradiated RPV steels compared with Master Curve predictions.....	5-65
Figure 5-20(g)	As-measured 8T $K_{Ic}$ data for both un-irradiated and irradiated RPV steels compared with Master Curve predictions.....	5-66
Figure 5-20(h)	As-measured 9T $K_{Ic}$ data for both un-irradiated and irradiated RPV steels compared with Master Curve predictions.....	5-67
Figure 5-20(i)	As-measured 10T $K_{Ic}$ data for both un-irradiated and irradiated RPV steels compared with Master Curve predictions.....	5-68

Figure 5-20(j)	As-measured 11T $K_{Ic}$ data for both un-irradiated and irradiated RPV steels compared with Master Curve predictions.....	5-69
Figure 6-1	Comparison of how $RT_{NDT}$ positions two different heats of RPV steel relative to the $K_{Ic}$ curve.....	6-12
Figure 6-2	Comparison of how $RT_{T_0}$ positions two different heats of RPV steel relative to the $K_{Ic}$ curve.....	6-13
Figure 6-3.	HSST-02 data and the $K_{Ic}$ curve indexed using $RT_{NDT}$ (solid curve) and $RT_{T_0}$ (dashed curve) positions. ....	6-14
Figure 6-4	Implicit margin for various RPV steels.....	6-15
Figure 7-1	Paths for estimation of the ART using current technology .....	7-15
Figure 7-2	Paths for implementation of Master Curve estimation of the ART compared with current technology .....	7-16
Figure 7-3	Variation of $RT_{T_0}$ with neutron fluence for Kewaunee and Maine Yankee materials .....	7-17
Figure 7-4	Comparison of ART values calculated by various techniques .....	7-18
Figure 7-5	Comparison of irradiated Kewaunee fracture toughness data and bounding $K_{Ic}$ curve based on $RT_{T_0}$ .....	7-21
Figure 7-6	Variation of $RT_{T_0}$ with neutron fluence for Kewaunee and Maine Yankee materials .....	7-22
Figure 7-7	Comparison of ART values calculated by various techniques .....	7-23

## EXECUTIVE SUMMARY

This investigation provides a technical basis for, and empirical support of, use of the Master Curve index temperature ( $T_o$ ) as a means to directly measure the adjusted reference temperature for an irradiated RPV steel. Our investigation focuses in the following four areas:

1. The technical basis for application of the Master Curve to RPV steels,
2. The bias and accuracy of  $T_o$  values measured using ASTM E1921,
3. Determination of an  $T_o$ -based index temperature ( $RT_{T_o}$ ) for the  $K_{Ic}$  curve, and
4. A margins strategy for  $RT_{T_o}$  that matches the intent of Reg. Guide 1.99 Rev. 2 procedures.

We use a database of fracture toughness values for reactor pressure vessel steels (both irradiated and unirradiated) to address items 1 through 3. This database includes over 1,600 E1921 valid fracture toughness values from plates, welds, and forgings. The conclusions of this investigation are as follows:

1. The three premises of the Wallin Master Curve are supported by the great preponderance (>90%) of the empirical database for RPV steels. The Master Curve applies with equal accuracy to irradiated and unirradiated steels.
2. When  $T_o$  is estimated in accordance the requirements of E1921, the resultant values are unbiased with regard to test temperature, level of deformation at fracture, and number of tests conducted. The standard deviation of E1921  $T_o$  estimates relative to  $T_o$  estimates determined using considerably larger data sets is 14°F for the RPV steels considered.
3. A recent draft ASME code case advocates addition of 35°F to  $T_o$  (determined by E1921) to establish a temperature to index the ASME  $K_{Ic}$  curve. This temperature is called  $RT_{T_o}$ . The value of 35°F exceeds that needed to maintain an equivalent level of safety to current  $RT_{NDT}$  based methodologies by 18°F. Consequently, use of  $RT_{T_o}$  as an indexing parameter for the  $K_{Ic}$  curve is more conservative than use of  $RT_{NDT}$ . Furthermore, the  $T_o$ -based toughness estimation methodology reduces considerably the degree of scatter in fracture toughness data, and contains implicit margins on toughness which are consistent for every steel considered.  $RT_{T_o}$  is therefore superior to  $RT_{NDT}$  as an index temperature for the  $K_{Ic}$  curve.
4. Measurements of  $T_o$  are made in both the irradiated and unirradiated conditions for the limiting weld in the Kewaunee RPV (Linde 1092 Heat 1P3571) and for this weld in Kewaunee's sister plant, Maine Yankee. These values are used to develop  $RT_{T_o}$  estimates, along with associated margins that satisfy the intent of Reg. Guide 1.99 Rev. 2. Based on these analyses, ART values are determined for the Kewaunee vessel as: 234°F for EOL (33 EFPY) and 249°F for extended EOL (51 EFPY). These values are based on irradiated  $T_o$  measurements, reflect conservative assumptions about the effects of neutron damage on fracture toughness, and are adjusted for heat uncertainty.

## 1.0 INTRODUCTION

United States law [10 CFR 50] requires nuclear licensees to demonstrate that the effects of progressive embrittlement by neutron irradiation do not compromise the safe operation of their reactor pressure vessel (RPV). Two analyses must be performed. Firstly, safe limits of pressure and temperature ( $P$ - $T$  limits) for normal heatup and cooldown operations are determined. Secondly, licensees must demonstrate the ability of the RPV to maintain integrity even during an emergency shutdown (i.e., the pressurized thermal shock, PTS, event).

The variation of the RPV steel's fracture toughness with temperature provides a key input to both analyses. Currently, the ASME  $K_{IR}$  and  $K_{IC}$  curves, indexed to the current state of embrittlement by shifting the curve to the  $RT_{NDT}$  of the RPV, provides this toughness characterization. The  $K_{IR}$  and  $K_{IC}$  curves were developed in 1973 [WRC 175] as a lower bound to a database of valid linear elastic fracture mechanics (LEFM) toughness values for a variety of unirradiated RPV steels tested at both static and dynamic loading rates. The  $RT_{NDT}$  which quantifies the current state of vessel embrittlement, is determined by testing Charpy V-notch (CVN) specimens removed periodically from RPV surveillance capsules. The use of this indirect process to quantify the effects of irradiation on toughness was an expedient necessitated by the extremely large specimen size considered necessary in 1973 to produce "valid" LEFM fracture toughness values.

While a successful approach, this procedure includes margins that are both implicit and conservative. These lead to an overly pessimistic assessment of vessel integrity, potentially resulting in premature discontinuation of license. For example, *all* steels in *all* RPVs are assumed to have the lower bound toughness represented by the  $K_{IR}$  and  $K_{IC}$  curves. This is true for some, but not for all, RPV steels. Technological advancements in the last 25 years provide for more accurate RPV integrity assessment. The objective of this report is to provide the technical basis for alternatives to current RPV licensing strategies, and to apply these alternatives to an application for operating license being made by the Kewaunee Nuclear Power Plant, which is operated by the Wisconsin Public Service Corporation.



## 2.0 RATIONALE AND OBJECTIVE

The low-alloy ferritic steels used in the construction of nuclear pressure vessels exhibit a ductile to brittle fracture transition. This behavior is illustrated in Figure 2-1, where the energy absorbed by a CVN specimen during fracture decreases from relatively high values at high temperatures (upper shelf) to low values at lower temperatures (lower shelf). Therefore, plant operation requires that the reactor vessel be heated to a temperature above the lower shelf region (i.e., into the transition region) before pressure is applied and significant stresses are developed in the vessel. A reference transition temperature is used to locate the ductile-to-brittle transition temperature and define allowable operating limits. The ductile-to-brittle transition temperature depends not only on the material condition but also on the rate and mode of loading. Different types of tests therefore produce different ductile-to-brittle transition temperatures. Definition of a meaningful reference transition temperature for reactor pressure vessel applications therefore requires use of a test method that considers the combined effects of material, loading rate, and notch geometry in an effort to match the conditions experienced in the vessel. For tests of nuclear pressure vessel steels, a notch or flaw is required to increase the ductile-to-brittle transition to any temperature of practical significance.

The reference temperature currently used for reactor pressure vessel analysis is  $RT_{NDT}$ .  $RT_{NDT}$  is defined in ASME Code, Section III, NB-2300, which is consistent with current regulations as defined in 10 CFR 50, Appendix G. The current definition, which employs both Charpy V-notch and drop weight testing to determine  $RT_{NDT}$ , was instituted in the Summer 1972 Addenda to the Code. Prior to 1972, reference temperature was not used and the ductile-to-brittle transition temperature was defined solely in terms of the Charpy V-notch impact energy transition curve. This use of the reference temperature was motivated by the development of new test techniques and improvements in the understanding of fracture.

A structural model links the reference temperature to the behavior of the vessel. Originally, the Fracture Analysis Diagram (FAD) developed by Pellini and Puzak [1963] provided this linkage. Subsequent development of fracture mechanics techniques led to revisions of Section III and Section XI of the ASME Code in 1972. These revisions changed the structural model from the FAD approach to two reference toughness curves ( $K_{IR}$  and  $K_{Ic}$ ) based on Linear Elastic Fracture Mechanics (LEFM) concepts. These curves are linked to the observed ductile-to-brittle transition behavior of the material through  $RT_{NDT}$ . However, the relationship between the reference toughness curves and  $RT_{NDT}$  is purely empirical. The 1972 revisions to the Code remain the basis for all reactor pressure vessel analyses performed today.

In the 25 years since 1972, the technical community has achieved dramatic progress in the understanding of fracture. A recent development called the Master Curve [Wallin, Saario, and Törrönen; 1984] has drawn much of this understanding together into a comprehensive approach to characterization of fracture in the transition region. This new approach provides both a new definition of the reference temperature for the ductile-to-brittle transition in fracture toughness,  $T_o$ , and an improved reference toughness curve. The Master Curve provides significant technical enhancements compared with technology currently incorporated in the ASME code for two primary reasons. First, there is a direct relationship between the reference

temperature ( $T_o$ ) and the reference curve, eliminating the need for the empirical relationship between the  $K_{lc}$  curve and  $RT_{NDT}$ . Second, the reference temperature can be directly and accurately determined for a wide variety of pressure vessel steels, including irradiated steels. These technical developments motivate application of Master Curve technology to assessment reactor pressure vessel at the Kewaunee Nuclear Power Plant, as described herein.

Most changes in codes and regulations are necessarily evolutionary. The approach taken in this report is to justify the use of Master Curve technology while maintaining the principles and structure of the current ASME code. This approach is consistent with efforts currently underway within the PVRC.  $T_o$  is used to calculate an index temperature,  $RT_{T_o}$ , which is defined to ensure functional equivalence with the index temperature  $RT_{NDT}$  described in current ASME code. This functional equivalence between  $RT_{T_o}$  and  $RT_{NDT}$  permits use of  $RT_{T_o}$  in lieu of  $RT_{NDT}$  while maintaining consistency with the intent and practice of current ASME code. Section 6 addresses the definition of  $RT_{T_o}$  in greater detail.

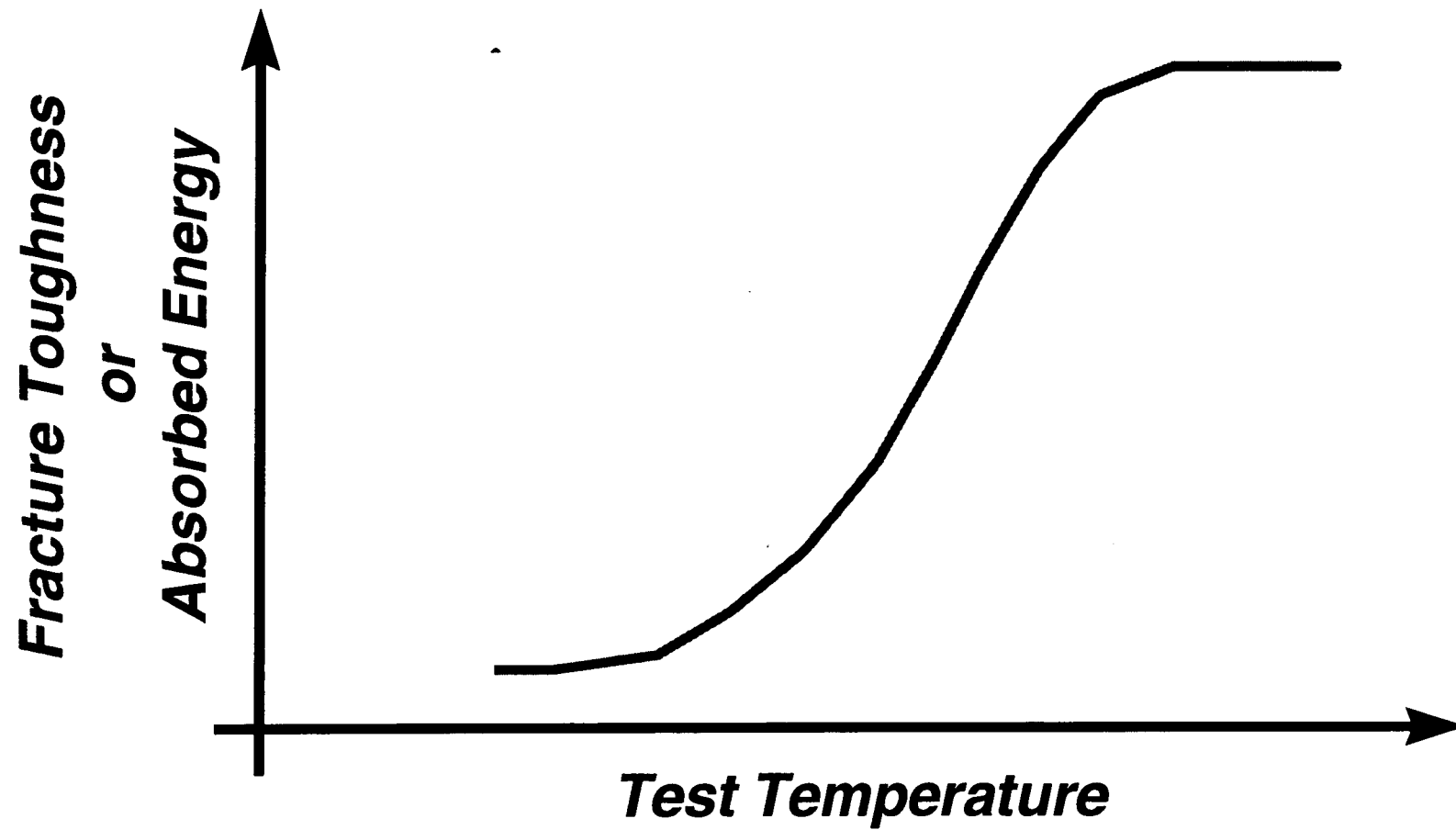


Figure 2-1 Schematic Transition Curve for an RPV Steel

### 3.0 SCOPE OF REPORT

This report develops the case for an alternative RPV assessment strategy by the following logic:

- Section 4 describes the existing strategy for RPV assessment. This discussion includes a description of the technical basis for current procedures as well as their specific implementation in both industry consensus standards (ASME) and federal law (Code of Federal Regulations, or CFR).
- Section 5 describes the technological advances which have transpired since the current procedure was adopted in the 1970s that enable the development of alternative RPV assessment strategies. A substantial fracture toughness database is assembled for RPV steels. This database is used to demonstrate and justify the appropriateness of the Master Curve to assessment of nuclear RPVs.
- Section 6 uses the technological advances described in Section 5 to develop an alternative strategy for RPV assessment. This development is done in a manner that is consistent with current assessment procedures (Section 4), but uses the best of currently available technology (Section 5).
- Section 7 applies both the current and the newly proposed assessment procedures to estimate the current fracture toughness condition of the RPV at Kewaunee. Additionally, this section includes a commentary on the relative merits of the various assessment strategies considered.
- Section 8 summarizes the findings of this investigation.

## 4.0 EXISTING ASSESSMENT STRATEGY

### 4.1 HISTORICAL DEVELOPMENT LEADING TO CURRENT REQUIREMENTS

The early prototype and first generation commercial nuclear power plants were designed to the ASME Code, Sections I or VIII. These Code sections did not have toughness requirement for the pressure vessel steels. Consequently, supplementary requirements were adopted for the low alloy ferritic pressure vessel steels used to fabricate these reactor vessels. The first edition of Section III of the ASME Code was published in 1963 and included toughness testing requirements for non-ductile failure based on the Fracture Analysis Diagram (FAD) approach, developed by Pellini and Puzak [1963]. The use of ductile-to-brittle transition temperature data dates from this version of the Code.

In the mid to late 1960s, the nuclear industry initiated work through the Pressure Vessel Research Committee (PVRC) to evaluate material property changes (including fracture mechanics properties) through the thickness of thick-walled pressure vessel steels. The Atomic Energy Commission (AEC) through the Advisory Committee on Reactor Safeguards (ACRS) recommended expansion of these PVRC activities to better address public health and safety concerns relative to nuclear power. The PVRC responded with the appointment of a Subcommittee on Heavy-Section Steels, which established an industry and government cooperative program having this goal.

By the late 1960s, results from the Nuclear Regulatory Commission's (NRC) Heavy Section Steel Technology (HSST) program led to recommendations for revisions of the 1963 edition of Section III to reflect advancements in fracture mechanics technology. In early 1971 a PVRC Task Group was formed to formalize these recommendations for ASME Code revisions. The recommendations of this PVRC Task Group were completed in August 1972 and presented to the Code committees. The ASME Code developed Code Case 1514 in early 1972, revisions to Section III, NB-2300 were made, and Appendix G was added. The PVRC documentation was adjusted to reflect the Code revisions, and a PVRC Task Group report was issued as [WRC-175]. Bulletin 175 also contained the reference fracture toughness curve for dynamic and crack arrest data ( $K_{IR}$ ) which was used to provide a conservative bound against brittle (non-ductile) fracture for normal operational conditions. The PVRC recommendations utilized fracture mechanics technology that had never before been formally applied in a design code. Later applications to other components and classes of materials has taken place in the Code, as well as the development of flaw evaluation procedures and criteria in Section XI. Nevertheless, the fracture toughness basis for ASME Code Sections III and XI is still that of WRC Bulletin 175, issued in 1973.

The following Section (4.2) summarizes the technological basis for Section III and XI requirements.

## 4.2 LINEAR ELASTIC FRACTURE MECHANICS

### 4.2.1 Technical Basis

Current Code requirements adopt the methodologies of linear elastic fracture mechanics (*LEFM*) to ensure the safety of nuclear RPVs against non-ductile fracture during both routine operation and potential accident conditions. A brief review of *LEFM* technology is presented here to place into context how the limitations of this technology influenced the nuclear RPV assessment procedures adopted in 1973.

#### 4.2.1.1 Theoretical Basis

*LEFM* provides a mathematical means to relate the three variables which combine to control the fracture integrity of a structure: stress, flaw size, and fracture toughness. In *LEFM* these variables have the following characteristic relationship:

$$K_I = \sigma \sqrt{\pi a} \cdot F\left(\frac{a}{W}\right) \quad (4-1)$$

where

$K_I$  is the applied fracture driving force, or the fracture toughness,

$\sigma$  is the stress,

$a$  is the flaw size, and

$F(a/W)$  is the geometry factor.

The utility of *LEFM* arises from the ability to calculate  $F(a/W)$  factors for both laboratory test specimens and structures. This enables the use of critical- $K_I$  values measured in the laboratory with simple test specimens to predict the fracture behavior of considerably more complex structures.

In *LEFM*, the following relationship exists between  $K_I$  and the stress (and strain) fields near a crack tip:

$$\sigma_{ij} = \frac{K_I}{\sqrt{2\pi r}} \cdot f_{ij}(\theta) \quad (4-2)$$

where

$r$  is the distance from the crack tip.

Under certain conditions,  $K_I$  quantifies completely and uniquely *all* of the stresses and *all* of the strains within some finite radius from the crack tip. Thus, provided the zone over which

Eq. (4-2) applies completely surrounds the fracture process zone,  $K_I$  characterizes when failure will occur irrespective of the physical process which controls fracture.

The effort to ensure that Eq. (4-1) applies places a significant restraint on *LEFM* approaches. This restraint has influenced engineers' view of the applicability regimes of various fracture mechanics technologies for the last quarter century. These aspects of *LEFM* are discussed in the following sections.

#### 4.2.1.2 Restraint Imposed by *LEFM*

In order to apply *LEFM* approaches to reasonably ductile materials, the test specimens used to measure fracture toughness must be exceedingly large. As implied by the "LE" in *LEFM*, the theory that underlies Eqs. (4-1) and (4-2) assumes linear elastic material behavior. Thus, the extent of plastic deformation experienced by a specimen or structure must be small relative to the overall size of that specimen or structure for *LEFM* to predict accurately the fracture event. As RPVs are fabricated from heavy wall sections, this limitation does not significantly impede accurate characterization of cracks in RPV structures using *LEFM*. However, this requirement results in the need to test large specimens.

The size of the plastic zone ahead of a deforming crack in a thick structure is as follows:

$$d_{plastic} = \frac{1}{3\pi} \left( \frac{K_I}{\sigma_y} \right)^2 \quad (4-3)$$

where

$\sigma_y$  is the yield strength.

This plastic zone size can be compared with the specimen dimensions required by ASTM Test Standard E399 to obtain a valid  $K_{Ic}$  value. The E399 dimensional requirement is as follows:

$$a, b, B \geq 2.5 \left( \frac{K_I}{\sigma_y} \right)^2 \quad (4-4)$$

where

$a, b, B$  are the crack length, remaining ligament, and thickness, respectively.

Comparison of Eqs. (4-3) and (4-4) reveals that E399 requires that the smallest length scale in the specimen ( $a, b$ , or  $B$ ) exceed the size of the plastic zone by a factor of  $2.5 \cdot 3 \cdot \pi$ , or approximately 25. This requirement was arrived at by testing specimens of progressively greater thickness to determine the thickness above which the fracture toughness values became constant [Scrawley and Brown; 1963].

Expressing the size requirement in this manner (as a multiple of plastic zone diameters) provides an indication of when the assumptions which underlie *LEFM* break down. However, selection of the numeric factor in Eq. (4-4) requires judgment. The value of 2.5 was motivated by the desire to have a test standard which applies equally well to all metallic materials. Nevertheless, certain technical groups supported use of a material specific numeric factor in Eq. (4-4). When the E399 standard was developed, Rolfe and Novack [1964] provided empirical evidence to support a factor of 1.0 for structural steel. This proposal would extend the measurement capacity of small specimens (Figure 4-1), however no such standards action was completed when nuclear RPVs and surveillance capsules were being designed. The ASTM E399 value of 2.5 is so restrictive for RPV steels that it was not possible to include specimens in surveillance capsules that met the *LEFM* size requirements. This forced nuclear surveillance programs to adopt indirect means (i.e., correlations between Charpy V-Notch specimens and toughness) to assess the fracture toughness of RPV steels in the irradiated condition.

#### 4.2.1.3 View on Toughness

Within a linear elastic framework, the variation of toughness with section thickness depicted in Figure 4-2 is expected. As discussed in Section 4.2.1.2, there is a critical plastic zone size above which the techniques of *LEFM* apply accurately. The fracture toughness remains constant with increasing section thickness above this limit. Barring metallurgical effects, there is no need to test specimens having sizes considerably greater than this critical dimension. Below this critical dimension the fracture toughness increases due to loss of constraint against plastic flow from the crack tip region, a plasticity effect not addressed adequately by *LEFM*. In this regime the concept of Elastic-Plastic Fracture Mechanics, or *EPFM*, is required. *EPFM* is discussed in Section 5.1 in greater detail.



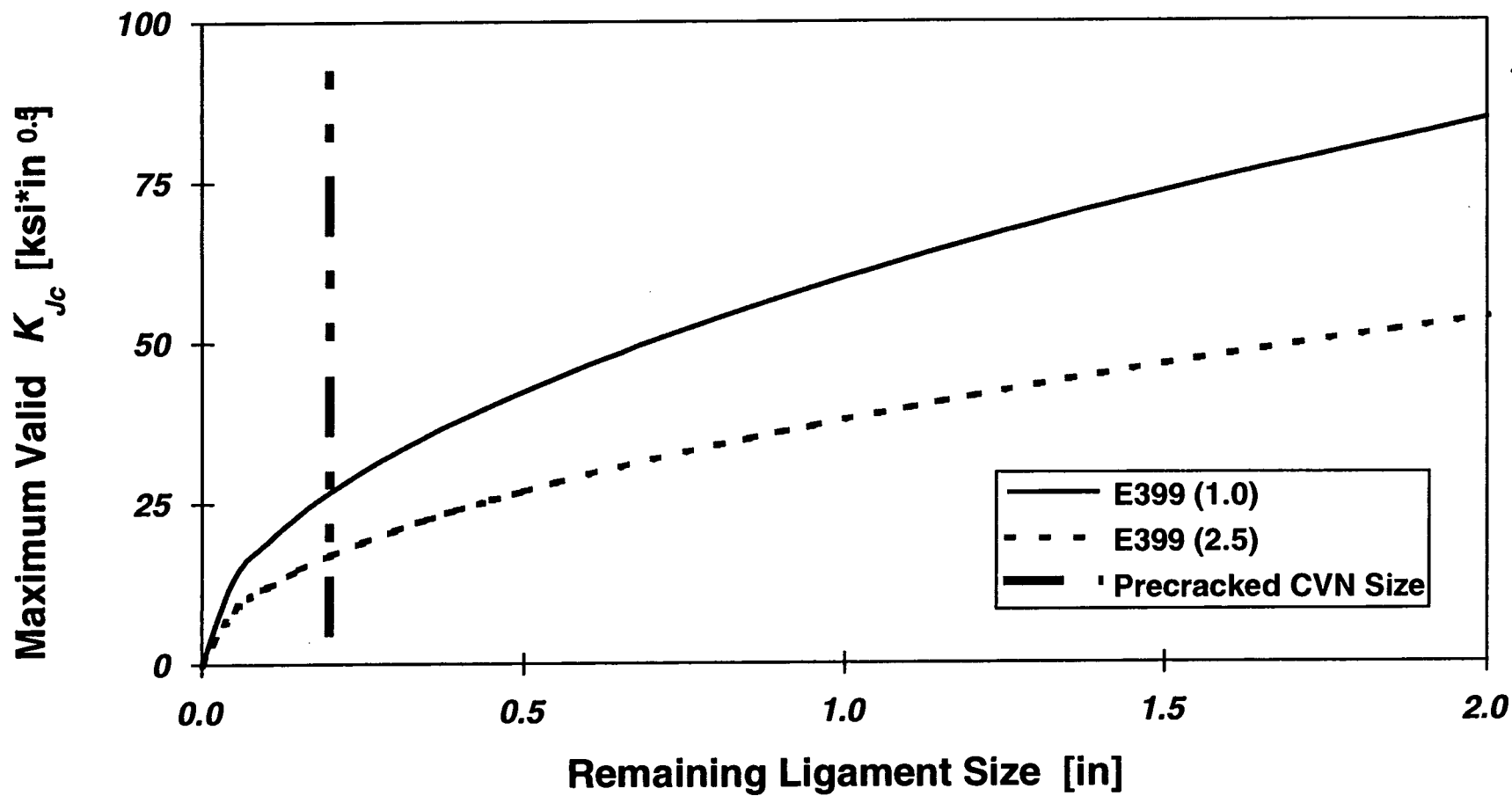


Figure 4-1 A comparison of material independent LEM size requirements (the E399 (2.5) curve) and LEM size requirements specific to RPV steels (the E399 (1.0) curve)

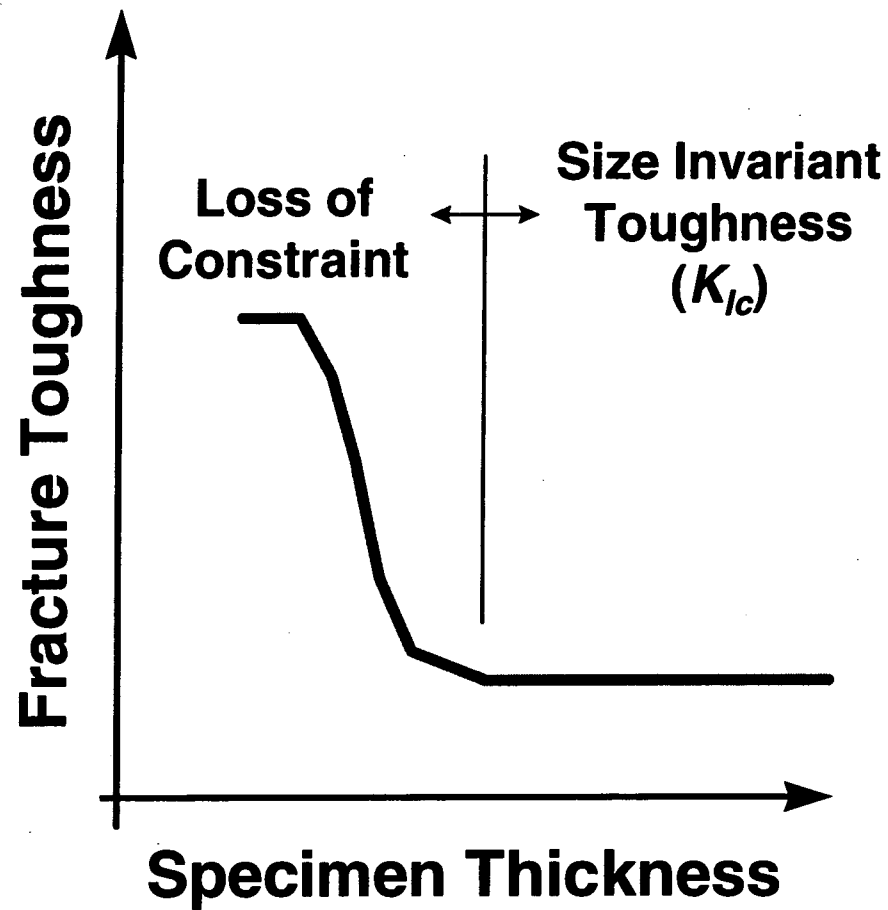


Figure 4-2 A perspective on the variation of fracture toughness with specimen thickness motivated by an understanding of *LEFM*

## 5.0 TECHNICAL ADVANCES SINCE 1973

The following three developments since the 1973 adoption of the ASME  $K_{IR}$  and  $K_{IC}$  curves establish a basis for updating the methodology used for RPV assessments while simultaneously improving their accuracy. These developments are as follows:

1. The development of elastic-plastic fracture mechanics (*EPFM*),
2. Increased understanding of the micro-mechanisms of cleavage fracture, and
3. The availability of considerably more fracture toughness data on reactor pressure vessel steels.

These developments establish the basis for the "Master Curve" concept first introduced by Wallin, et al. [1984]. This section includes a review of these developments, a description of the Master Curve, and a critical examination of its applicability to nuclear RPV assessment.

### 5.1 ELASTIC-PLASTIC FRACTURE MECHANICS

The concept of *EPFM*, an extension of the earlier methods of *LEFM* which enables treatment of specimens and structures that undergo significant plastic deformation prior to failure, emerges as a key enabling technology. In the case of RPVs, Federal regulations require demonstration of integrity against postulated brittle fracture conditions. While *LEFM* provides a reasonable model of vessel fracture under these conditions, it characterizes inadequately the fracture of specimens removed from surveillance capsules. These specimens, owing to their small size, experience significant plastic deformation prior to fracture, even when fracture occurs by cleavage. This plasticity invalidates the use of  $K$  as a fracture characterizing parameter because, under these conditions,  $K$  no longer completely describes all of the stresses and all of the strains in the fracture process zone. In these situations the  $J$ -integral [Rice and Rosengren, 1968] provides an analogous role to  $K$  as it describes uniquely all of the stresses and all of the strains in the vicinity of a crack tip deforming under elastic-plastic conditions, viz.:

$$\frac{\sigma_{ij}}{\sigma_o} = \left( \frac{J}{\alpha \epsilon_o \sigma_o I_n r} \right)^{\frac{1}{n+1}} \sigma_{ij}(\theta; n) \quad (5-1)$$

where

$\sigma_o$  is the yield stress,

$\epsilon_o$  is the yield strain,

$I_n$  is an integration constant,

$\alpha$  is a parameter in a Ramberg-Osgood constitutive model, and

$n$  is the work hardening coefficient in a Ramberg-Osgood constitutive model.

*EPFM* can characterize the fracture process to much higher deformation levels than *LEFM* because its mathematical basis accounts appropriately for the effects of plastic flow. Figure 5-1 illustrates the effect schematically. This difference between *LEFM* and *EPFM* has two practical implications:

- *EPFM* methods lose validity at much higher deformation levels than *LEFM* methods, and/or
- Much smaller specimens can be tested when fracture toughness is expressed in terms of critical  $J$  values.

Koppenhoefer, et al. [1995] examined these effects by calculating a ratio between the E399 size requirements (Eq. (4-4)) and a fairly restrictive *EPFM* size requirement [Dodds, et al., 1992]. Figure 5-2 provides these ratios, expressed in terms of maximum valid  $K_{Ic}$ . For a typical RPV steel (yield strength of 60 ksi, tensile strength of 90 ksi) these graphs demonstrate that *EPFM* provides approximately eight times the toughness measurement capacity (or  $1/8^{\text{th}}$  of the dimensional requirements) of *LEFM*. Thus, by using *EPFM* one can measure valid fracture toughness values using specimens that are only  $1/8^{\text{th}}$  of the size required for *LEFM* validity. *EPFM* validity limits are discussed further in Section 5.2.2.

## 5.2 CLEAVAGE FRACTURE MICRO-MECHANISMS

As discussed in Section 4.2.1.2, in the 1960s fracture toughness was understood to be a material property equally appropriate to the characterization of any metal. This perspective was partially influenced by the belief that a material property should relate to structural durability in the same way that material properties relate to structural strength, and partially influenced by practical considerations. In the 1960s the understanding of the micro-scale mechanisms which cause fracture was not sufficiently mature to incorporate into a methodology useful for structural design. Moreover, the computational standard of the day was inadequate to resolve micro-mechanical failure criteria at the fine size scale needed to enable prediction of structural performance based on small specimen test data. Both of these situations changed dramatically in the intervening decades.

Here we review what has emerged as an appropriate micro-mechanical model of fracture by transgranular cleavage (Section 5.2.1). The insights gained from this model carry with them the following significant practical implications for the assessment of RPV structures:

1. They provide a new basis for establishing size limits / measurement capacities for fracture toughness specimens. This basis is more fundamentally sound and less restrictive than the current basis, which derives solely from limitations inherent to a phenomenological description of fracture based on linear elasticity (Section 5.2.2).
2. They provide for a physically motivated statistical model of fracture toughness data scatter in the transition regime (Section 5.2.3.1).

3. They provide a means to account for the effect of structural size on fracture toughness (Section 5.2.3.2).
4. They suggest that all RPV steels experience a similar variation of fracture toughness with temperature, an observation which simplifies considerably the task of characterizing the fracture toughness transition.

### 5.2.1 Micro-Mechanical Models for Cleavage Fracture

Ritchie, Knott, and Rice (RKR) [1973] were the first to link explanations of the cause for cleavage fracture based on dislocation mechanics with the concepts of *LEFM*. By 1973 both phenomenological [Orowan, 1948] and dislocation-based [Smith, 1966; Smith, 1968] models suggested that cleavage fracture required achievement of a critical stress level. The RKR model combined this criteria with the (then) recently published solutions for stresses ahead of a crack in an elastic-plastic solid [Rice and Rosengren, 1968; Hutchinson, 1968; Rice and Johnson, 1970] to predict successfully the variation of the critical stress intensity factor with temperature in the low transition regime of a mild steel. These researchers also introduced the concept that achievement of this critical stress at a single point ahead of the crack tip was not a sufficient criteria for fracture. They postulated, and subsequently demonstrated, that the critical stress value had to be exceeded over a microstructurally relevant size scale (e.g., multiples of grain sizes, multiples of carbide spacing) for failure to occur.

The RKR model provides a description which is both consistent with the physics of the cleavage fracture process and predicts successfully the results of fracture toughness experiments. However, the model has limited engineering utility because the predictions depend strongly on two parameters (the critical stress for cleavage fracture, or  $\sigma_c$ , and the critical distance over which  $\sigma_c$  is achieved) which are both difficult to measure and can only be determined inferentially. Consequently, while the RKR model provides many useful insights, its application to design and assessment of component integrity has been limited.

### 5.2.2 Predictive Application of a RKR-like Model

Recent contributions by Dodds, et al. [1992] have improved the engineering utility of RKR-like models. Dodds used finite element models having extremely high resolution in the crack tip region to quantify the crack-tip fields in finite bodies. Their analyses revealed that these fields remain self-similar to those characteristic of small-scale yielding (*SSY*, or the infinite body reference condition) even under deformation conditions beyond *J*-dominance. At these high deformation levels, the stress fields in finite bodies can be expressed as a scalar multiple of those in *SSY*. Combining this scalar with *J* re-captures a complete description of the crack-tip fields.

These investigators used their finite element results as input to a RKR-like model, thus produced a methodology capable of predicting the effect of geometry and loading condition on fracture toughness. This methodology differed from that originally proposed by RKR in two important aspects:

1. The model only attempted to scale fracture toughness values between different geometry and loading conditions rather than predict toughness values from fundamental material variables, and
2. The observation of self-similar crack-tip stress fields in all geometries made the model predictions insensitive to the critical RKR parameters (critical stress, critical distance). Thus, even though this new methodology used a physically realistic cleavage fracture model, the predictions of the model were insensitive to the critical micro-scale parameters, thereby eliminating the need to measure them.

The Dodds model successfully predicts the relative toughness of specimens which fail at different constraint levels. In the context of the diagram in Figure 4-2, this model operates in the *EPFM* regime. Additionally, the model motivated specimen size limits for fracture testing (i.e., the position of the vertical line on Figure 4-2) on a fundamentally different basis than adopted for *LEFM* [Dodds, et al., 1992; Koppenhoefer, et al., 1995].

For *LEFM*, validity limits derive from criteria regarding acceptable differences of plastic zone size between laboratory specimens and very large structures [ASTM E399] (see Section 4.2.1.2). Such a basis is appropriate as it relates directly to when the mathematical basis of a *LEFM* description fails to model adequately the physical process. However, the concept of a limiting plastic zone size is irrelevant in *EPFM* because, as illustrated schematically in Figure 5-1, the mathematics which underlies *EPFM* models the physical deformation process up to and beyond full ligament yielding.

Dodds and co-workers proposed that the size limitations on *EPFM* validity be established as the *J* level at which the driving force for cleavage fracture (as defined by a RKR-like model) deviates significantly from that characteristic of the *SSY*, or infinite body, reference state. Their analyses suggests a size limit of the following form:

$$a, b, B \geq M \cdot \left( \frac{J_{critical}}{\sigma_{flow}} \right) \quad (5-2)$$

where  $\sigma_{flow}$  is the flow stress (average of yield and ultimate). Three dimensional analysis of single edge notch bend (SE(B)) fracture specimens both with and without sidegrooves suggests a value of  $M=50$  is appropriate [Nevalainen and Dodds, 1995]. Figure 5-3 compares this size requirement with that of Eq. (4-4) for *LEFM*. Of particular interest are bend specimens having dimensions equivalent to the CVN specimens placed in RPV surveillance capsules. *LEFM* limits restrict the measurement capacity of this specimen to  $20 \text{ ksi}\sqrt{\text{in}}$ , a value below the lower shelf of the ASME  $K_{Ic}$  curve. Conversely, the new size limits reveal the precracked CVN as capable of measuring size invariant toughness values of up to  $80 \text{ ksi}\sqrt{\text{in}}$  for the steel used in this example (Yield strength of 60 ksi, Tensile strength of 90 ksi). This elevated measurement capacity permits determination of structurally relevant toughness values using specimens currently placed in RPV surveillance capsules.

## 5.2.3 Stochastic Effects and the "Master Curve"

### 5.2.3.1 Description of the WST Model

While successful in accounting for deterministic differences between structural configurations, the model proposed by Dodds, et al. fails to predict the large degree of scatter characteristic of cleavage fracture data. Additionally, the Dodds model does not account for the size effect on *LEFM* valid data, first demonstrated experimentally by Landes and Shaffer [1980] and described by them as a "weakest link" effect.

In their 1984 paper, Wallin, Saario, and Törrönen (WST) suggest a connection between the micro-mechanics of cleavage fracture and the essentially phenomenological observation of a "master" toughness transition curve. The model accounts predictively for the scatter in cleavage fracture toughness data, the weakest link effect, and the variation of fracture toughness with temperature. The WST model includes the following features:

- WST assume that failure occurs when a sufficient stress ( $\sigma_c$ ) is achieved in the vicinity of a particle of sufficient size ( $r_c$ ),
- WST assume that carbide failure initiates fracture, and
- The applied- $K$  (or applied- $J$ ) indexes the variation of the stress in the crack-tip region.

On this basis, the probability of cleavage failure at a particular value of applied- $K$  (or applied- $J$ ) is determined as follows:

1. Failure is assumed to occur when a sufficient stress is achieved in the vicinity of a particle of sufficient size. The relationship between the particle radius ( $r$ ) and applied stress ( $\sigma$ ) needed to cause fracture is assumed to obey the following relationship [Griffith, 1920]:

$$r = \frac{\pi(\gamma_s + w_p)E}{2(1 - \nu^2)\sigma^2} \quad (5-3)$$

where  $E$  is Young's modulus,  $\nu$  is Poisson's ratio,  $\gamma_s$  is the surface energy of the matrix, and  $w_p$  is the plastic work necessary for crack propagation.

2. The critical fracture event is assumed to be failure of a carbide. The material is therefore described in the model in terms of the carbide distribution. WST assume an exponential form for this distribution, as illustrated in Figure 5-4(a) and described by the following equation:

$$\text{Probability}\{r \geq r^*\} = S \cdot \exp[-Q \cdot r] \quad (5-4)$$

where  $S$  and  $Q$  are constants, and  $r^*$  is the particle size of interest.

3. The variation of the applied stress in the crack-tip region is indexed to the applied- $K$  (or applied- $J$ ), and is determined from either asymptotic or finite element solutions of the following form:

$$\frac{\sigma_{ij}}{\sigma_o} = \left( \frac{J}{\alpha \epsilon_o \sigma_o I_n r} \right)^{\frac{1}{n+1}} \sigma_{ij}(\theta; n) \quad (5-5)$$

where  $\sigma_o$  is the yield stress,  $\epsilon_o$  is the yield strain,  $I_n$  is an integration constant, and  $\alpha$  and  $n$  are parameters in a Ramberg-Osgood constitutive model.

4. The probability of failure is related to the applied- $K$  (or applied- $J$ ) in the following manner:
- The applied- $K$  (or applied- $J$ ) is set to a value.
  - This value is used to calculate the applied stress in the crack tip region, using Eq. (5-5).
  - The applied stress is used in Eq. (5-3) to determine radius of the particle needed to cause fracture.
  - The probability distribution of Eq. (5-4) at this radius quantifies the probability of failure for this applied- $K$  (or applied- $J$ ) value.

Repetition of steps (a) through (d) for progressively higher levels of applied- $K$  (or applied- $J$ ) produces a relationship between the probability of failure and the applied fracture driving force, as illustrated in Figure 5-4(b).

5. A temperature dependency is introduced to the model by assuming that the sum of the matrix surface energy and the plastic work necessary for crack propagation in Eq. (5-3) increases with temperature ( $T$ ) as follows:

$$\gamma_s + w_p = A + B \cdot \exp[C \cdot T] \quad (5-6)$$

where  $A$ ,  $B$ , and  $C$  are constants.

Subsequent refinements to the WST model include adoption of a minimum fracture toughness value ( $K_{min} = 18.18 \text{ ksi}\sqrt{\text{in}}$ ) to address fracture on the lower shelf ( $K_{lc} \ll 45 \text{ ksi}\sqrt{\text{in}}$ ). On the lower shelf, fracture is controlled by crack propagation, rather than a crack initiation, criteria. Such fracture processes cannot be represented by a weakest-link model and, consequently, are not treated rigorously by the WST model. Thus, incorporation of a minimum fracture toughness value into the WST model represents an approximate, rather than a rigorous, treatment of the lower shelf behavior.



### 5.2.3.2 Features of the WST Model Important to Nuclear RPV Assessment

Three features of the WST model warrant further discussion because of their significant practical benefits when applied to nuclear RPV assessment.

1. The WST model demonstrates that the scatter in fracture toughness ( $K$ ) data for specimens which fail in small-scale yielding is characterized by a Weibull distribution with a slope of 4 (the Weibull slope is analogous to the standard deviation in Normal statistics) [Wallin, 1984]. This observation spawned the development of testing protocols [ASTM E1921-97] which assume a fixed dispersion (i.e., Weibull slope = 4) and so need only measure the central tendency of the distribution. These protocols enable estimation of data tolerance bounds based on limited sample replication.
2. The WST model incorporates the weakest link size effect observed by Landes and Schaffer [Wallin, 1985], thereby enabling the use of toughness results from small laboratory specimens to predict the fracture behavior of large structural components [Wallin, 1995].
3. The WST model incorporates the variation of fracture toughness with temperature in the lower transition regime for ferritic steels [Wallin, Saario, and Törrönen, 1984; Wallin, 1993], a variation now known as the Master Curve. This feature enables estimation of the entire lower transition curve based on testing at one temperature.

Section 5.3 provides an empirical evaluation of these features using of a substantial database of fracture toughness data for RPV steels.

### 5.2.3.3 ASTM Master Curve Testing Standard

Over the past 13 years, the WST Master Curve concept has evolved to the point of being adopted as a testing standard by ASTM [ASTM E1921-97]. Specifics of this standard are summarized here as this information is needed in the Section 5.3.

- A Master Curve is established for a material by determining an index temperature,  $T_o$ .  $T_o$  is the temperature at which the median fracture toughness of a 1T (i.e., a 1-in. thick) fracture mechanics specimen equals 90.9 ksi $\sqrt{\text{in}}$  (or 100 MPa $\sqrt{\text{m}}$ ). Both the reference size (1-in.) and the reference toughness (100 MPa $\sqrt{\text{m}}$ ) are selected purely for convenience. This selection is not required by the theory, nor does it influence structural assessments made using the Master Curve.
- Fracture test validity depends on the following two factors:
  1. The measured  $K_{Ic}$  value must fall below a limiting value established based on the work of Ruggieri et al. [1998]. This  $K_{Ic}$  limit ensures that measured  $K_{Ic}$  values and, thereby, the calculated  $T_o$  value, are not effected by the finite size of the test specimen. This  $K_{Ic}$  limit is as follows:

$$K_{Jc(\text{limit})} = \sqrt{\frac{Eb\sigma_y}{30}} \quad (5-7)$$

2. The amount of stable crack extension that occurs prior to cleavage failure cannot exceed 5% of the initial remaining ligament length.
- If 1T specimens are not tested, measured  $K_{Jc}$  values are converted to equivalent 1T values using the following formula, which is derived from a weakest link failure model [Wallin, 1985]:

$$K_{Jc|_{1T}} = 18.18 + \left( K_{Jc|_{\text{Measured}}} - 18.18 \right) \cdot \left[ \frac{B_{\text{Measured}}}{1} \right]^{1/4} \quad (5-8)$$

- Replicate tests of a single specimen size at a single temperature are conducted to determine  $T_o$ . Table 5-1 expresses the minimum number of valid replicates required as a function of the median fracture toughness of the data set.
- Once a data set having the minimum number of valid replicates is obtained,  $T_o$  is determined as follows:

Step 1: Determine  $K_o$ :

$$K_o = \left[ \frac{\sum_{i=1}^N \left( \text{Min} \{ K_{Jc}, K_{Jc(\text{limit})} \} - 18.18 \right)^4}{r - 0.3068} \right]^{1/4} + 18.18 \quad (5-9)$$

where

$N$  is the total number of specimens tested, and

$r$  is the number of specimens that satisfy the ASTM validity criteria.

Step 2: Determine  $K_{Jc(\text{med})}$ :

$$K_{Jc(\text{med})} = 0.9124 \cdot (K_o - 18.18) + 18.18 \quad (5-10)$$

Step 3: Determine  $T_o$ :

$$T_o = T_{\text{Test}} - 94.74 \cdot \ln \left[ \frac{K_{Jc(\text{med})} - 27.27}{63.63} \right] \quad (5-11)$$

Step 4: This  $T_o$  value may be increased to account for the uncertainty associated with limited sample sizes as follows (see Table 5-2 for values of  $\beta$  as a function of the median fracture toughness):

$$T_o|_{\text{mod}} = T_o + \frac{\beta}{\sqrt{N}} \quad (5-12)$$

- The median and 5% / 95% bounding Master Curves for a 1T specimen are determined as follows (see Table 5-3 for values of A and B appropriate to the different curves):

$$K_{Jc}|_{1T} = A + B \cdot \exp\left[\frac{T - T_o}{94.74}\right] \quad (5-13)$$

- $K_{Jc}$  values from Eq. (5-13) for 1-in. long crack fronts are converted to crack fronts of different lengths using the following formula:

$$K_{Jc}|_{Thick2} = 18.18 + \left(K_{Jc}|_{1T} - 18.18\right) \cdot \left[\frac{1}{B_{Thick2}}\right]^{1/4} \quad (5-14)$$

### 5.3 CLEAVAGE FRACTURE TOUGHNESS DATA

When ASME adopted the  $K_{Jc}$  curve in 1973, the data basis consisted of 163 quasi-static fracture toughness experiments performed on 11 heats of unirradiated RPV steel (and their weldments). As detailed in Table 5-4, specimen sizes ranging from 1- to 11-in. were tested [Marston, 1978]. Considerably more toughness data is now available (Tables 5-4 and 5-5). To date, Westinghouse has compiled fracture toughness data for 29 heats of steel / weldments in the unirradiated condition (27 for RPV steels, 2 for non-RPV steels), and an additional 10 heats of RPV steel in an irradiated condition. Figure 5-5 compares the quantity of fracture toughness data now available to that which provided the basis for the original ASME  $K_{Jc}$  curve. The amount of unirradiated data has increased by a factor of nearly 7. Moreover, a significant quantity of fracture toughness data are now available for irradiated materials (302 values, or 1.85 times more than the original 163 *unirradiated* datum). In this section, we use this empirical basis to examine the three key features of the WST Master Curve concept identified in Section 5.2.3.1, and questions associated with the ASTM test standard identified by Mayfield, et al. [1997].

- Section 5.3.1: The validity of characterizing the scatter in transition fracture toughness data using a Weibull distribution having a fixed slope of 4.
- Section 5.3.2: The validity of scaling fracture toughness data for differences in structural size based on a weakest link model.
- Section 5.3.3: The universality of the master curve shape.
- Section 5.3.4: The influence of test temperature and of the degree of deformation prior to fracture on  $T_o$ .

We conclude this argument in Section 5.3.5 with a test of the Master Curve as it could be applied in a reactor vessel integrity assessment.

In combination, the information in Sections 5.3.1 through 5.3.5 provides an empirical evaluation of the applicability of the Master Curve to RPV steels. Furthermore, cognizant that the range of chemistry, tensile properties, and product forms included in our A508/A533 database may not fully represent the diversity of conditions in the operating nuclear fleet, we carry two data sets for non-RPV steels through these analysis. These non-RPV steels differ more from each other, and from RPV steels, than any two heats of RPV steel differ from one another. Consequently, these data for non-RPV steels support our argument that the Master Curve applies to all RPV steels by providing evidence that steels of strength and chemical composition which extend beyond those characteristic of nuclear grade RPV steels are still modeled well by the Master Curve.

The two non-RPV steels considered in this study are A470 (a high strength/high alloy rotor forging) and A36 (a low strength/low alloy plate used in bridge construction and other civil engineering structures). Table 5-6 summarizes the strength and composition of these steels and compares them to the RPV steels that populate the bulk of the database. Figure 5-6 demonstrates that the tensile properties of these two non-RPV steels differ markedly from each other, and more importantly, bound the range of tensile properties in the operating nuclear fleet both before and after irradiation.

### 5.3.1 Weibull Description of Fracture Toughness Data

The WST Master Curve model and ASTM Master Curve testing protocols assume that the experimental data conforms to a Weibull distribution with a fixed slope (dispersion) of 4. This premise is tested using available data for RPV steels.

A best fit is determined for all iso-temperature/iso-size data sets that have at least five specimens. Table 5-7 summarizes the results of this analysis, performed on 75 data groupings (44 from unirradiated RPV steels, 14 from unirradiated non-RPV steels, 17 from irradiated RPV steels). The best fit Weibull slope was statistically significant at the 99% level for 95% of these data groupings, demonstrating the broad conformance of these data to Weibull distributions. Figure 5-7 compares these best-fit slope values with the 95% confidence bounds on the theoretical value of 4 [Wallin, 1984]. The data lie largely within these confidence bounds, and do not exhibit any obvious dependence on specimen size. These data provide experimental testament to the appropriateness of a Weibull slope of 4 in the limit of a very large data set.

### 5.3.2 Weakest Link Size Scaling of Fracture Toughness Data

The WST model includes the following relationship, derived from a weakest-link model of cleavage fracture, between toughness and crack front length:

$$K_{Jc} \Big|_{Thick2} = 18.18 + \left( K_{Jc} \Big|_{Thick1} - 18.18 \right) \cdot \left[ \frac{B_{Thick1}}{B_{Thick2}} \right]^{1/4} \quad (5-15)$$

Figures 5-8(a) and 5-8(b) illustrate this trend. The adequacy of this model is tested in the following way:

1. A data set is identified that has fracture toughness data for specimens of various sizes at a single temperature. Only data which satisfy the validity requirements of ASTM E1921-97 are used.
2. These fracture toughness values are normalized to 1T equivalence using Eq. (5-8).
3. These 1T equivalent toughness values are plotted as a function of specimen thickness. If Eq. (5-15) accounts properly for the deterministic effect of crack front length on toughness, then the slope of a line fit through these data should be statistically indistinguishable from zero. We test for this condition by applying Student's T-test to the best-fit slope at a 99% confidence level.

Figure 5-9 re-visits the two data sets from Figure 5-8, but now presented as 1T equivalent toughness *vs.* specimen thickness. These plots demonstrate the success of the weakest link model, Eq. (5-8), in predicting the deterministic differences in toughness between specimens of different crack front lengths. Table 5-8 summarizes the results from 43 data groupings analyzed in this way, the last column providing results from the T-test described as Step 3. This test demonstrates that no statistically superior relationship to Eq. (5-8) exists for 91% of the data groupings (39 out of 43) considered here. Thus, the weakest-link methodology developed by WST, and adopted by ASTM in testing standard E1921-97 to account for the deterministic effect of specimen size on toughness, predicts trends that agree with the great preponderance of available empirical evidence for RPV steels and their weldments both before and after irradiation.

### 5.3.3 The Universality of the Master Curve Shape

The WST Master Curve assumes that the median fracture toughness of a steel (when normalized to 1T thickness) varies with temperature by the following relationship:

$$K_{Jc|1T} = 27.27 + 63.63 \cdot \exp\left[\frac{T - T_o}{94.74}\right] \quad (5-16)$$

If this functional form provides an appropriate description of a particular data set, the variation of the fracture toughness residuals (i.e., the deviation of an experimental  $K_{Jc}$  value from the prediction of Eq. (5-16)) with increasing temperature will have zero slope and zero y-intercept, as illustrated in Figure 5-10. In this section, the goodness-of-fit of the Master Curve to available experimental data is assessed relative to these criteria. The following analytical procedure is employed:

1. A candidate data set is identified.

2. All cleavage fracture toughness data are considered irrespective of if they satisfy ASTM E1921-98 validity requirements (Eq. (5-7)) or not. As illustrated in Figure 5-11, censoring the  $K_{Ic}$  values per ASTM biases the  $K_{Ic}$  residuals toward negative values. Such a bias unfairly penalizes this assessment of the Master Curve shape, making use of "invalid" cleavage fracture toughness values necessary in this context.
3. A  $T_0$  value is calculated for the data set using the maximum likelihood technique of Moskovic [1993] (see Section 5.3.3.2 for a further examination of  $T_0$  calculation methodologies).
4. All measured toughness values are converted to 1T equivalence using Eq. (5-8) and are plotted along with the Master Curve (Eq. (5-16)).
5. The  $K_{Ic}$ -residual (i.e., the vertical distance from a datum to the Master Curve) is calculated and plotted on a second graph at the same  $T - T_0$  value.
6. A best fit slope and intercept is estimated from the variation of  $K_{Ic}$ -residual vs.  $T - T_0$  using the method of least squares. If Eq. (5-16) properly describes the variation of toughness with temperature, these slope and intercept values should be statistically indistinguishable from zero. We test for this condition by applying Student's T-test at a 99% confidence level.

This analysis is performed on the following three data sets:

- Aggregated data sets
  - All available unirradiated data
  - All available irradiated data
- Each data set individually.

#### 5.3.3.1 Analysis of Aggregated Data Sets

Analysis of the aggregated unirradiated and irradiated data is conducted over various temperature ranges to determine if the Master Curve fits better over some temperature ranges than others. Goodness-of-fit is assessed over the temperature ranges indicated in Figures 5-12 and 5-13 for the aggregated unirradiated and the aggregated irradiated data, respectively. Figure 5-14 demonstrates that the slopes and intercepts calculated from Figures 5-12 and 5-13 are statistically indistinguishable from zero over the following temperature ranges:

- Unirradiated:  $T - T_0 = \pm 140^\circ\text{F}$
- Irradiated:  $T - T_0 = \pm 100^\circ\text{F}$

This analysis demonstrates that no statistically superior curve shape exists in the temperature interval of  $T - T_0 = \pm 140^\circ\text{F}$  for unirradiated RPV steels, and  $T - T_0 = \pm 100^\circ\text{F}$  for irradiated RPV

steels. These temperature intervals are superimposed on the data in Figures 5-12 and 5-13 and compared with the temperature range populated by the data. The smaller temperature range over which the Master Curve agrees with  $K_{Ic}$  data for irradiated steels occurs as a natural consequence of the range of empirical data being more limited for irradiated steels, i.e.:

- Range of Unirradiated  $K_{Ic}$  data:  $-260^{\circ}\text{F} < T - T_0 < +200^{\circ}\text{F}$
- Range of Irradiated  $K_{Ic}$  data:  $-200^{\circ}\text{F} < T - T_0 < +140^{\circ}\text{F}$

The temperature range of Master Curve agreement is approximately the same percentage (60%) of the range of available data for both unirradiated and irradiated RPV steels.

The less than ideal fit of the Master Curve to experimental data at extremely high and at extremely low temperatures occurs for three reasons.

- At Both High and Low Temperatures: Rigorous statistical agreement of a theoretical curve with an empirical database should not be expected to the limits of the empirical data because of the significant influence the limited observations as these extreme temperatures exert on the best fit curve.
- At Low Temperatures: At temperatures on the lower shelf, the lack of fit results from the loss of a weakest-link controlled failure mechanism, as noted previously by Wallin [1995].
- At High Temperatures: At higher temperatures, the lack of agreement between the Master Curve and available fracture toughness data may result from the intervention of upper shelf failure modes.

These factors notwithstanding, the small magnitude of the best-fit slope and intercept values determined here (see Figure 5-15) suggest that a minor adjustment of the coefficients in Eq. (5-16) would produce a better fit over a wider temperature range. Furthermore, even in its existing form, the Master Curve describes a variation of  $K_{Ic}$  with temperature in good agreement with experimental data over toughness and temperature ranges of considerable practical interest for establishing heat up and cool down curves, and for performing PTS assessments.

In summary, available empirical evidence suggests that the Master Curve provides robust predictions of the effects of temperature on the fracture toughness of RPV steels (and their weldments) both before and after irradiation. No statistically superior curve shape exists in the temperature interval of  $T - T_0 = \pm 140^{\circ}\text{F}$  for unirradiated steels, and  $T - T_0 = \pm 100^{\circ}\text{F}$  for irradiated steels. Only very minor adjustments to existing Master Curve coefficients could extend this temperature range to encompass all existing fracture toughness data for RPV steels.

### 5.3.3.2 Analysis of Individual Data Sets

Table 5-9 summarizes the results of the goodness-of-fit analyses for each data set. Most data sets do not differ from the Master Curve in a manner which suggests that another curve shape

would be more appropriate. The lightly shaded rows in Table 5-9 indicate data sets which do not match the Master Curve shape at a 99% confidence level. These data sets are as follows:

- Marston A508 Cl. 2
- Marston A533B Cl. 1 (HSST Plate 02)
- Morland A533B Cl. 1
- McCabe A533B Cl. 1 (HSST Plate 13A)
- Lidbury A 508 Cl. 3
- Sorem A36 Plate
- McCabe Midland WF 70 Beltline Weld
- McCabe Midland WF-70 Nozzle Weld

The insights provided in Section 5.3.3.1 motivate a re-analysis of these data sets to determine if a limited number of toughness data at high and/or low temperatures are exerting undue influence over a much larger data set. This re-analysis, reflected by the lightly shaded rows of Table 5-9, show that elimination of limited quantities of high temperature data restores agreement with the Master Curve shape for four of these eight data sets:

- Morland A533B Cl. 1 6 data eliminated (2.5%)
- McCabe A533B Cl. 1 (HSST Plate 13A) 3 data eliminated (2.4%)
- Lidbury A 508 Cl. 3 16 data eliminated (23%)
- Sorem A36 Plate 3 data eliminated (1.7%)

Re-analysis of the Marston data for HSST Plate 02 is motivated by a different reason. The  $K_{Ic}$  values for the 10T and 11T specimens (5 values total) all lie above than the 95% Master Curve upper bound, a very unusual occurrence for this size data set. Re-analysis of the HSST-02  $K_{Ic}$  residuals without the 10T and 11T data suggests that the Master Curve has an appropriate shape for these data.

Accepting these re-analyses, the Master Curve shape describes adequately 24 out of 25 unirradiated data sets for RPV steels, 2 out of 2 unirradiated data sets for non-RPV steels, and 7 out of 9 irradiated data sets for RPV steels. In total, 92% of all available data sets, and 95% of all  $K_{Ic}$  data, exhibit a variation of fracture toughness with test temperature consistent with that described by the Master Curve.

### 5.3.4 Effect of Test Variables on $T_0$ Determination Bias and Accuracy

#### 5.3.4.1 Test Temperature and Deformation Effects on ASTM $T_0$ Estimates

ASTM E1921-97 permits the conduct of  $K_{Ic}$  tests to determine  $T_0$  over a wide range of temperatures. Furthermore, these specimens can experience deformation conditions prior to



failure that range from well contained plasticity to full ligament yielding. This latitude of permissible test conditions has led some to express concern regarding the possibility for variation in  $T_o$  within the limits allowed by the ASTM standard [Mayfield, et al., 1997]. Here we address these concerns using available fracture toughness data.

Table 5-7 summarizes  $T_o$  values estimated using ASTM protocols.  $T_o$  values for all iso-temperature data groupings which meet ASTM requirements (44 for unirradiated RPV steels, 14 for non-RPV steels, and 17 for irradiated RPV steels) are calculated. Table 5-7 includes  $T_o$  values calculated using the Maximum Likelihood (ML) technique of Moskovic [1993]. While both the ML and ASTM  $T_o$  values are estimates, we regard ML  $T_o$  values as a better experimental estimate because they are based on much larger data sets than ASTM  $T_o$  values (77 values for ML  $T_o$  estimates vs. 10 for ASTM  $T_o$  estimates, on average). Furthermore, these data sets sample the entire transition fracture range. Figure 5-16 presents data which examines the influence of both test temperature and degree of yielding before failure on the departure of ASTM  $T_o$  values from the best experimental estimate of  $T_o$ . We apply the following statistical test to the data presented in Table 5-7 and Figure 5-16:

The ASTM  $T_o$  values are considered accurate (i.e., differing by no more than the scatter inherent to the data) relative to the best experimental estimate of  $T_o$  provided that both the slope and intercept of a line fit through the data are statistically indistinguishable from zero (based on a Student's-T test at a 99% confidence level). This criteria may be interpreted as follows:

- **Figure 5-16(a):** The test temperature at which  $K_{Ic}$  experiments are conducted exert no systematic influence on the value of  $T_o$  over a temperature range of  $-50^\circ\text{F} < T - T_o < +175^\circ\text{F}$ .
- **Figure 5-16(b):** The deformation prior to fracture experienced by  $K_{Ic}$  test specimens exerts no systematic influence over the resultant value of  $T_o$  over a deformation range of  $30 < M_{\text{MINIMUM}} < 1,100$ .  $M_{\text{MINIMUM}}$  is defined as follows based on the maximum  $K_{Ic}$  in a data set used to estimate  $T_o$ .

$$M_{\text{MINIMUM}} = \frac{E \cdot b \cdot \sigma_{ys}}{K_{Jc \text{ Maximum}}^2} \quad (5-17)$$

Table 5-10 summarizes the results of this statistical test, which is applied to the following data groupings: all data, unirradiated RPV steels, non-RPV steels, and irradiated RPV steels. These data demonstrate that neither test temperature or the degree of deformation prior to fracture exerts a systematic influence on  $T_o$  values. Thus, there is no empirical basis for the concern that  $T_o$  values can differ significantly from each other, provided the validity requirements of ASTM E1921-97 are satisfied.

### 5.3.4.2 ASTM $T_o$ Estimate Bias and Accuracy

Figure 5-17 compares ASTM  $T_o$  values with the best experimental estimate of  $T_o$ . These data are used to quantify the accuracy and bias inherent to ASTM  $T_o$  estimates. ASTM  $T_o$  estimates are unbiased if, on average, they agree with the best experimental estimate of  $T_o$ . In the context of Figure 5-17, this implies that the slope and intercept of a line fit through the data points should not differ significantly from unity and zero, respectively. A Student's T-test of the residuals associated with this zero-bias fit reveals that the slope and intercept do not differ from unity and zero, respectively, at a 99% confidence level. The accuracy characteristic of ASTM  $T_o$  estimates is quantified by using normal statistics to determine the expected uncertainty of an ASTM  $T_o$  estimate relative to the best experimental estimate of  $T_o$ . This calculation reveals a standard deviation on ASTM  $T_o$  estimates of 15°F for the data considered here.

Figure 5-18 re-presents the data from Figure 5-17 but now with the ASTM  $T_o$  estimate increased by one standard deviation ( $\sigma = \beta/\sqrt{N}$ ) to account for measurement uncertainties, as recommended by E1921-97 (see Eq. (5-12)). For 87% of the available data, this estimate of  $T_o$  (i.e., ASTM  $T_o + \beta/\sqrt{N}$ ) provides a higher reference temperature than the best experimental estimate of  $T_o$ .

### 5.3.5 Applications Test of the Master Curve

The information presented in Sections 5.3.2 through 5.3.5 examined the appropriateness of individual aspects of the WST Master Curve methodology relative to a large fracture toughness database for RPV steels. These results suggest that the Master Curve effectively predicts the following aspects of fracture toughness data for RPV steels in the great majority of cases:

- The scatter characteristic of replicate measurements of cleavage fracture toughness data made at a fixed temperature,
- The deterministic effect of crack-front length, or specimen "size," on cleavage fracture toughness at a fixed temperature, and
- The variation of cleavage fracture toughness with temperature between lower and upper shelf.

These features of the Master Curve must be satisfied simultaneously to achieve an accurate prediction for anticipated RPV applications (which will have the following characteristics, see Figure 5-19 for a graphical representation):

- A limited quantity of small specimens (PC-CVNs,  $\frac{1}{2}$ -Ts, or 1-Ts) could be tested at a single low temperature, e.g., a temperature below  $T_o$ . The quantity and size of specimens is limited by volume considerations in nuclear surveillance capsules. ASTM validity requirements dictate that testing of such small specimens occur at temperatures that are generally below  $T_o$ .

- These data will be used to predict the variation of median and bounding fracture toughness values with temperature characteristic of cracks which may exist in RPVs.

The viability of the Master Curve in this application is tested using available fracture toughness data in Figure 5-20. To avoid issues associated with selecting an "appropriate" crack front length for RPV applications, we examine the ability of the Master Curve to predict the variation of toughness with temperature for crack front lengths between 0.394-in. and 11-in., a range of nearly 30:1. Figure 5-20 partitions available fracture toughness data by specimen size to permit comparison of measured toughness values with Master Curve predictions. The Master Curve accurately predicts the variation of both median and bounding fracture toughness values for specimens ranging in size from precracked CVNs to 9Ts. The Master Curve significantly underpredicts the limited fracture toughness data for larger specimens (four 10T values and a single 11T value). It is unclear if this underprediction is a consequence of the extremely limited data quantity at these dimensions, if there is something anomalous about these data, or if this signals some breakdown in the theory. Regardless, the data demonstrate that the Master Curve conservatively predicts fracture toughness, even for these extremely long cracks.

#### 5.4 SUMMARY: AN EMPIRICAL BASIS FOR THE MASTER CURVE

The applicability of the WST Master Curve methodology to nuclear RPV assessment rests on three premises:

- The scatter in transition fracture toughness data is characterized by a Weibull distribution having a fixed slope of 4.
- The deterministic effect of crack front length, or specimen "size," on fracture toughness is quantifiable based on a weakest link model.
- The variation with temperature of both median and bounding values of fracture toughness is described by a single curve appropriate to both irradiated and unirradiated RPV steels. All RPV steels are indexed to this curve by determining their  $T_0$  value, where  $T_0$  is the temperature at which the median fracture toughness of a 1T (i.e., a 1-in. thick) fracture mechanics specimen equals 90.9 ksi $\sqrt{\text{in}}$ .

A database of fracture toughness values for RPV steels is assembled to evaluate these premises. The database contains 37 different steels, distributed as follows:

- 27 Unirradiated RPV Steels  
8 plates, 11 welds, 1 HAZ, 7 forgings.
- 2 Unirradiated non-RPV Steels  
1 plate, 1 forging.
- 10 Irradiated  
1 plate, 9 welds.

- 2,043 fracture toughness values (1,664 ASTM valid)
 

Unirradiated RPV:	1,431 values	(1,115 ASTM valid)
Unirradiated non-RPV:	300 values	(247 ASTM valid)
Irradiated:	312 values	(302 ASTM valid)
- Specimen sizes range from fatigue precracked CVNs up through 11T compact tension specimens.

This empirical evidence supports the following conclusions:

- The Weibull Distribution: All available fracture toughness data provide experimental testament to the validity of a fixed slope of 4 in the limit of a very large data set.
- Deterministic Size Effect: 91% of available fracture toughness data support prediction of the deterministic effect of crack front length, or specimen "size," based on a weakest link model.
- Universal Transition Curve Shape
  - *Based on Data Sets Treated Individually*: 92% of all available data sets (and 95% of all data) substantiate the variation of fracture toughness with test temperature predicted by the WST Master Curve.
  - *Based on Data Sets Treated in Aggregate*: Available fracture toughness data suggests that the Master Curve provides robust predictions of the effects of temperature on the fracture toughness of RPV steels (and their weldments) both before and after irradiation. No statistically superior curve shape could be derived for unirradiated or irradiated RPV steels in the temperature intervals of  $T - T_0 = \pm 140^\circ\text{F}$  and  $T - T_0 = \pm 100^\circ\text{F}$ , respectively. Only minor adjustments to existing Master Curve coefficients are needed to extend this temperature range to encompass all existing fracture toughness data.
- Effect on Test Variables on  $T_0$  Determination Bias and Accuracy
  - *Bias*: No systematic effects of either test temperature or specimen deformation prior to failure are evident. Provided that ASTM validity requirements are satisfied, an estimate of  $T_0$  may be regarded as unbiased in comparison with an experimental estimate based on the entire transition curve.
  - *Accuracy*: In 87% of the cases for which data is available, an estimate of  $T_0$  as  $[ \text{ASTM } T_0 + \beta/\sqrt{N} ]$  is conservative (i.e., provides a higher  $T_0$  value) relative to the best experimental estimate of  $T_0$ .
- Application of the Master Curve to RPV Assessment: The Master Curve accurately predicts the variation of both median and bounding fracture toughness values for

specimens ranging in size from precracked CVNs through 9Ts, and conservatively predicts the limited fracture toughness data for larger 10T and 11T specimens. This finding suggests that  $T_0$  determined based on a limited sampling of small specimens tested at a single temperature can predict accurately (or conservatively) the variation of fracture toughness with temperature characteristic of cracks which may exist in nuclear RPVs.

Unless specifically stated otherwise, these conclusions apply to both irradiated and to unirradiated RPV steels, and to two non-RPV steels. The two non-RPV steels have tensile properties that bound those characteristic of RPV steels, both before and after irradiation. The good agreement of these two non-RPV steels to the premises of the Master Curve suggest that the applicability of the Master Curve to *all* steels used in the operating nuclear fleet may be more general than can be established solely on the merits of the empirical evidence detailed herein.

<b>A 1T Equivalent <math>K_{Jc(med)}</math> Value of at Least [ksi*in<sup>0.5</sup>]</b>	<b>Requires this many valid specimens</b>
76.4	6
60.0	7
52.7	8
48.2	9
45.5	10
Below 45.5	Not valid by this test method

<b>A 1T Equivalent <math>K_{Jc(med)}</math> Value of at Least [ksi*in<sup>0.5</sup>]</b>	<b><math>\beta</math> [°F]</b>
75.4	32.4
60.0	33.8
52.7	36.2
48.2	38.5
44.5	40.9
Below 44.5	Not valid by this test method

**Table 5-3 Master Curve Coefficients from ASTM E1921-97**

Curve	A	B
95% Upper Tolerance Bound	31.5	92.9
Median	27.3	63.6
5% Lower Tolerance Bound	23.1	34.4

Table 5-4 Count of ASTM E1921-97 valid specimens in the fracture toughness database

Author	Material ID	Product Form	Irradlation Condition	RT <sub>NDT</sub> [°F]	T <sub>o</sub> [°F]	T-T <sub>o</sub> Range		Count for Specimens that are ASTM Valid										
						Min [°F]	Max [°F]	PC CVN	1/2T	1T	1.25T	2T	3T	4T	6T	8T	9T	10T
<b>Un-Irradiated RPV Steels</b>																		
Marston	A508 Cl. 2	Forging	None	51	-60	-90	60					7	1	1				
Marston	A508 Cl. 2	Forging	None	65	-55	-120	41					9			1			
Marston	A508 Cl. 2	Forging	None	50	-124	-196	24			9	4							
Marston	A533B Cl. 1	Plate	None	65	-74	-247	77			11	2							
Marston	A533B Cl. 1	HAZ	None	0	-132	-118	68			5	1							
Marston	A533B Cl. 1	Weld	None	0	-57	-264	57			4		3		1				
Marston	A533B Cl. 1	Weld	None	-45	-151	-169	-49			7	3							
Marston	HSST-01	Plate	None	20	-1	-149	-149			17								
Marston	HSST-01	Weld	None	0	-105	-70	55			2			5	1				
Marston	HSST-02	Plate	None	0	-17	-233	67			41	5	4	5			4		
Marston	HSST-03	Plate	None	20	31	-181	-181			9								
Nanstad	72W	Weld	None	-9.4	-70	-168	138			31	20	16	3	4				
Nanstad	73W	Weld	None	-29.2	-78	-160	119			35	20	16	2	4				
VanDerSluys	A508 Cl. 3	Plate	None	-22	-157	9	99			143								
Morland	A533B Cl. 1	Plate	Nene	5	-149	19	163			37	51							
Alexander	A508 Cl. 2	Plate	None	149	-2	-97	52			20	9	4						
McCabe	A533B Cl.1 (13A)	Plate	None	-9.4	-109	-129	184			38	48	26	6					
Ingham	A533B Cl. 1	Plate	None	5	-159	29	227	7		28	25	16			11			
McCabe 94	Midland WF70 Beltline	Weld	None	27	-71	-77	103			8	29	12	2					
McCabe 94	Midland WF70 Nozzle	Weld	None	27	-34	-114	66			7	25							
McGowan	HSST-02	Plate	None		-8	-140	82			23								
McGowan	68W	Weld	None		-133	-79	111			10								
McGowan	69W	Weld	None		5	-153	70			19								
McGowan	70W	Weld	None		-77	-134	46			10								
McGowan	71W	Weld	None		-41	-98	55			7								
Iwadata	A508	Forging	None	-13	-46	-192	60			39	56	10	4					
Lidbury	A508	Forging	None		-159	2	225	11				45			15			
<b>Non-RPV Steels</b>																		
Iwadata	A470	Forging	None	-31	-116	-204	94			62	36	8	11	6				
Sorem	A36	Plate	None		-68	-252	100			66		58						



Table 5-4 (cont.) Count of ASTM E1921-97 valid specimens in the fracture toughness database

Author	Material ID	Product Form	Irradiation Condition	RT <sub>NDT</sub> [°F]	T <sub>0</sub> [°F]	T-T <sub>0</sub> Range		Count for Specimens that are ASTM Valid											
						Min [°F]	Max [°F]	PC CVN	1/2T	1T	1.25T	2T	3T	4T	6T	8T	9T	10T	11T
<b>Irradiated RPV Steels</b>																			
Nanstad 92	72W	Weld	Irrad	138	85	-187	118			32		23		14					
Nanstad 92	73W	Weld	Irrad	179	99	-202	122			27		23		11					
Nanstad 97	Midland WF70 Beltline	Weld	1x10 <sup>19</sup>		88	-146	106	18	11	18									
Nanstad 97	Midland WF70 Beltline	Weld	0.5x10 <sup>19</sup>		37	-26	-26	7											
Nanstad 97	Midland WF70 Nozzle	Weld	1x10 <sup>19</sup>		135	-57	32	9	13	6									
McGowan	HSST-02	Plate	Irrad		127	-140	49			28									
McGowan	68W	Weld	Irrad		-111	-90	53			15									
McGowan	69W	Weld	Irrad		66	-98	56			16									
McGowan	70W	Weld	Irrad		-33	-160	38			16									
McGowan	71W	Weld	Irrad		2	-101	30			15									
<b>T-T<sub>0</sub> Range</b>																			
	<b>Condition</b>	<b># of Data Sets</b>	<b>Total # of Datum</b>			<b>Min [°F]</b>	<b>Max [°F]</b>	<b>PC CVN</b>	<b>1/2T</b>	<b>1T</b>	<b>1.25T</b>	<b>2T</b>	<b>3T</b>	<b>4T</b>	<b>6T</b>	<b>8T</b>	<b>9T</b>	<b>10T</b>	<b>11T</b>
	Original ASME Basis	11	163			-264	77	0	0	105	0	31	0	13	7	2	0	4	1
	Current Unirradiated (RPV)	27	1115			-264	227	18	129	640	0	153	45	77	12	25	11	4	1
	Current Unirradiated (Non-RPV)	2	247			-252	100	0	128	36	58	8	11	6	0	0	0	0	0
	Current Irradiated	10	302			-202	122	34	24	173	0	46	0	25	0	0	0	0	0
	All Data	39	1664			-264	227	52	281	849	58	207	56	108	12	25	11	4	1

Table 5-5 Count of all specimens in the fracture toughness database

Author	Material ID	Product Form	Irradiation Condition	T-T <sub>0</sub> Range			Count for All Specimens										
				T <sub>0</sub> [°F]	Min [°F]	Max [°F]	PC CVN	1/2T	1T	1.25T	2T	3T	4T	6T	8T	9T	10T
<b>Un-irradiated RPV Steels</b>																	
Marston	A508 Cl. 2	Forging	None	-60	-90	60						7		1	1		
Marston	A508 Cl. 2	Forging	None	-55	-120	41						9				1	
Marston	A508 Cl. 2	Forging	None	-124	-196	24					9	4					
Marston	A533B Cl. 1	Plate	None	-74	-247	77					11	2					
Marston	A533B Cl. 1	HAZ	None	-132	-118	68					5	1					
Marston	A533B Cl. 1	Weld	None	-57	-264	57					4			3		1	
Marston	A533B Cl. 1	Weld	None	-151	-169	-49					7	3					
Marston	HSST-01	Plate	None	-1	-149	-149					17						
Marston	HSST-01	Weld	None	-105	-70	55					2			5	1		
Marston	HSST-02	Plate	None	-17	-233	67					41	5		4	5		4
Marston	HSST-03	Plate	None	31	-181	-181					9						
Nanstad	72W	Weld	None	-70	-168	138					31	20		16	3	4	
Nanstad	73W	Weld	None	-78	-160	119					35	20		16	2	4	
VanDerSluys	A508 Cl. 3	Forging	None	-157	9	99					155						
Morland	A533B Cl. 1	Plate	None	-149	19	163				64	93						
Alexander	A508 Cl. 2	Forging	None	-2	-97	52					20	9		4			
McCabe	A533B Cl.1 (13A)	Plate	None	-109	-129	184				38	51	26		6			
Ingham	A533B Cl. 1	Plate	None	-159	29	227	44				70	61		30			12
McCabe 94	Midland WF70 Beltline	Weld	None	-71	-77	103				12	31	12		2			
McCabe 94	Midland WF70 Nozzle	Weld	None	-34	-114	66				7	25						
McGowan	HSST-02	Plate	None	-8	-140	82					25						
McGowan	08W	Weld	None	-133	-79	111					10						
McGowan	69W	Weld	None	5	-153	70					21						
McGowan	70W	Weld	None	-77	-134	46					10						
McGowan	71W	Weld	None	-41	-98	55					7						
Iwadata	A508	Forging	None	-46	-192	60					83	56		10		4	
Lidbury	A508	Forging	None	-159	2	225	34							69			16
<b>Non-RPV Steels</b>																	
Iwadata	A470	Forging	None	-116	-204	94					63	36		8	11	6	
Sorem	A36	Plate	None	-68	-252	100					118		58				

**Table 5-5 (cont.) Count of all specimens in the fracture toughness database**

Author	Material ID	Product Form	Irradiation Condition	T-T <sub>0</sub> Range			Count for All Specimens											
				T <sub>0</sub> [°F]	Min [°F]	Max [°F]	PC CVN	1/2T	1T	1.25T	2T	3T	4T	6T	8T	9T	10T	11T
<b>Irradiated RPV Steels</b>																		
Nanstad 92	72W	Weld	Irrad	85	-187	118			33		23	14						
Nanstad 92	73W	Weld	Irrad	99	-202	122			32	23	11							
Nanstad 97	Midland WF70 Beltline	Weld	1x10 <sup>19</sup>	88	-146	106	18	11	21									
Nanstad 97	Midland WF70 Beltline	Weld	0.5x10 <sup>19</sup>	37	-26	-26	7											
Nanstad 97	Midland WF70 Nozzle	Weld	1x10 <sup>19</sup>	135	-57	32	9	13	6									
McGowan	HSST-02	Plate	Irrad	127	-140	49			28									
McGowan	68W	Weld	Irrad	-111	-90	53			15									
McGowan	69W	Weld	Irrad	66	-98	56			16									
McGowan	70W	Weld	Irrad	-33	-160	38			16									
McGowan	71W	Weld	Irrad	2	-101	30			16									
<b>T-T<sub>0</sub> Range      Count for All Specimens</b>																		
	Condition	# of Data Sets	Total # of Datum	Min [°F]	Max [°F]	PC CVN	1/2T	1T	1.25T	2T	3T	4T	6T	8T	9T	10T	11T	
	Original ASME Basis	11	163	-264	77	0	0	105	0	31	0	13	7	2	0	4	1	
	Current Unirradiated (RPV)	27	1431	-264	227	78	204	745	0	189	69	91	12	26	12	4	1	
	Current Unirradiated (Non-RPV)	2	300	-252	100	0	181	36	58	8	11	6	0	0	0	0	0	
	Current Irradiated	10	312	-202	122	34	24	183	0	46	0	25	0	0	0	0	0	
	All Data	39	2043	-264	227	112	409	964	58	243	80	122	12	26	12	4	1	

Table 5-6 Strength and composition of steels in the fracture toughness database

Author	Material ID	Product Form	C	Mn	P	S	Si	Cr	Ni	Mo	Cu	V	Co	Al	As	Sn	$\sigma_{ys}$ [ksi]	$\sigma_{uts}$ [ksi]	% Elongation	% RA
<b>Un-Irradiated RPV Steels</b>																				
Marston	A508 Cl. 2	Forging	Not Reported																	
Marston	A508 Cl. 2	Forging	Not Reported																	
Marston	A533B Cl. 1	Plate	Not Reported																	
Marston	A533B Cl. 1	HAZ	Not Reported																	
Marston	A533B Cl. 1	Weld	Not Reported																	
Marston	A533B Cl. 1	Weld	Not Reported																	
Marston	HSST-01	Plate	Not Reported																	
Marston	HSST-01	Weld	Not Reported																	
Marston	HSST-02	Plate	Not Reported																	
Marston	HSST-03	Plate	Not Reported																	
Nanstad	72W	Weld	0.093	1.6	0.006	0.006	0.44	0.27	0.6	0.58	0.23	0.003	0.03	0.006	0.002	0.003	72	88	20	67
Nanstad	73W	Weld	0.098	1.56	0.005	0.005	0.45	0.25	0.6	0.58	0.31	0.003	0.03	0.006	0.002	0.003	71	87	22	68
VanDerSluys	A508 Cl. 3	Forging	0.19	1.42	0.003	0.003	0.2	0.15	0.76	0.48				0.017			66	87	25	76
Morland	A533B Cl. 1	Plate	0.21	1.44	0.006	0.005	0.28	0.18	0.67	0.48	0.05			0.021			68	90	25	66
Alexander	A508 Cl. 2	Forging	0.21	0.57	0.007	0.012	0.24	0.35	0.74	0.66		<0.01					79	101	16	61
McCabe	A533B Cl.1 (13A)	Plate	0.25	1.34			0.29		0.55	0.52							64	87		
Ingham	A533B Cl. 1	Plate	Same as Morland																	
McCabe	Midland WF70 Beltline	Weld	0.083	1.607	0.017	0.006	0.622	0.1	0.574	0.41	0.256	0.006	0.04	0.05	0.07					
McCabe	Midland WF70 Nozzle	Weld	0.083	1.604	0.016	0.007	0.605	0.11	0.574	0.39	0.29	0.008	0.015	0.018	0.006					
McGowan	HSST-02	Plate	0.23	1.55	0.009	0.014	0.2	0.04	0.67	0.53	0.14	0.003					68	90	18	68
McGowan	68W	Weld	0.15	1.38	0.008	0.009	0.16	0.04	0.13	0.6	0.04	0.007					80	94	17	72
McGowan	69W	Weld	0.14	1.19	0.01	0.009	0.19	0.09	0.1	0.54	0.12	0.005					93	105	16	69
McGowan	70W	Weld	0.1	1.48	0.011	0.011	0.44	0.13	0.63	0.47	0.056	0.004					69	86	19	68
McGowan	71W	Weld	0.12	1.58	0.011	0.011	0.54	0.12	0.63	0.45	0.046	0.005					68	87	19	68
Iwadata	A508 Cl. 3	Forging	0.21	1.36	0.009	0.004	0.29	0.19	0.64	0.52		<0.01					70	92	27	70

Table 5-6 (cont) Strength and composition of steels in the fracture toughness database

Author	Material ID	Product Form	C	Mn	P	S	Si	Cr	Ni	Mo	Cu	V	Co	Al	As	Sn	$\sigma_{ys}$ [ksi]	$\sigma_{UTS}$ [ksi]	% Elongation	% RA
<b>Non-RPV Steels</b>																				
Iwadata	A470 Cl. 6	Forging	0.23	0.3	0.009	0.011	0.05	1.81	3.79	0.44		0.13					111	126	18	65
Sorem	A36	Plate	0.2	1.11	0.007	0.023	0.029										36	67	38	67
<b>Irradiated RPV Steels</b>																				
Lidbury	A508 Cl. 3	Forging	Not Reported																	
McCabe	72W	Weld	Same as 72W Un-Irradiated														89	105	21	
McCabe	73W	Weld	Same as 73W Un-Irradiated														95	108	19	
McCabe	Midland WF70 Beltline	Weld	Same as Midland WF70 Beltline Not Reported																	
McCabe	Midland WF70 Beltline	Weld	Same as Midland WF70 Beltline Un- Irradiated Not Reported																	
McCabe	Midland WF70 Nozzle	Weld	Same as Midland WF70 Nozzle Un-Irradiated Not Reported																	
McGowan	HSST-02	Plate	Same as HSST-02 Un-Irradiated														89	109	17	57
McGowan	68W	Weld	Same as 68W Un-Irradiated														82	94	16	71
McGowan	69W	Weld	Same as 69W Un-Irradiated														103	114	16	65
McGowan	70W	Weld	Same as 70W Un-Irradiated														77	94	19	65
McGowan	71W	Weld	Same as 71W Un-Irradiated														78	94	19	62

Table 5-7  $T_o$  Weibull slope values calculated from the fracture toughness database

Author	Material ID	B [ln]	W/B	Test Temperature [°F]	$K_{Ic}$ Test Specimen Counts				ASTM E1921-98 $T_o$ Calculation					Weibull Slope Calculations				
					Total	E1921-98 Valid	Required by E1921-98	# Having $M$ Below 50	$K_{Ic}$ [ksi $\sqrt{in}^{0.5}$ ]	$K_{IcMedian}$ [ksi $\sqrt{in}^{0.5}$ ]	$T_o$ [°F]	$\sigma$ [°F]	Maximum Likelihood $T_o$ [°F]	Best Fit Slope	R <sup>2</sup> on Slope	T statistic on Slope	99% Significance	
<b>Un-Irradiated RPV Steels</b>																		
Marston	HSST-02	2	2	-50	7	7	7	0	74	69	-9.8	12.8	-17	11.58	0.72	3.58	No	
Nanstad	72W	1	2	-112	6	6	6	0	83	77	-88.6	13.2	-70	2.38	0.94	8.16	Yes	
Nanstad	72W	1	2	-58	6	6	6	0	108	100	-71.0	13.2	-70	8.13	0.81	4.07	Yes	
Nanstad	73W	1	2	-112	9	9	7	0	79	73	-81.6	11.3	-78	3.49	0.88	7.13	Yes	
Nanstad	73W	1	2	-58	6	6	6	0	108	100	-70.7	13.2	-78	4.25	0.87	5.15	Yes	
Nanstad	73W	1	2	5	8	7	6	2	212	195	-88.7	12.2	-78	6.39	0.96	11.32	Yes	
Alexander	A508 Cl. 2	1	2	-0.4	10	10	6	0	87	81	15.4	10.2	-2	2.73	0.95	13.00	Yes	
McCabe	A533B Cl. 1 (13A)	0.5	2	-103	20	20	6	3	105	97	-112.2	7.2	-109	4.52	0.87	11.11	Yes	
McCabe	A533B Cl. 1 (13A)	1	2	-103	26	26	6	0	109	101	-116.7	6.4	-109	2.31	0.97	27.74	Yes	
McCabe	A533B Cl. 1 (13A)	2	2	-103	12	12	6	0	116	108	-125.0	9.4	-109	3.54	0.97	16.75	Yes	
McCabe	A533B Cl. 1 (13A)	4	2	-103	6	6	6	0	113	105	-122.1	13.2	-109	3.12	0.97	10.90	Yes	
Ingham	A533B Cl. 1	0.98	1	-92.2	12	10	6	7	175	161	-162.7	10.2	-159	4.33	0.96	14.29	Yes	
Ingham	A533B Cl. 1	1.97	1	-58	12	12	6	2	226	208	-156.7	9.4	-159	3.18	0.97	17.96	Yes	
Ingham	A533B Cl. 1	3.94	1	-59.8	6	6	6	0	189	174	-133.9	13.2	-159	4.31	0.98	15.04	Yes	
Ingham	A533B Cl. 1	3.94	1	14	9	7	6	4	468	429	-160.6	12.2	-159	3.13	0.92	7.53	Yes	
Ingham	A533B Cl. 1	9.06	1	14	6	6	6	0	354	325	-132.1	13.2	-159	3.41	0.95	9.19	Yes	
VanDerSluys	A508 Cl. 3	1	2	-148	50	50	6	0	108	99	-158.9	4.6	-157	4.22	0.98	49.91	Yes	
VanDerSluys	A508 Cl. 3	1	2	-103	55	55	6	0	144	133	-150.9	4.4	-157	5.45	0.95	30.87	Yes	
VanDerSluys	A508 Cl. 3	1	2	-58	50	38	6	28	220	203	-154.0	5.3	-157	3.63	0.92	20.92	Yes	
Morland	A533B Cl. 1	0.49	2	-94	12	9	6	6	159	147	-153.9	10.8	-149	3.27	0.92	9.25	Yes	
Morland	A533B Cl. 1	0.49	2	-130	6	6	6	0	95	88	-125.4	13.2	-149	4.87	0.96	9.42	Yes	
Morland	A533B Cl. 1	0.49	2	-94	10	7	6	5	162	149	-155.8	12.2	-149	3.95	0.92	7.47	Yes	
Morland	A533B Cl. 1	0.98	2	-94	10	10	6	0	125	116	-125.2	10.2	-149	4.31	0.99	26.05	Yes	
Morland	A533B Cl. 1	0.98	2	-94	8	8	6	0	178	164	-166.2	11.5	-149	3.35	0.97	13.56	Yes	
Morland	A533B Cl. 1	0.98	2	-94	10	10	6	1	168	155	-159.8	10.2	-149	3.59	0.79	5.41	Yes	
McCabe 94	Midland WF70 Beltline	0.5	2	-58	6	6	6	1	110	102	-73.4	13.2	-71	4.24	0.97	12.30	Yes	
McCabe 94	Midland WF70 Beltline	1	2	-13	7	7	6	1	174	160	-82.6	12.2	-71	3.05	0.65	3.04	No	
McCabe 94	Midland WF70 Beltline	1	2	-58	6	6	6	0	95	89	-54.4	13.2	-71	3.50	0.96	9.32	Yes	
McCabe 94	Midland WF70 Nozzle	0.5	2	-58	7	7	6	0	84	79	-37.7	12.2	-34	2.69	0.97	13.23	Yes	
McCabe 94	Midland WF70 Nozzle	1	2	-13	8	8	6	0	105	98	-22.6	11.5	-34	4.47	0.90	7.46	Yes	

Table 5-7 (cont)  $T_o$  Weibull slope values calculated from the fracture toughness database

Author	Material ID	B [in]	W/B	Test Temperature [°F]	$K_{Ic}$ Test Specimen Counts				ASTM E1921-98 $T_o$ Calculation					Weibull Slope Calculations			
					Total	E1921-98 Valid	Required by E1921-98	# Hoving # Below 50	$K_{Ic}$ [ksi $\sqrt{\text{in}}^{0.5}$ ]	$K_{Ic,Median}$ [ksi $\sqrt{\text{in}}^{0.5}$ ]	$T_o$ [°F]	$\sigma$ [°F]	Maximum Likelihood $T_o$ [°F]	Best Fit Slope	$R^2$ on Slope	T statistic on Slope	99% Significance
Lidbury	A508	3.15	1	5	20	16	6	18	440	403	-163.3	8.1	-159.4	11.49	0.95	16.73	Yes
Lidbury	A508	3.15	1	-22	10	10	6	0	294	270	-148.9	10.2	-159.4	4.97	0.93	10.68	Yes
Lidbury	A508	3.15	1	-49	11	11	6	0	216	199	-142.9	9.8	-159.4	4.23	0.91	9.73	Yes
Lidbury	A508	3.15	1	-85	8	8	6	0	166	153	-149.7	11.5	-159.4	3.05	0.94	9.55	Yes
Lidbury	A508	7.87	1	5	8	8	6	0	347	318	-139.1	11.5	-159.4	2.71	0.94	9.85	Yes
Iwadate	A508	0.5	2	-148	7	7	7	0	68	62	-90.7	12.8	-46.42	4.36	0.84	5.15	Yes
Iwadate	A508	0.5	2	-76	30	30	7	0	78	73	-44.7	6.2	-46.42	4.42	0.97	29.74	Yes
Iwadate	A508	1	2	-76	8	8	7	0	79	74	-45.9	12.0	-48.42	4.40	0.92	8.43	Yes
Iwadate	A508	0.5	2	-4	13	13	6	3	105	97	-13.1	9.0	-46.42	6.74	0.97	18.57	Yes
Iwadate	A508	0.5	2	-4	27	21	6	14	128	119	-38.3	7.1	-46.42	4.65	0.96	22.52	Yes
Iwadate	A508	1	2	-4	12	12	6	0	123	113	-32.6	9.4	-46.42	8.22	0.93	11.22	Yes
Iwadate	A508	1	2	-4	12	12	6	0	121	112	-30.7	9.4	-46.42	6.43	0.85	7.44	Yes
Iwadate	A508	2	2	-4	6	6	6	0	146	135	-54.1	13.2	-46.42	5.21	0.86	4.88	Yes
Iwadate	A508	1	2	14	10	10	6	4	180	166	-59.9	10.2	-46.42	5.54	0.97	15.16	Yes
Non-RPV Steels																	
Iwadate	A470	0.5	2	-148	28	28	6	0	82	77	-124.0	6.1	-116.04	3.56	0.95	21.78	Yes
Iwadate	A470	3	2	-148	7	7	6	0	92	65	-139.0	12.2	-116.04	2.80	0.92	7.51	Yes
Iwadate	A470	0.5	2	-76	8	8	6	0	114	105	-95.5	11.5	-116.04	3.58	0.95	10.29	Yes
Iwadate	A470	0.5	2	-76	27	26	6	3	126	118	-107.7	6.4	-118.04	4.07	0.92	16.65	Yes
Iwadate	A470	1	2	-76	8	8	6	0	130	121	-112.3	11.5	-118.04	5.02	0.83	5.43	Yes
Iwadate	A470	1	2	-76	8	8	6	0	130	120	-111.9	11.5	-116.04	4.97	0.97	12.99	Yes
Sorem	A36	0.5	1	-105	16	16	7	5	74	69	-65.9	8.5	-67.55	6.86	0.92	12.96	Yes
Sorem	A36	1.25	1	-45	8	8	6	0	105	97	-53.8	11.5	-67.55	5.46	0.96	11.78	Yes
Sorem	A36	1.25	1	-18	8	8	6	6	138	127	-60.7	11.5	-67.55	10.71	0.99	20.13	Yes
Sorem	A36	0.49	2	-105	14	14	7	1	73	68	-63.3	9.0	-67.55	3.67	0.82	7.29	Yes
Sorem	A36	1.25	2	-105	8	8	7	0	66	62	-47.3	12.0	-67.55	8.57	0.97	14.08	Yes
Sorem	A36	0.49	2	-45	17	12	6	9	116	107	-88.9	9.4	-67.55	3.65	0.99	25.65	Yes
Sorem	A36	1.25	2	-45	7	7	7	0	81	75	-18.2	12.8	-67.55	7.96	0.91	7.19	Yes
Sorem	A36	1.25	2	0	22	9	6	17	168	155	-66.2	10.8	-67.55	7.47	0.96	13.67	Yes
Irradiated RPV Steels																	
Nanstad 92	72W	1	2	185	9	9	6	1	180	166	111.4	10.8	85	4.21	0.91	8.52	Yes
Nanstad 92	72W	1	2	203	6	6	6	0	188	173	124.3	13.2	85	9.29	0.81	4.19	Yes
Nanstad 92	72W	2	2	185	6	6	6	0	215	197	91.8	13.2	85	3.86	0.96	9.81	Yes
Nanstad 92	72W	2	2	208	6	6	6	0	217	199	108.9	13.2	85	3.87	0.96	9.50	Yes
Nanstad 92	73W	1	2	185	10	10	6	0	173	159	115.7	10.2	99	3.67	0.92	9.30	Yes
Nanstad 92	73W	2	2	203	10	10	6	0	202	186	116.3	10.2	99	3.54	0.95	12.62	Yes
Nanstad 97	Midland WF70 Nozzle	1	2	167	6	6	6	0	122	113	138.9	13.2	135	2.95	0.93	7.27	Yes

Table 5-7 (cont)  $T_0$  Weibull slope values calculated from the fracture toughness database

Author	Material ID	B [in]	W/B	Test Temperature [°F]	$K_{IC}$ Test Specimen Counts				ASTM E1921-98 $T_0$ Calculation					Weibull Slope Calculations			
					Total	E1921-98 Valid	Required by E1921-98	# Having $M$ Below 50	$K_{IC}$ [ksi $\sqrt{\text{in}}^{0.5}$ ]	$K_{IC, \text{Median}}$ [ksi $\sqrt{\text{in}}^{0.5}$ ]	$T_0$ [°F]	$\sigma$ [°F]	Maximum Likelihood $T_0$ [°F]	Best Fit Slope	$R^2$ on Slope	T statistic on Slope	99% Significance
Nanstad 97	Midland WF70 Nozzle	0.5	2	149	6	6	6	0	94	88	154.1	13.2	135	10.12	0.91	6.32	Yes
Nanstad 97	Midland WF70 Nozzle	1	2	113	7	7	8	0	82	76	137.4	12.2	135	4.92	0.93	8.23	Yes
Nanstad 97	Midland WF70 Nozzle	0.394	1	77	9	9	7	0	76	71	113.4	11.3	135	6.47	0.94	10.70	Yes
Nanstad 97	Midland WF70 Beltline	0.5	2	68	6	6	6	0	88	82	82.7	13.2	88	2.78	0.93	7.06	Yes
Nanstad 97	Midland WF70 Beltline	1	2	95	6	6	8	0	102	95	89.5	13.2	88	3.65	0.93	7.03	Yes
Nanstad 97	Midland WF70 Beltline	0.394	1	71.6	10	6	6	3	93	88	78.9	11.5	88	3.30	0.91	7.94	Yes
Nanstad 97	Midland WF70 Beltline	0.394	1	32	8	8	8	0	81	57	104.3	12.8	88	3.44	0.91	7.80	Yes
Nanstad 97	Midland WF70 Beltline	0.394	1	10.4	7	7	7	3	82	76	35.0	12.2	37	2.46	0.88	6.20	Yes
McGowan	HSST-02	1	2	122	10	10	6	0	92	85	130.8	10.2	127	5.50	0.85	4.75	Yes
McGowan	HSST-02	1	2	176	10	10	6	0	147	136	125.5	10.2	127	5.50	0.85	4.75	Yes



Table 5-8 Empirical assessment of the validity of the weakest link prediction of the statistical size effect on fracture toughness data

Author	Material ID	Test Temperature [F]	Thickness Range		No. of Data	Mean $K_{Jc/IT}$ [ksi*in <sup>0.5</sup> ]	Slope Fit to $K_{Jc/IT}$ vs. Thickness				
			Min. [in]	Max. [in]			Value [ksi*in <sup>0.5</sup> /in]	R <sup>2</sup>	T statistic	99% Significance	
<b>Un-Irradiated RPV Steels</b>											
Marston	HSST-02	0	2	10	7	105.2	5.0	0.535	2.398	-	
Nanstad	72W	-58	1	4	13	104.2	0.7	0.002	0.150	-	
Nanstad	72W	-22	1	4	9	141.2	8.1	0.109	0.924	-	
Nanstad	72W	5	1	4	9	128.8	13.9	0.139	1.062	-	
Nanstad	72W	50	2	8	11	243.4	4.2	0.034	0.563	-	
Nanstad	73W	-58	1	4	13	105.9	0.5	0.001	0.082	-	
Nanstad	73W	-22	1	4	11	145.0	12.3	0.335	2.130	-	
Nanstad	73W	5	1	4	15	177.7	-14.0	0.197	-1.784	-	
Nanstad	73W	23	2	8	10	231.0	11.7	0.440	2.507	-	
Alexander	A508 Cl. 2	-0.4	1	4	19	85.3	-1.3	0.004	-0.254	-	
McCabe	A533B Cl.1 (13A)	-103	0.5	4	64	98.2	3.2	0.015	0.976	-	
McCabe	A533B Cl.1 (13A)	-238	0.5	2	46	38.8	7.1	0.300	4.348	Yes	
Ingham	A533B Cl. 1	-95	0.394	1	10	137.4	113.7	0.683	4.150	Yes	
Ingham	A533B Cl. 1	-60	1	4	20	191.3	-3.6	0.005	-0.310	-	
Ingham	A533B Cl. 1	15	1	9	13	344.2	-3.8	0.013	-0.385	-	
Ingham	A533B Cl. 1	50	3	8	6	598.5	31.5	0.197	0.992	-	
McCabe 94	Midland WF70 Beltline	-58	0.5	2	17	100.2	5.2	0.033	0.712	-	
McCabe 94	Midland WF70 Beltline	-13	0.5	4	17	142.2	0.9	0.001	0.097	-	
McCabe 94	Midland WF70 Beltline	32	1	2	5	204.6	74.2	0.349	1.268	-	
McCabe 94	Midland WF70 Nozzle	-58	0.5	1	13	70.1	-19.4	0.082	-0.994	-	
Lidbury	A508	-49	3	8	15	189.9	-5.9	0.090	-1.130	-	
Lidbury	A508	5	3	8	24	367.4	-17.7	0.300	-3.100	Yes	
Iwadata	A508	-148	0.5	1	12	61.3	-12.7	0.160	0.190	-	
Iwadata	A508	-76	0.5	4	39	73.4	2.6	0.010	0.666	-	
Iwadata	A508	-4	0.75	4	36	119.2	6.3	0.050	1.340	-	
<b>Non-RPV Steels</b>											
Sorem	A36	-320	0.5	1.25	14	31.8	6.1	0.200	1.730	-	
Sorem	A36	-170	0.5	1.25	20	52.8	3.9	0.016	0.540	-	
Sorem	A36	-105	0.5	1.25	44	67.8	-4.0	0.018	-0.880	-	
Sorem	A36	-45	0.5	1.25	26	89.7	2.2	0.003	0.269	-	
Sorem	A36	0	0.5	1.25	9	111.7	0.4	0.000	0.054	-	
Iwadata	A470	-320	1	3	3	29.0	3.5	0.671	1.429	-	

**Table 5-8 (cont) Empirical assessment of the validity of the weakest link prediction of the statistical size effect on fracture toughness data**

Author	Material ID	Test Temperature [F]	Thickness Range		No. of Data	Mean $K_{Jc/IT}$ [ksi*in <sup>0.5</sup> ]	Slope Fit to $K_{Jc/IT}$ vs. Thickness			
			Min. [in]	Max. [in]			Value [ksi*in <sup>0.5</sup> /in]	R <sup>2</sup>	T statistic	99% Significance
Iwadata	A470	-148	0.5	3	39	78.4	1.3	0.006	0.457	-
Iwadata	A470	-103	1	4	7	97.8	10.0	0.620	2.860	-
Iwadata	A470	-76	0.375	4	61	116.7	16.8	0.260	4.560	Yes
Iwadata	A470	-49	1	4	4	149.8	-17.6	0.690	-2.090	-
Iwadata	A470	-22	1	4	5	154.2	-7.1	0.129	-0.670	-
<b>Irradiated RPV Steels</b>										
Nanstad 92	72W	122	1	4	12	125.7	-1.4	0.003	-0.175	-
Nanstad 92	72W	167	1	4	10	189.4	2.5	0.002	0.135	-
Nanstad 92	72W	185	1	4	19	181.1	13.9	0.137	1.646	-
Nanstad 92	72W	203	1	4	18	213.9	20.3	0.169	1.804	-
Nanstad 92	73W	122	1	4	9	125.2	-1.7	0.006	-0.208	-
Nanstad 92	73W	185	1	4	18	166.1	4.0	0.009	0.391	-
Nanstad 97	Midland WF70 Beltline	70	0.394	0.5	16	78.4	1.1	0.000	0.010	-
<b># of Data Groupings</b>										
<b># of <math>K_{Jc}</math> Values</b>										
		<b>Total</b>	<b>Fit Well</b>	<b>%</b>	<b>Total</b>	<b>Fit Well</b>	<b>%</b>			
<b>Un-Irradiated RPV Steels</b>		25	22	88%	454	386	85%			
<b>Non-RPV Steels</b>		11	10	91%	232	171	74%			
<b>Irradiated RPV Steels</b>		7	7	100%	102	102	100%			
<b>Total</b>		43	39	91%	788	659	84%			

Table 5-9 Empirical Assessment of the Validity of a Universal Shape for the Master Curve

Author	Material ID	Product Form	T <sub>0</sub> [°F]	T-T <sub>0</sub> Range		On All Data							Notes
				Min [°F]	Max [°F]	No. of Data	Intercept	T on Intercept	Slope	T on Slope	Intercept 99% Significant?	Slope 99% Significance	
Un-Irradiated RPV Steels													
Marston	A508 Cl. 2	Forging	-60	-90	60	9	-12.710	-1.221	-0.193	-1.268	-	-	
Marston	A508 Cl. 2	Forging	-55	-120	41	10	-1.637	-0.481	-0.051	-1.278	-	-	
Marston	A508 Cl. 2	Forging	-124	-196	24	13	-23.791	-4.674	-0.177	-4.385	Yes	Yes	
Marston	A533B Cl. 1	Plate	-74	-247	77	13	-0.713	-0.084	0.002	0.031	-	-	
Marston	A533B Cl. 1	HAZ	-132	-118	68	6	22.295	1.256	0.204	1.452	-	-	
Marston	A533B Cl. 1	Weld	-57	-264	57	8	14.418	2.913	0.093	2.872	-	-	
Marston	A533B Cl. 1	Weld	-151	-169	-49	10	12.244	1.107	0.144	1.395	-	-	
Marston	HSST-01	Plate	-1	-149	-149	17							Data only at one temperature
Marston	HSST-01	Weld	-105	-70	55	8	-1.582	-0.172	-0.067	-0.290	-	-	
Marston	HSST-02	Plate	-17	-233	67	70	10.588	3.143	0.096	3.270	Yes	Yes	
Marston	HSST-02	Plate	-17	-233	67	65	-2.822	-2.822	-0.020	-1.403	-	-	Data for 10T and 11T eliminated
Marston	HSST-03	Plate	31	-181	-181	9							Data only at one temperature
Nanstad	72W	Weld	-70	-168	138	74	-2.948	-0.424	-0.126	-1.582	-	-	
Nanstad	73W	Weld	-78	-160	119	77	1.583	0.386	0.037	0.700	-	-	
VanDerSluys	A508 Cl. 3	Forging	-157	9	99	155	1.989	0.324	-0.095	-1.005	-	-	
Morland	A533B Cl. 1	Forging	-148	19	163	157	25.428	1.685	-0.455	-3.263	-	Yes	
Morland	A533B Cl. 1	Plate	-149	19	163	153	-4.523	0.317	-0.178	-1.308	-	-	Data at T-T <sub>0</sub> = +199 eliminated
Alexander	A508 Cl. 2	Plate	-2	-97	52	29	-8.166	-1.388	-0.013	-0.102	-	-	
McCabe	A533B Cl. 1 (13A)	Plate	-109	-129	184	121	-11.413	-3.307	-0.138	-3.572	Yes	Yes	
McCabe	A533B Cl. 1 (13A)	Plate				118	-6.104	-1.749	-0.041	-1.206	-	-	Data at T-T <sub>0</sub> = +185 eliminated
Ingham	A533B Cl. 1	Plate	-159	29	227	217	-30.653	-1.868	0.243	2.140	-	-	
McCabe	Midland WF70 Beltline	Weld	-71	-77	103	57	-1.900	-0.378	0.112	1.279	-	-	
McCabe	Midland WF70 Nozzle	Weld	-34	-114	66	32	3.217	0.727	0.150	2.006	-	-	
McGowan	HSST-02	Plate	-8	-140	82	25	9.261	2.445	0.117	2.531	-	-	
McGowan	68W	Weld	-133	-79	111	10	-0.203	-0.016	0.148	0.822	-	-	
McGowan	69W	Weld	5	-153	70	21	-0.528	-0.137	-0.023	-0.521	-	-	
McGowan	70W	Weld	-77	-134	46	10	0.926	0.154	0.011	0.137	-	-	
McGowan	71W	Weld	-41	-98	55	7	1.922	0.167	0.001	0.006	-	-	
Lidbury	A508 Cl. 3	Forging	-159	2	225.2	119	-66.560	-3.380	0.609	4.354	Yes	Yes	
Lidbury	A508 Cl. 3	Forging	-159	2	180	103	-42.520	-2.166	0.346	2.250	-	-	Data above T-T <sub>0</sub> = +180 eliminated
Iwamoto	A508	Forging	-46	-192	60	153	-2.060	-1.050	-0.064	-1.820	-	-	

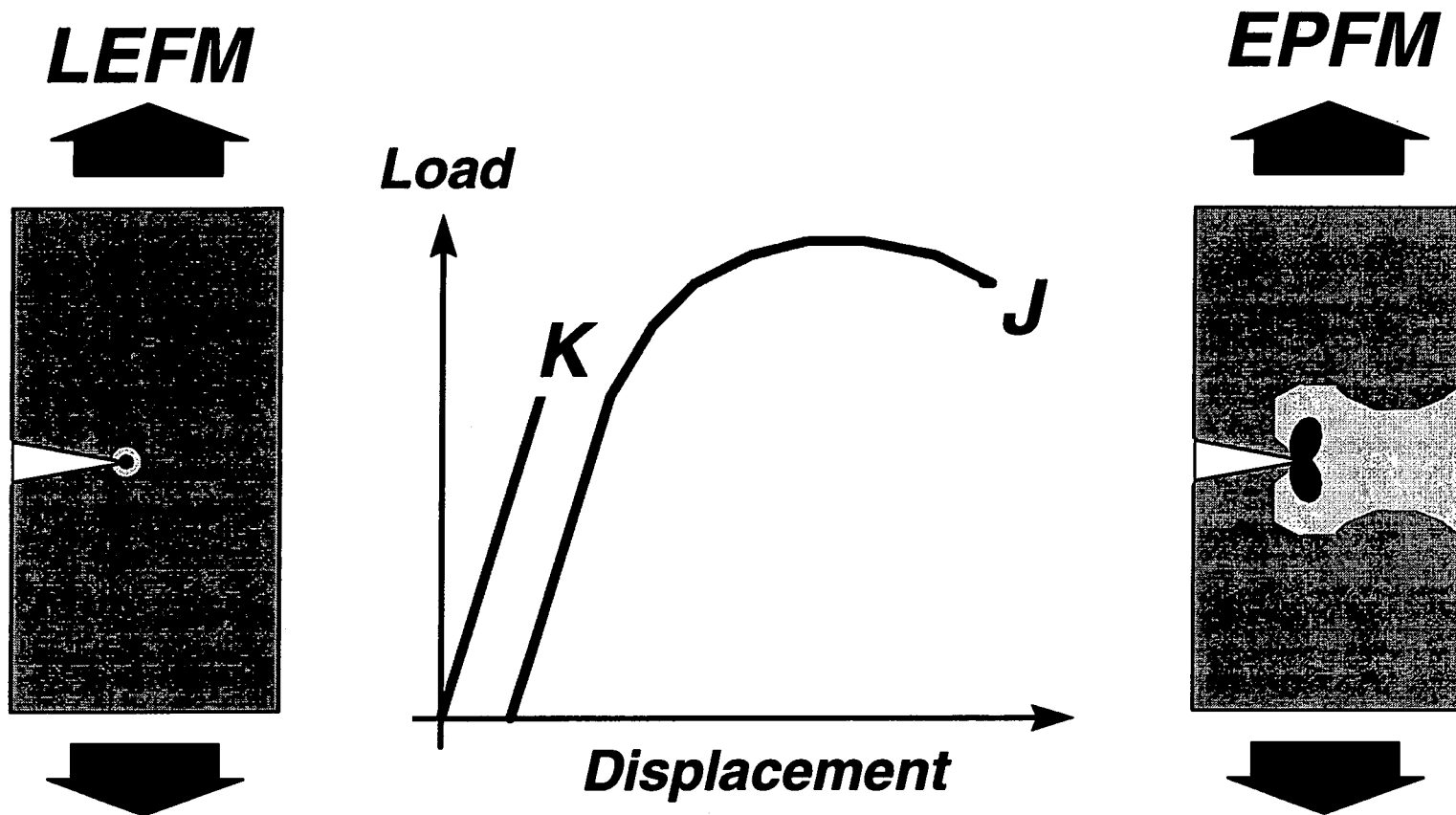
**Table 5-9 (cont) Empirical Assessment of the Validity of a Universal Shape for the Master Curve**

Author	Material ID	Product Form	T <sub>0</sub> [°F]	T-T <sub>0</sub> Range		On All Data							
				Min [°F]	Max [°F]	No. of Data	Intercept	T on Intercept	Slope	T on Slope	Intercept 99% Significant?	Slope 99% Significance	Notes
<b>Non-RPV Steels</b>													
Iwadate	A470	Forging	-116	-204	94	124	-2.680	-1.140	-0.109	-2.510	-	-	
Sorem	A36	Plate	-68	-252	100	176	-7.160	-3.390	-0.069	-2.930	Yes	Yes	
Sorem	A36	Plate	-68	-252	66	173	-5.740	-2.600	-0.052	-2.270	Yes	-	Data at T-T <sub>0</sub> = +100 eliminated
<b>Irradiated RPV Steels</b>													
McCabe	72W	Weld	85	-187	118	70	-0.266	-0.031	-0.201	-2.237	-	-	
McCabe	73W	Weld	99	-202	122	66	-1.994	-0.338	-0.126	-1.875	-	-	
McCabe	Midland WF70 Bellline	Weld	88	-146	106	50	-8.966	-1.812	-0.199	-2.608	-	Yes	
McCabe	Midland WF70 Bellline	Weld	37	-26	-26	7							Data only at one temperature
McCabe	Midland WF70 Nozzle	Weld	135	-57	32	28	-6.267	-1.973	-0.288	-3.456	-	Yes	
McGowan	HSST-02	Plate	127	-140	49	28	-1.115	-0.239	-0.004	-0.060	-	-	
McGowan	68W	Weld	-111	-90	53	15	2.326	0.470	0.085	1.030	-	-	
McGowan	69W	Weld	66	-98	56	16	-1.132	-0.211	-0.048	-0.520	-	-	
McGowan	70W	Weld	-33	-160	38	16	2.592	0.452	0.025	0.380	-	-	
McGowan	71W	Weld	2	-101	30	16	-3.209	-0.621	-0.114	-1.465	-	-	

Individual Data	Total	1,985
	Fit Well by Master Curve	1,894
	% Fit Well	95%
Data Sets	Total	36
	Fit Well by Master Curve	33
	% Fit Well	92%

**Table 5-10 Statistical Assessment of the Effects of Deformation and Test Temperature on ASTM E1921-97  $T_o$  Values**

Variation of $T_o$ Error with	Data Set	Tests on Intercept			Tests on Slope		
		T stat	T (99%)	Signif?	T stat	T (99%)	Signif?
$M_{Minimum}$	All Data	2.74	2.33	Yes	1.15	2.33	No
	Un-Irradiated RPV	0.96	2.33	No	0.36	2.33	No
	Non-RPV	2.11	2.65	No	1.20	2.65	No
	Irradiated RPV	1.45	2.58	No	0.30	2.58	No
Test Temp. - $T_o$	All Data	1.57	2.33	No	1.28	2.33	No
	Un-Irradiated RPV	0.07	2.33	No	1.11	2.33	No
	Non-RPV	1.72	2.65	No	0.60	2.65	No
	Irradiated RPV	1.32	2.58	No	2.66	2.58	Yes



**EPFM characterizes crack tip fields (process zone) to much higher deformation levels than LEFM, enabling rigorous interpretation of data from small specimens.**

Figure 5-1 Schematic Illustration of the Differences Between *LEFM* and *EPFM*

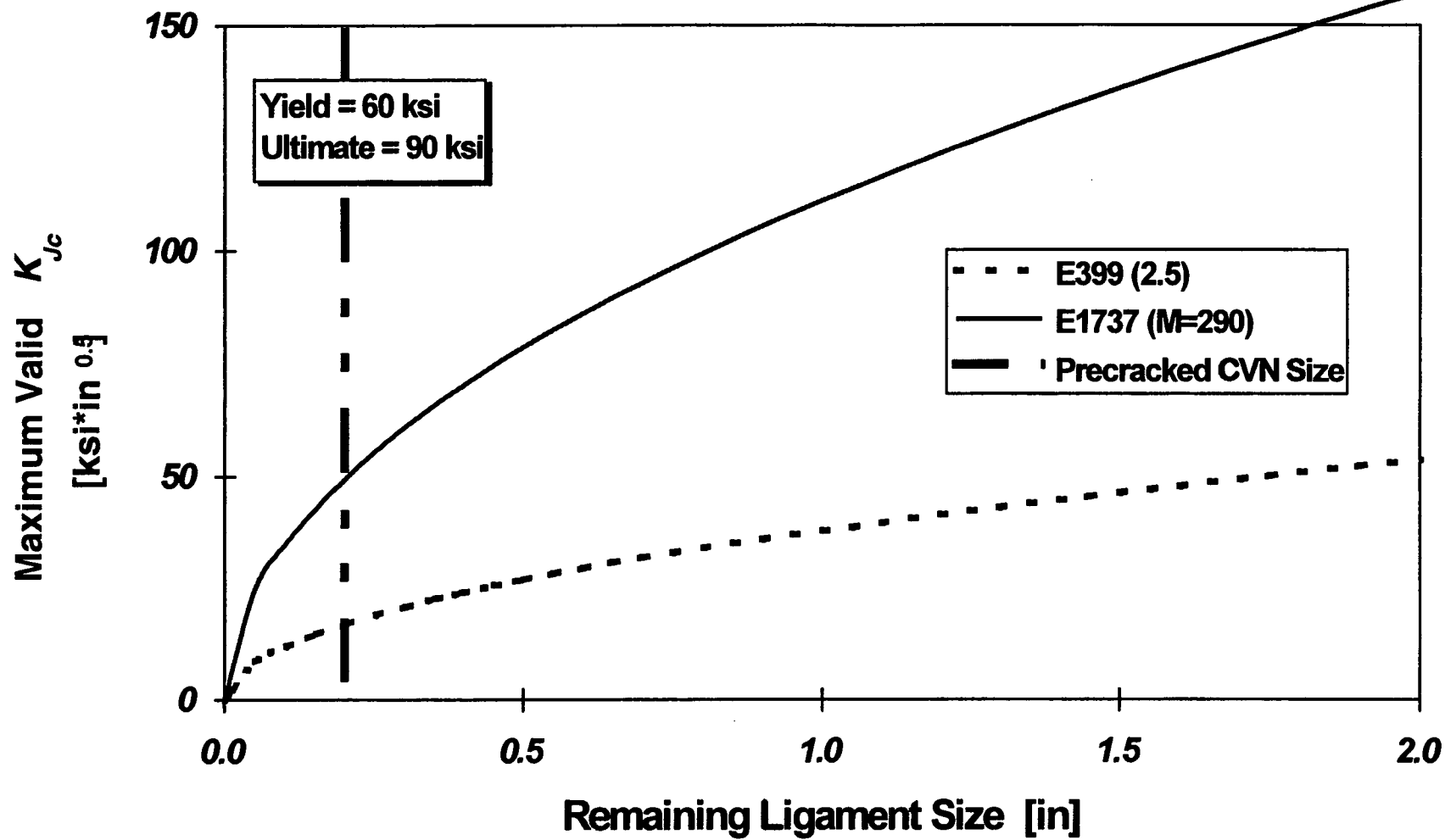


Figure 5-2 A Comparison of Material Independent *LEFM* Size Requirements (the E399 (2.5) curve) and a Conservative *EPFM* Size Requirement (the E1737 ( $M=200$ ) Curve)

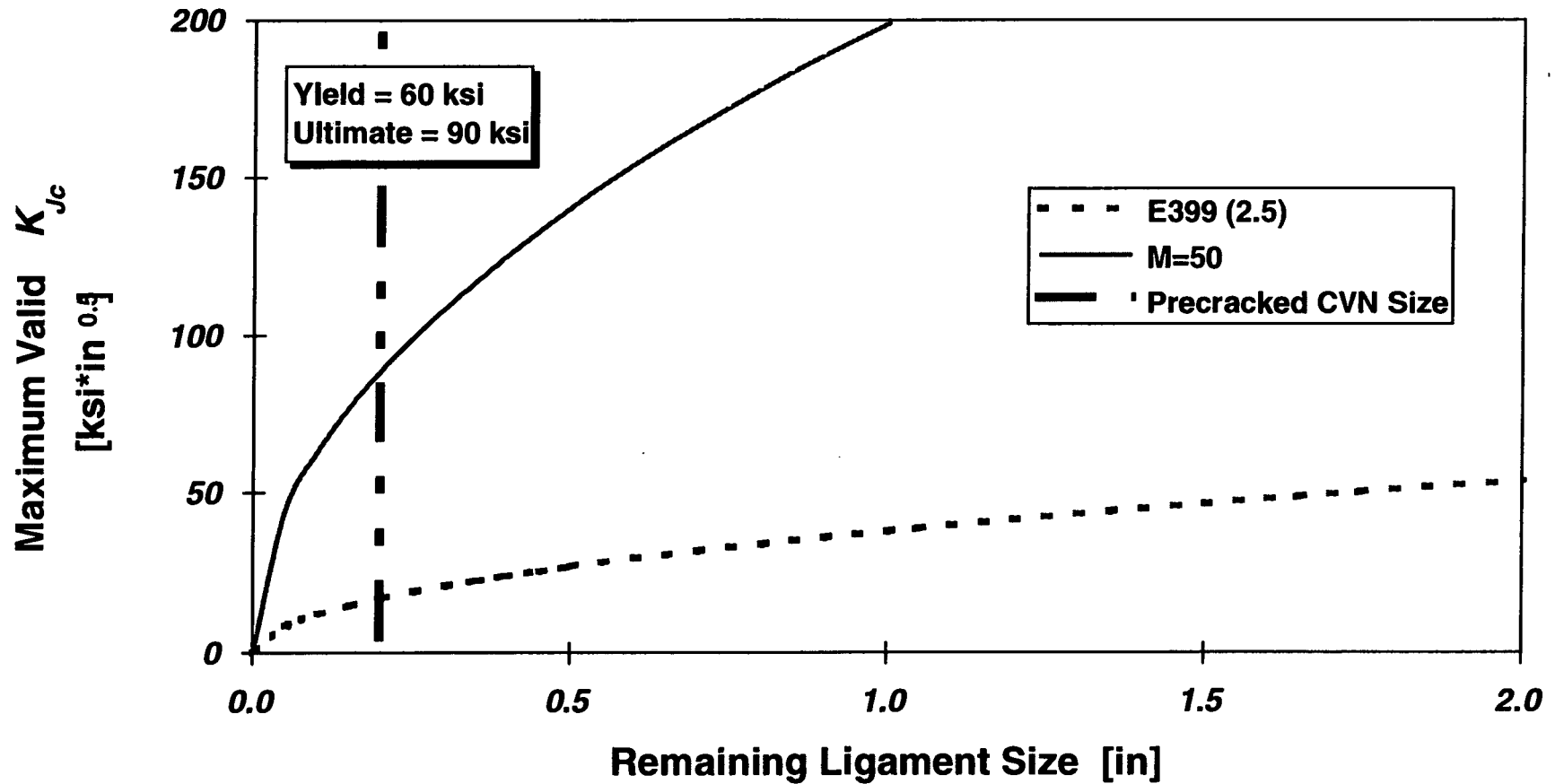
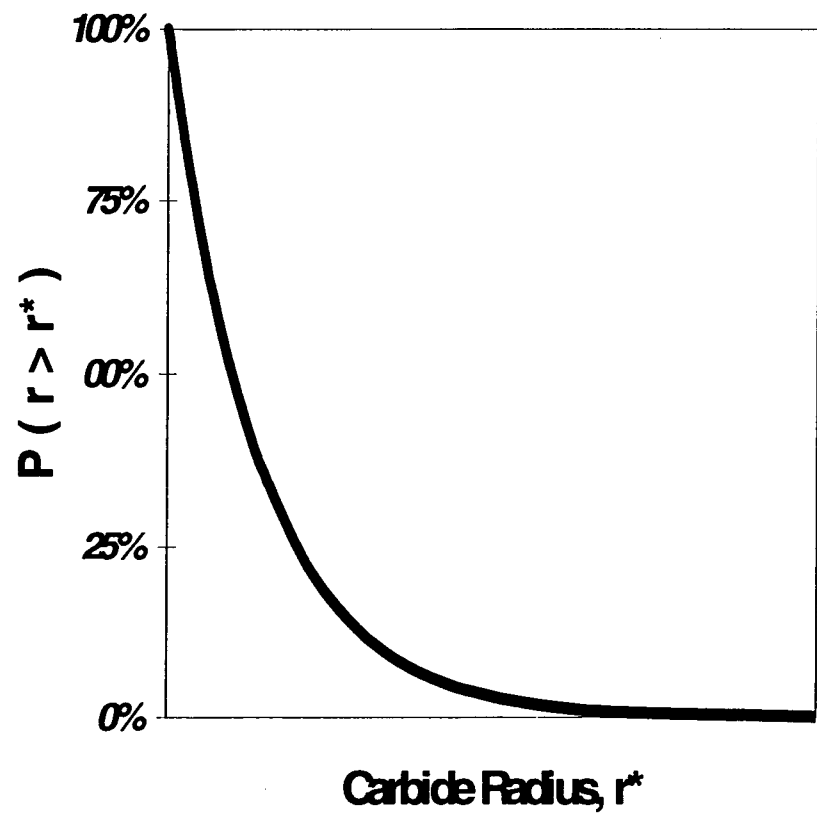
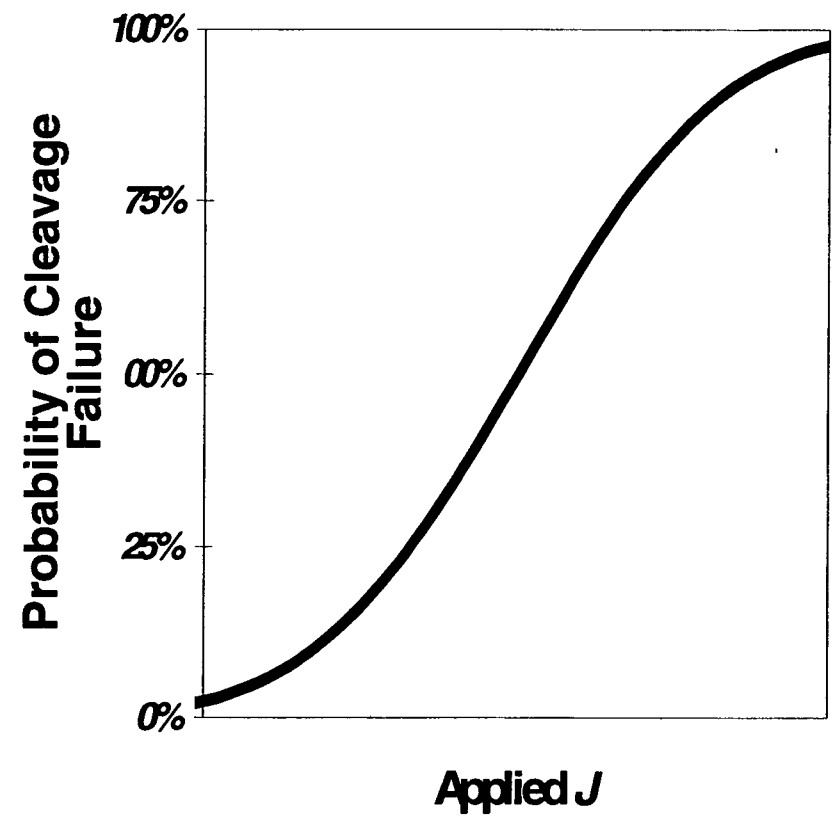


Figure 5-3 A comparison of material independent *LEFM* size requirements (the E399 (2.5) curve) and an *EPFM* size requirements specific to RPV steels (the M=50 curve)





(a)



(b)

Figure 5-4 Probability distribution function for carbide sizes (left), and variation of the probability of cleavage failure with increasing applied-J (right)

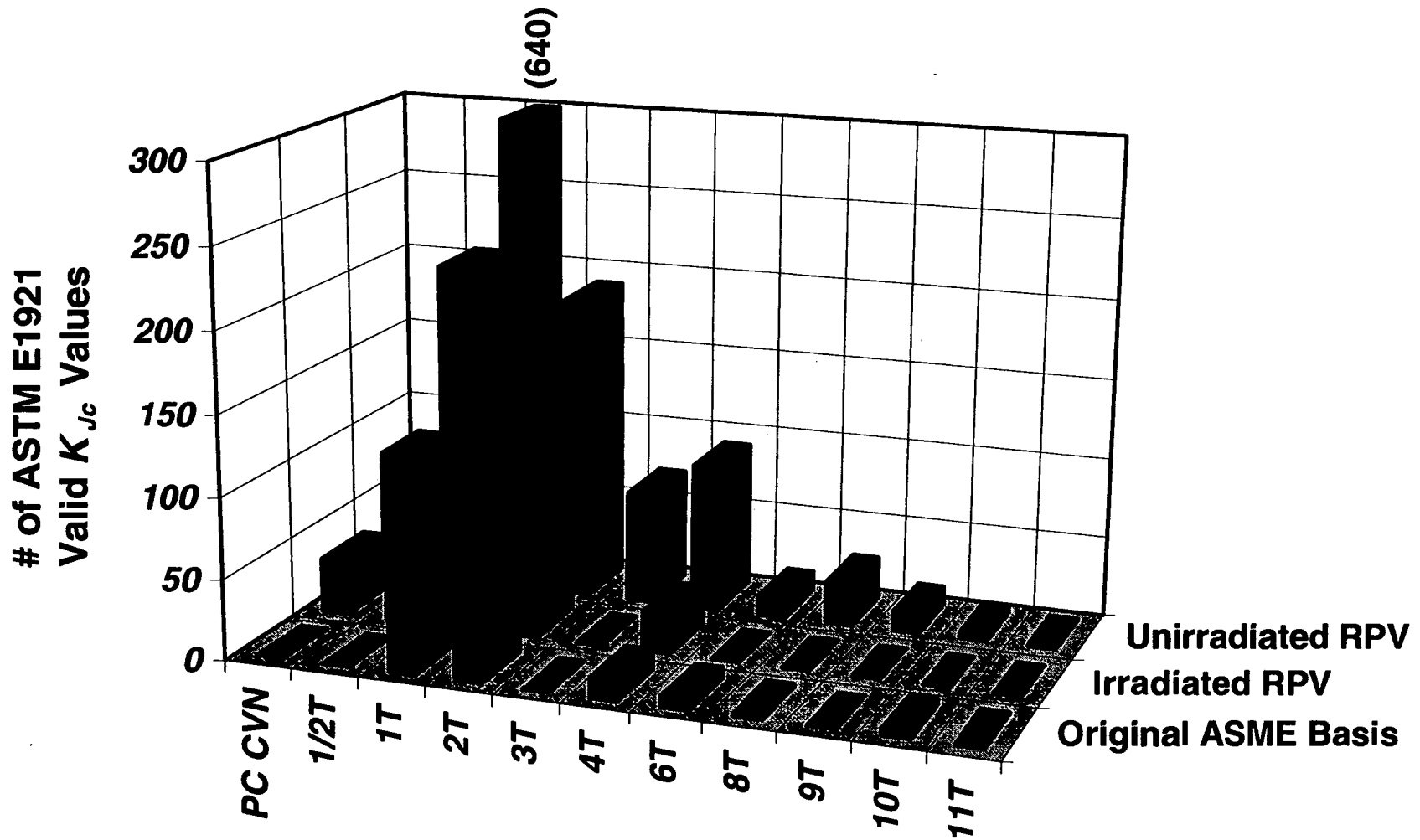


Figure 5-5 Comparison of the amount of quasi-static fracture toughness data that was available to support the  $K_{Jc}$  curve vs. the amount of data available today

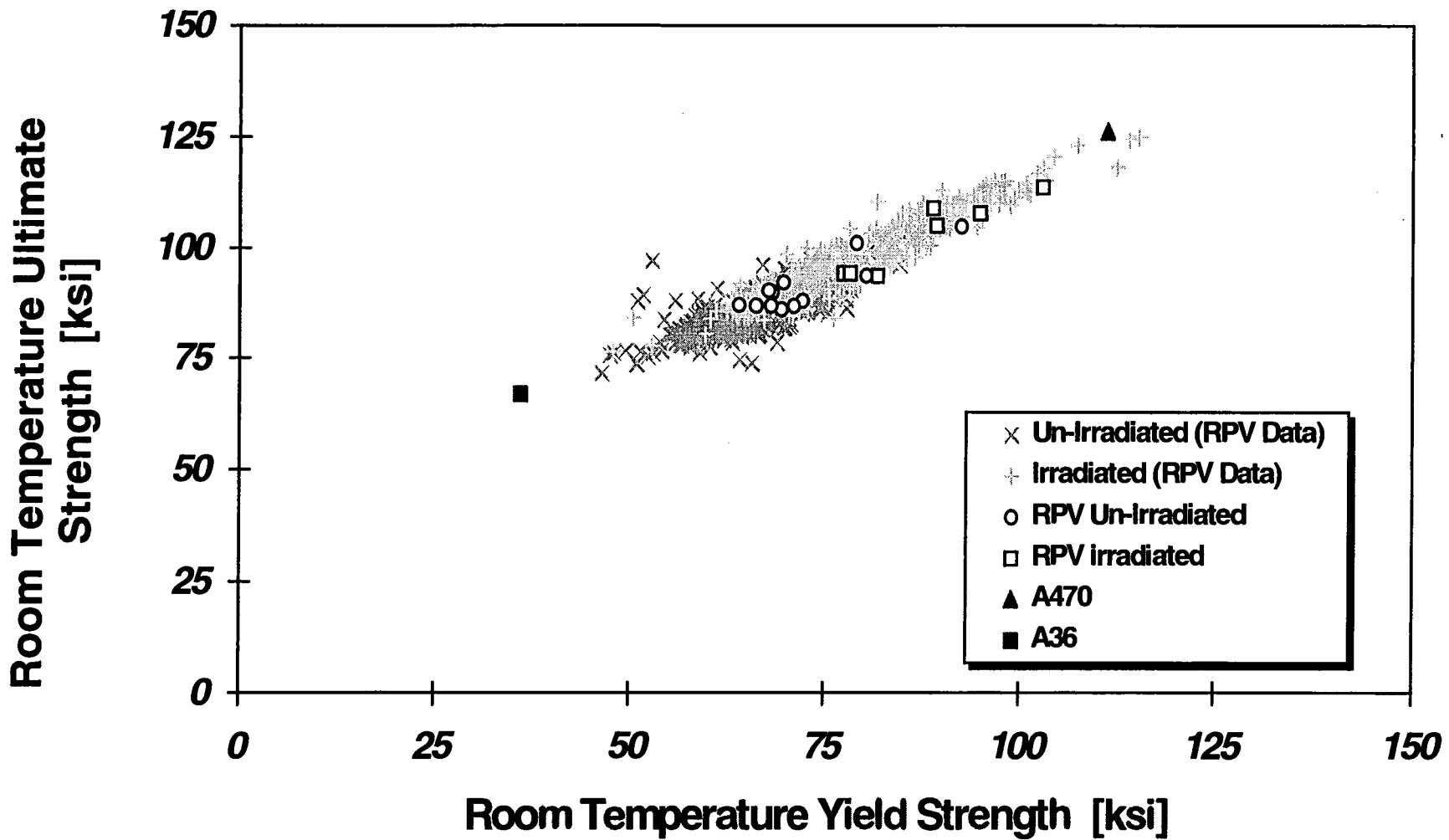


Figure 5-6 Variation of ultimate tensile strength with yield strength for steels in the fracture toughness database (filled and open symbols) compared with those characteristic of the operating nuclear fleet (light plusses and crosses)

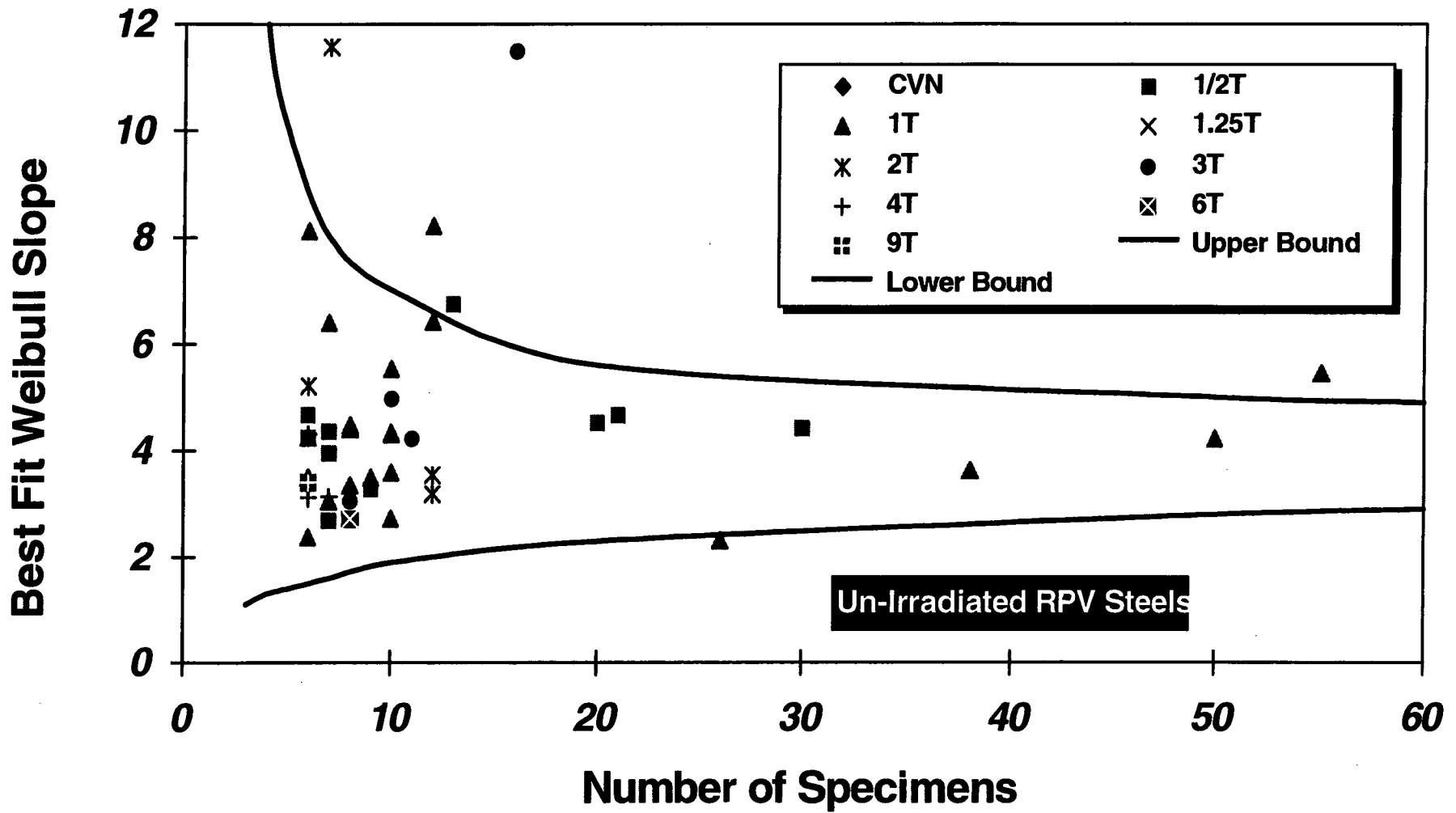


Figure 5-7(a) Best-fit Weibull slope vs. sample size for un-irradiated RPV steels

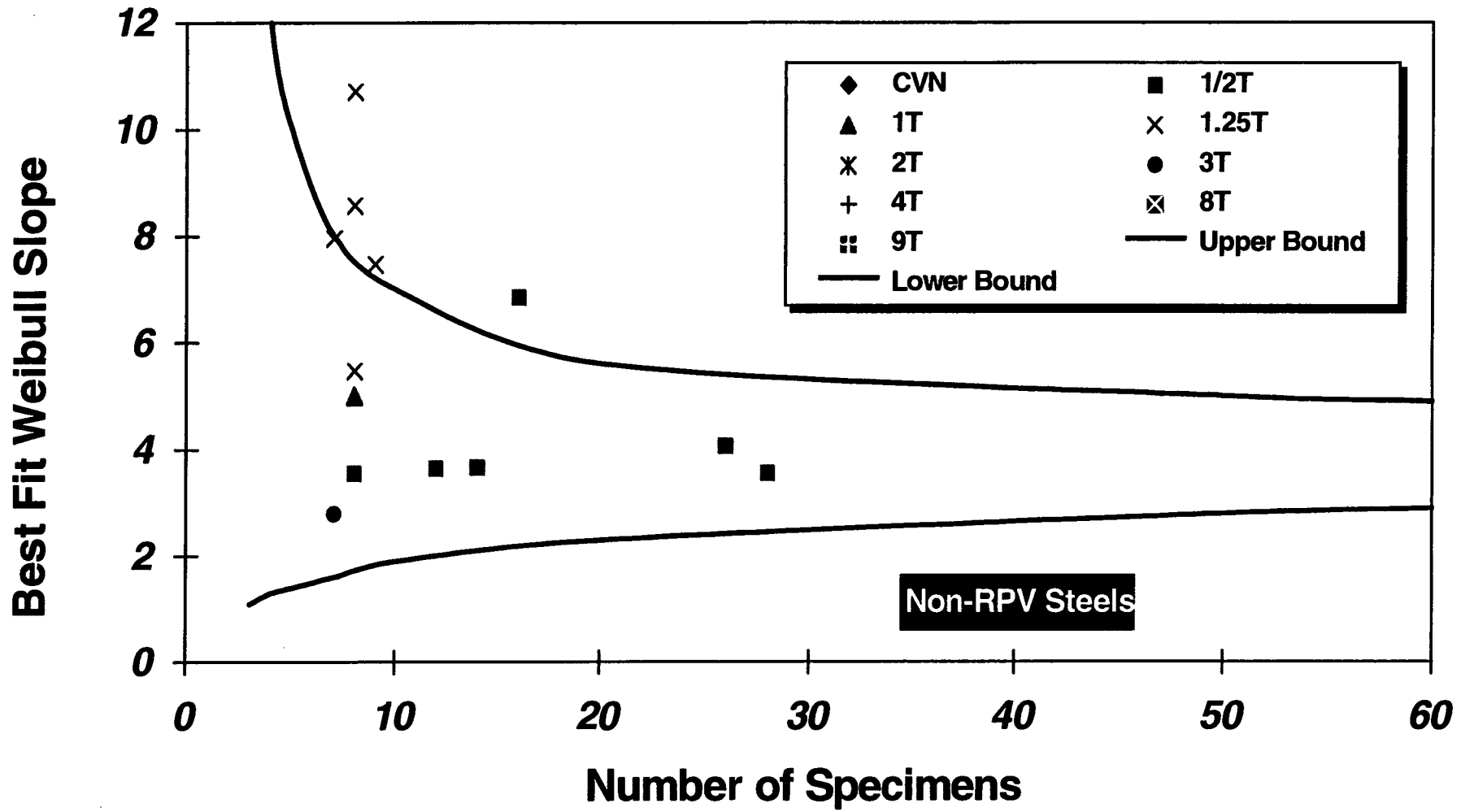


Figure 5-7(b) Best-fit Weibull slope vs. sample size for non-RPV steels

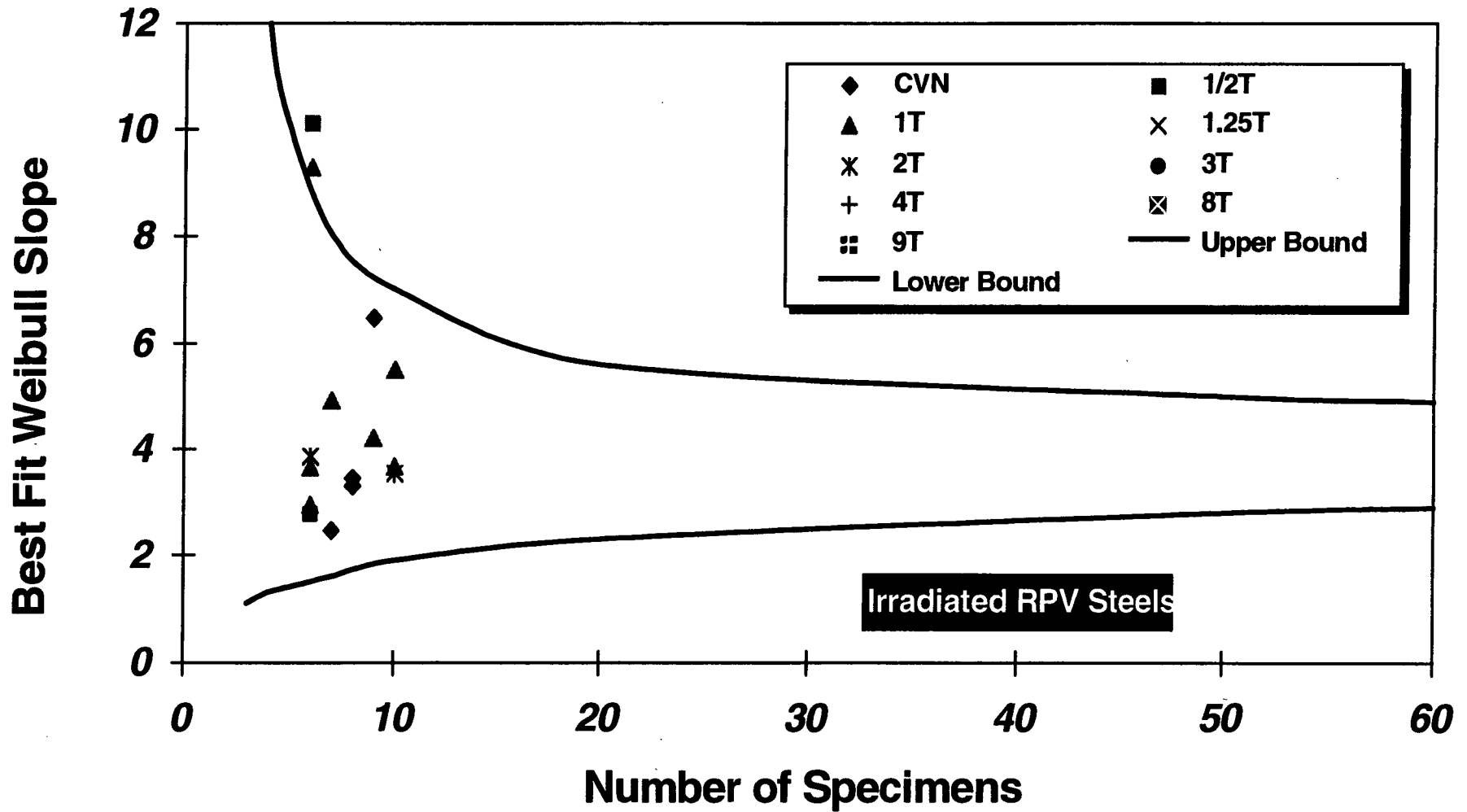


Figure 5-7(c) Best-fit Weibull slope vs. sample size for irradiated RPV steels

### Weld 72W Un-Irradiated at +50F

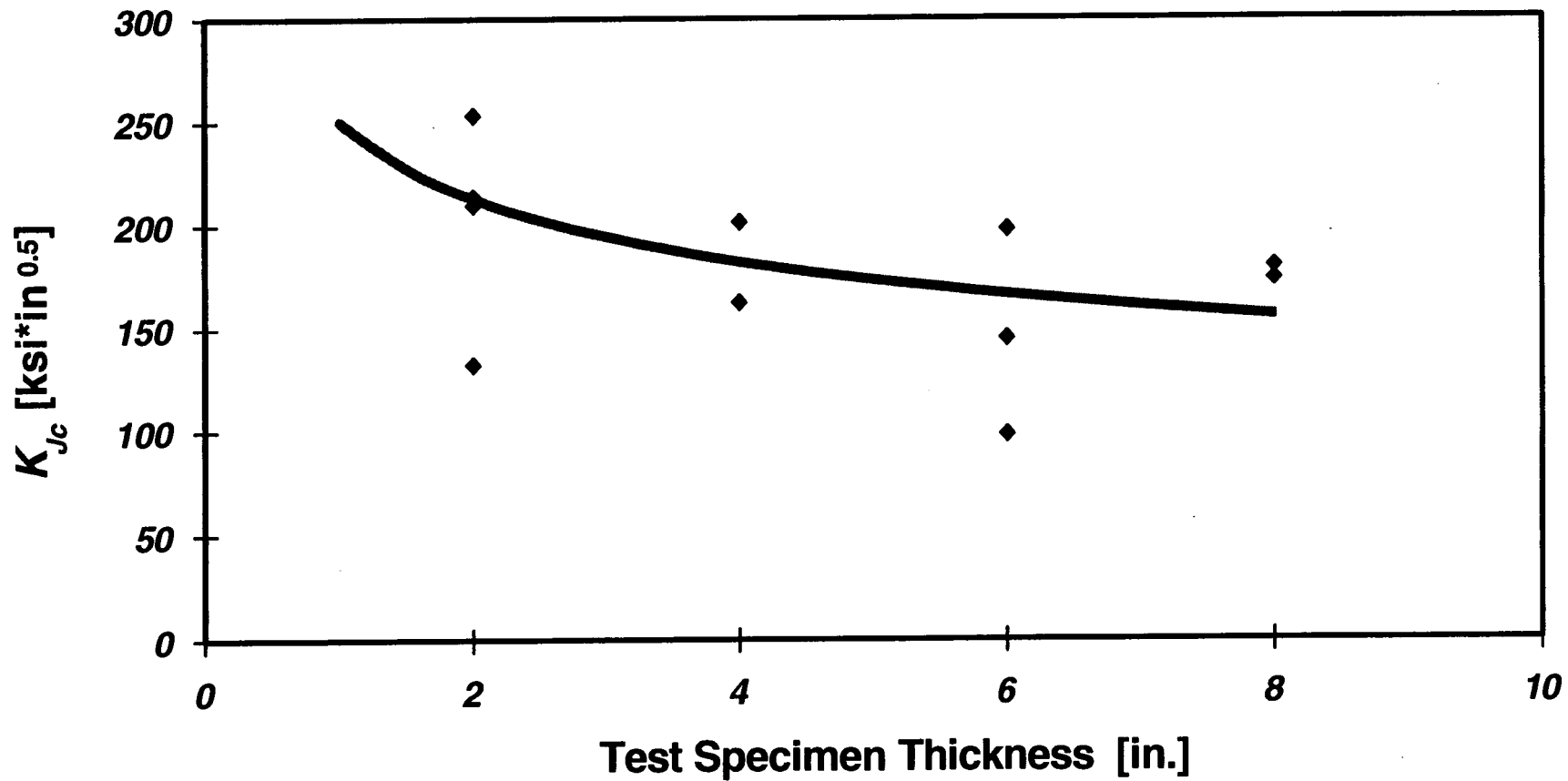


Figure 5-8(a) Measured  $K_{Jc}$  vs. specimen size for an un-irradiated RPV steel

**Weld 72W Irradiated at +203F**

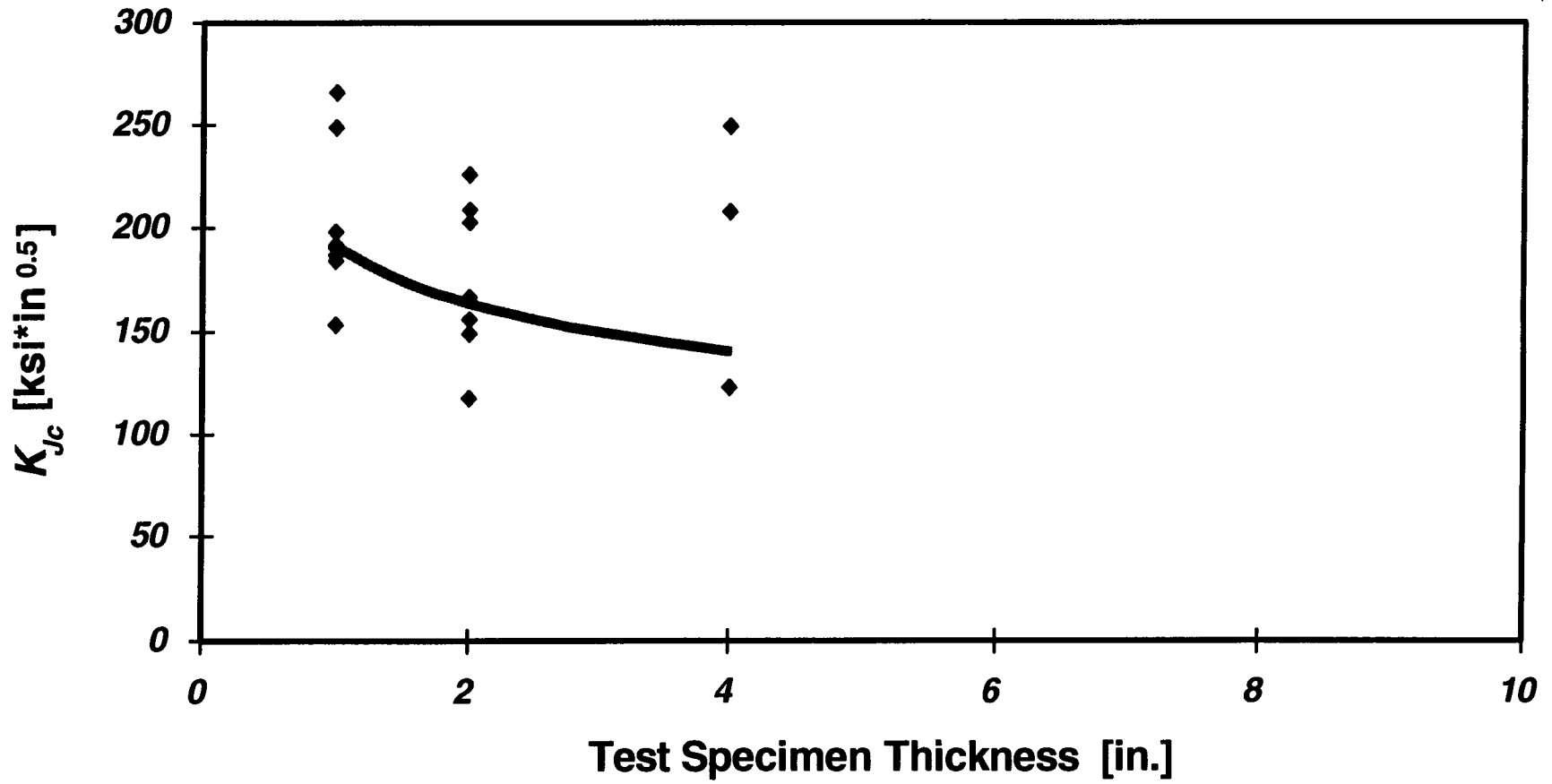


Figure 5-8(b) Measured  $K_{Jc}$  vs. specimen size for an irradiated RPV steel



### Weld 72W Un-Irradiated

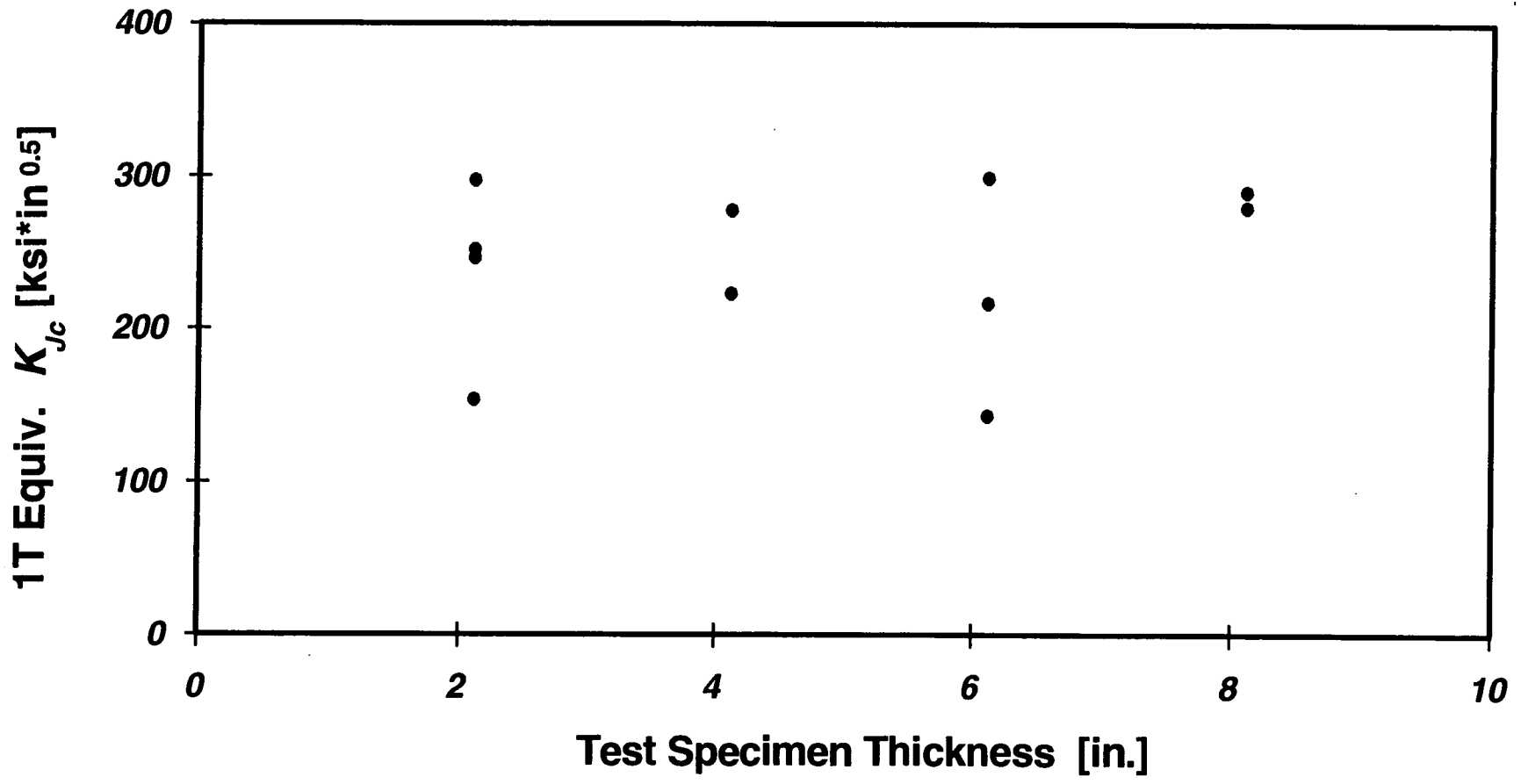


Figure 5-9(a) 1T equivalent  $K_{Jc}$  vs. specimen size for an un-irradiated RPV steel

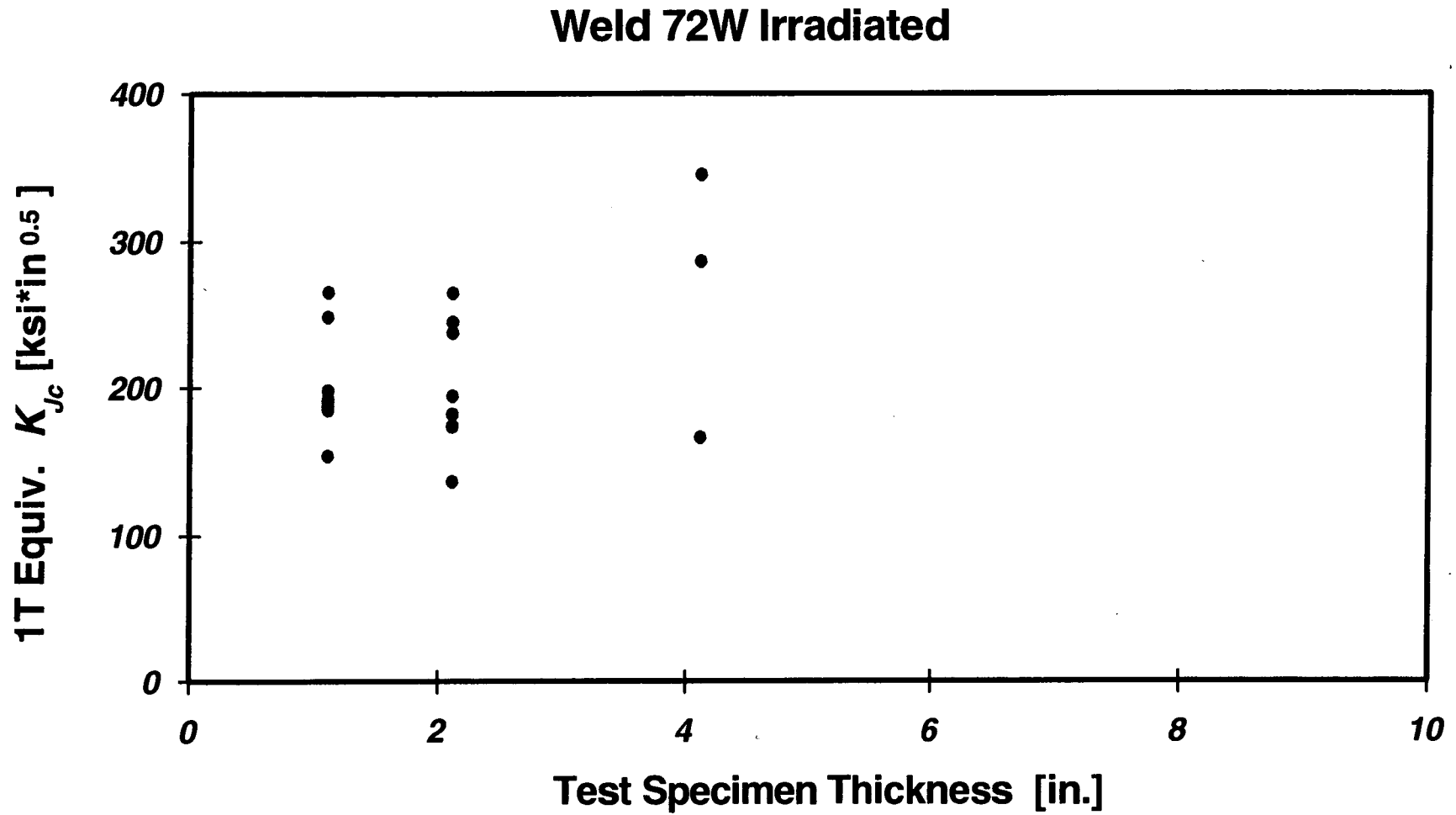


Figure 5-9(b) 1T equivalent  $K_{Jc}$  vs. specimen size for an irradiated RPV steel

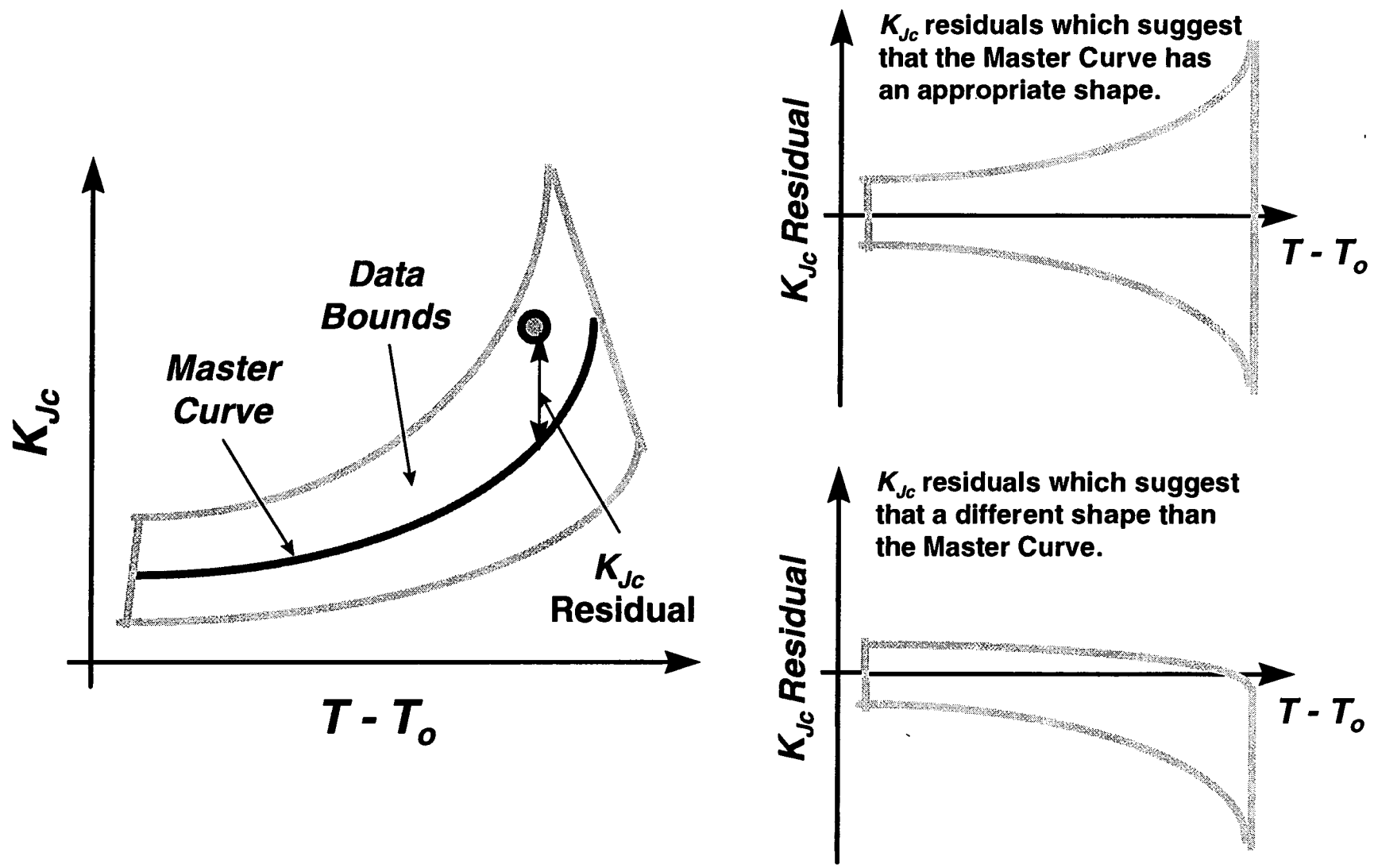


Figure 5-10 Schematic illustration of the goodness-of-fit test applied to the Master Curve shape

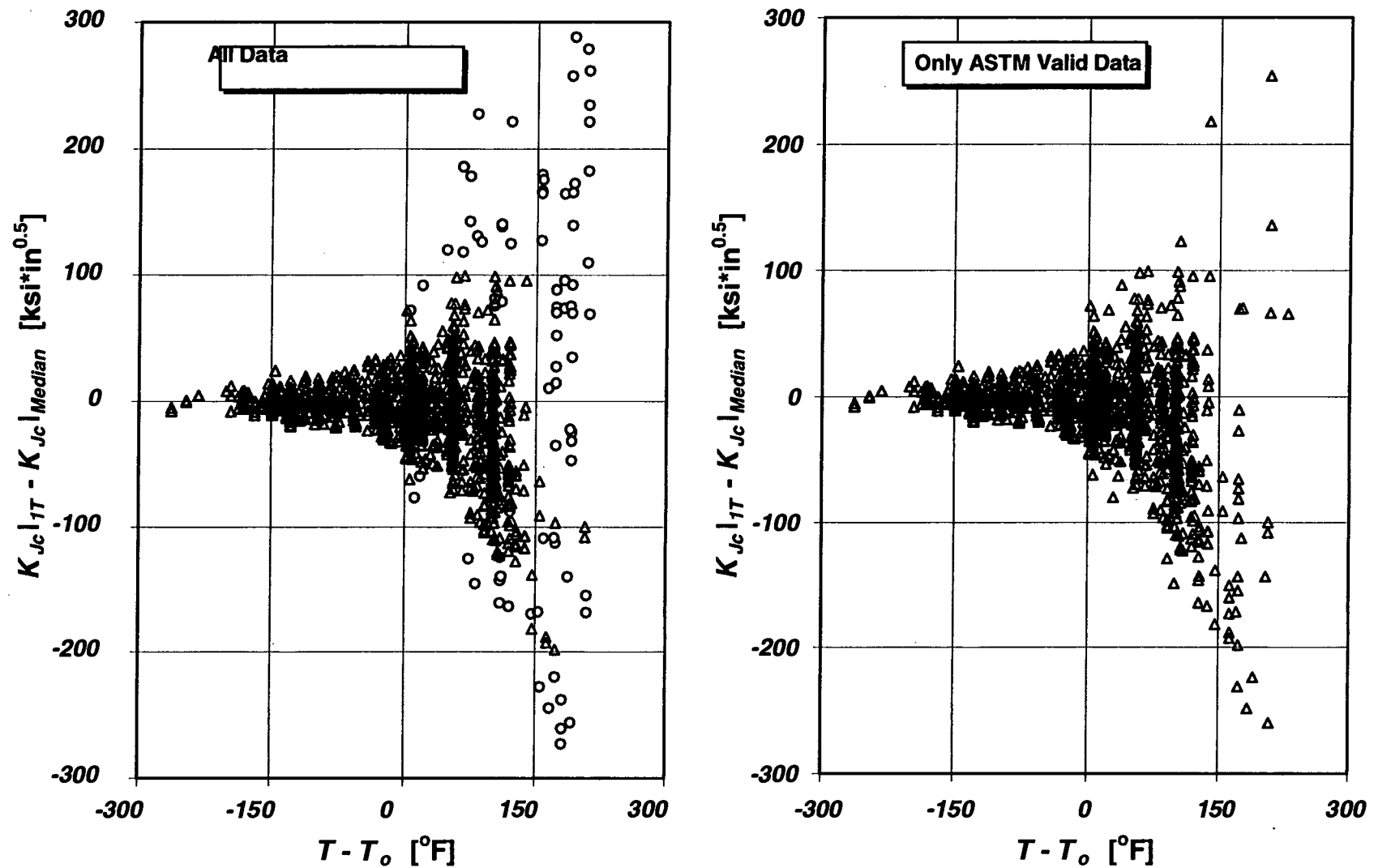


Figure 5-11 A comparison of  $K_{Jc}$  residuals for all available data (left) and for only ASTM valid data (right) illustrating the bias introduced by the ASTM censoring procedure

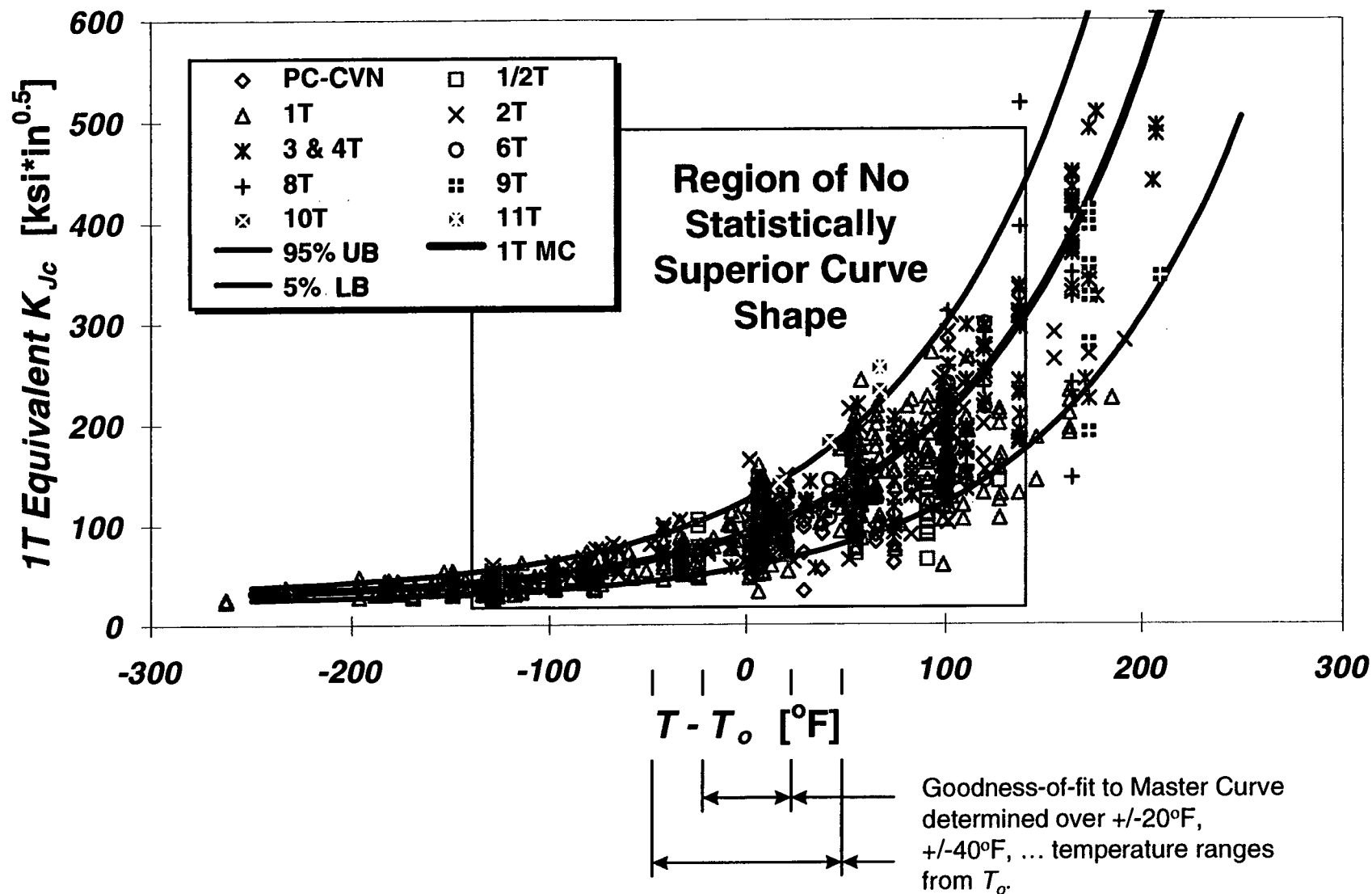


Figure 5-12 Aggregated fracture toughness data (ASTM valid only) for un-irradiated RPV steels

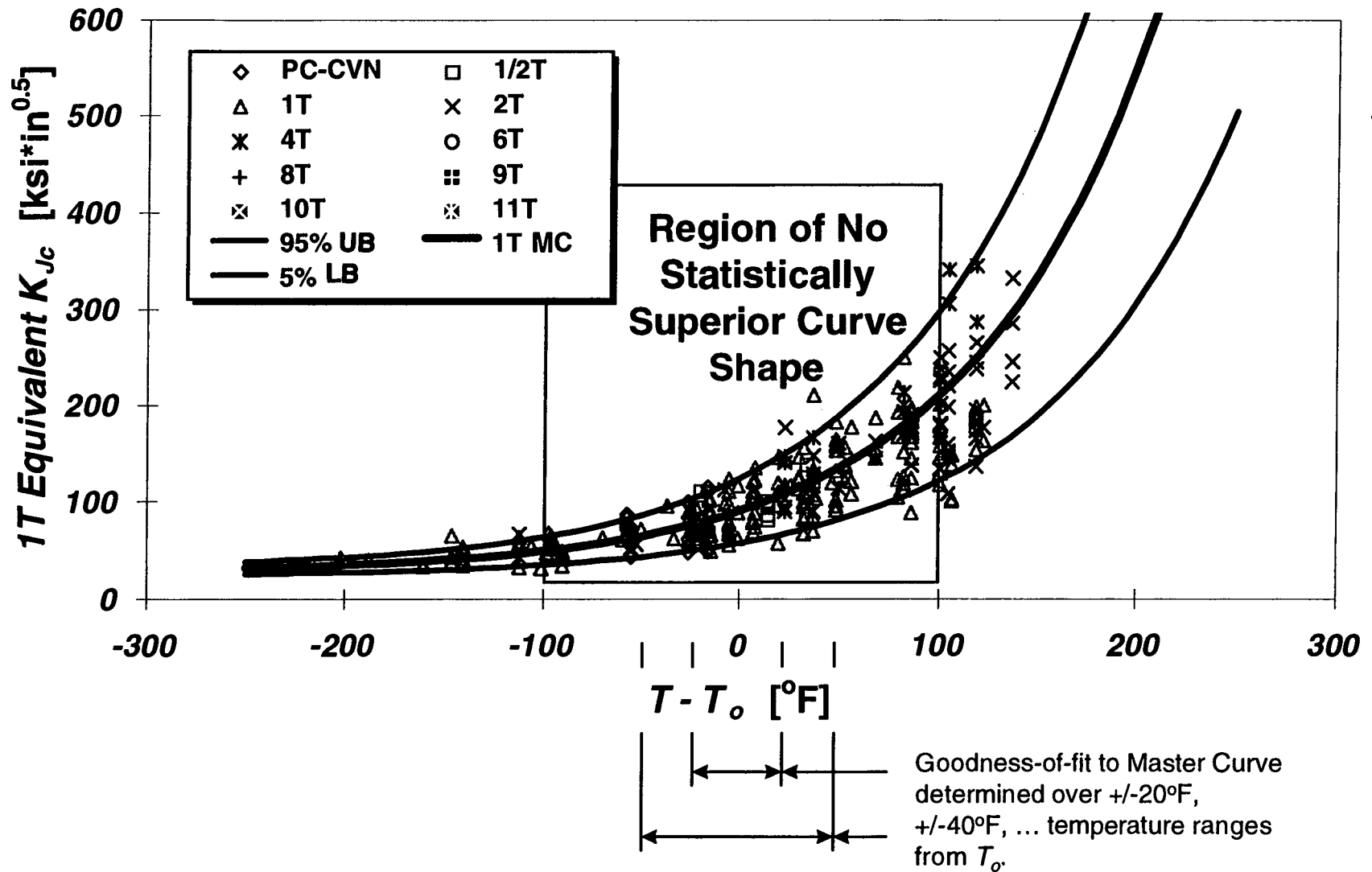


Figure 5-13 Aggregated fracture toughness data (ASTM valid only) for irradiated RPV steels.

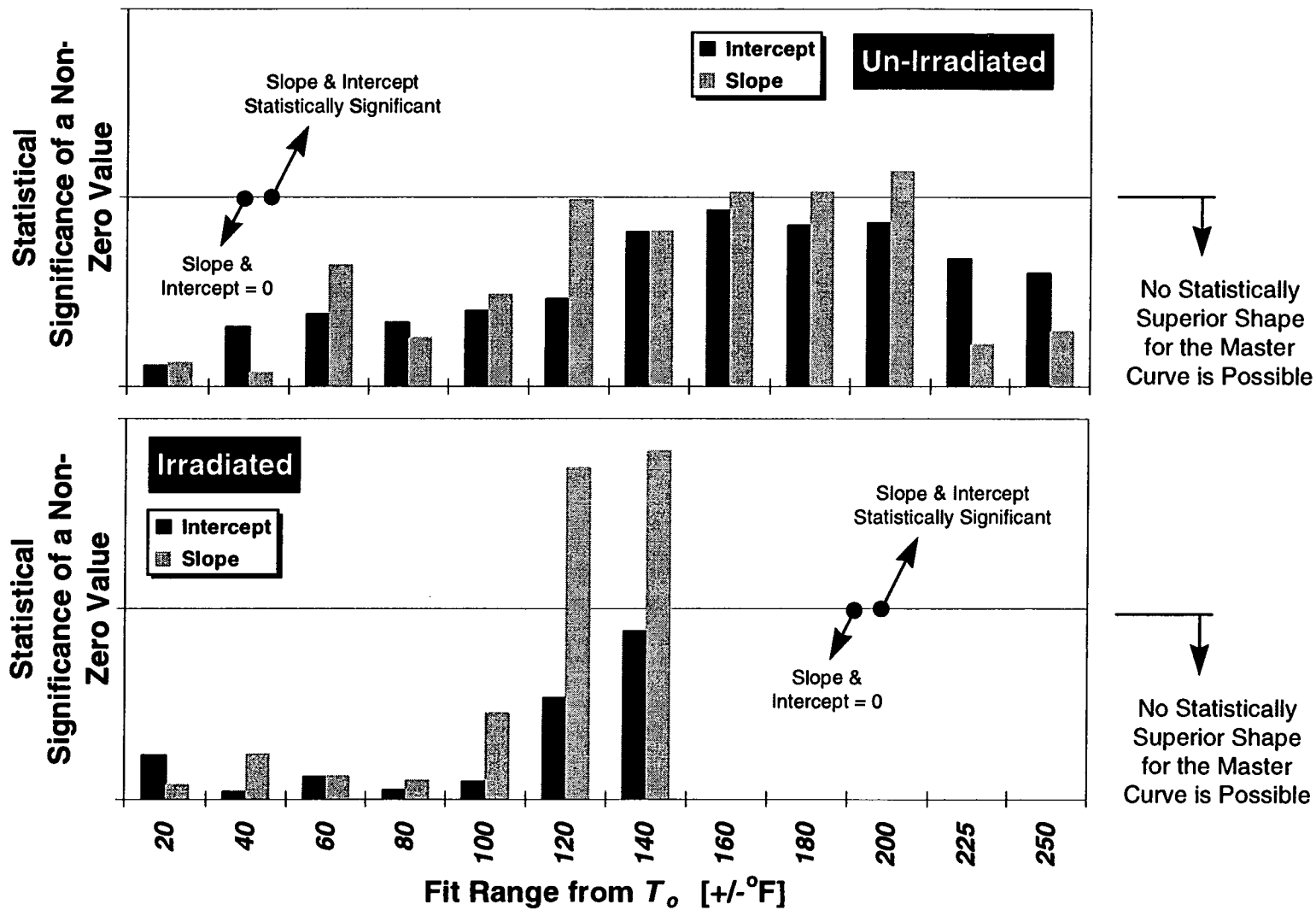


Figure 5-14 Statistical significance of slope and intercept values fit to  $K_{Ic}$  residuals over various temperature ranges for un-irradiated (Top) and irradiated (bottom) steels

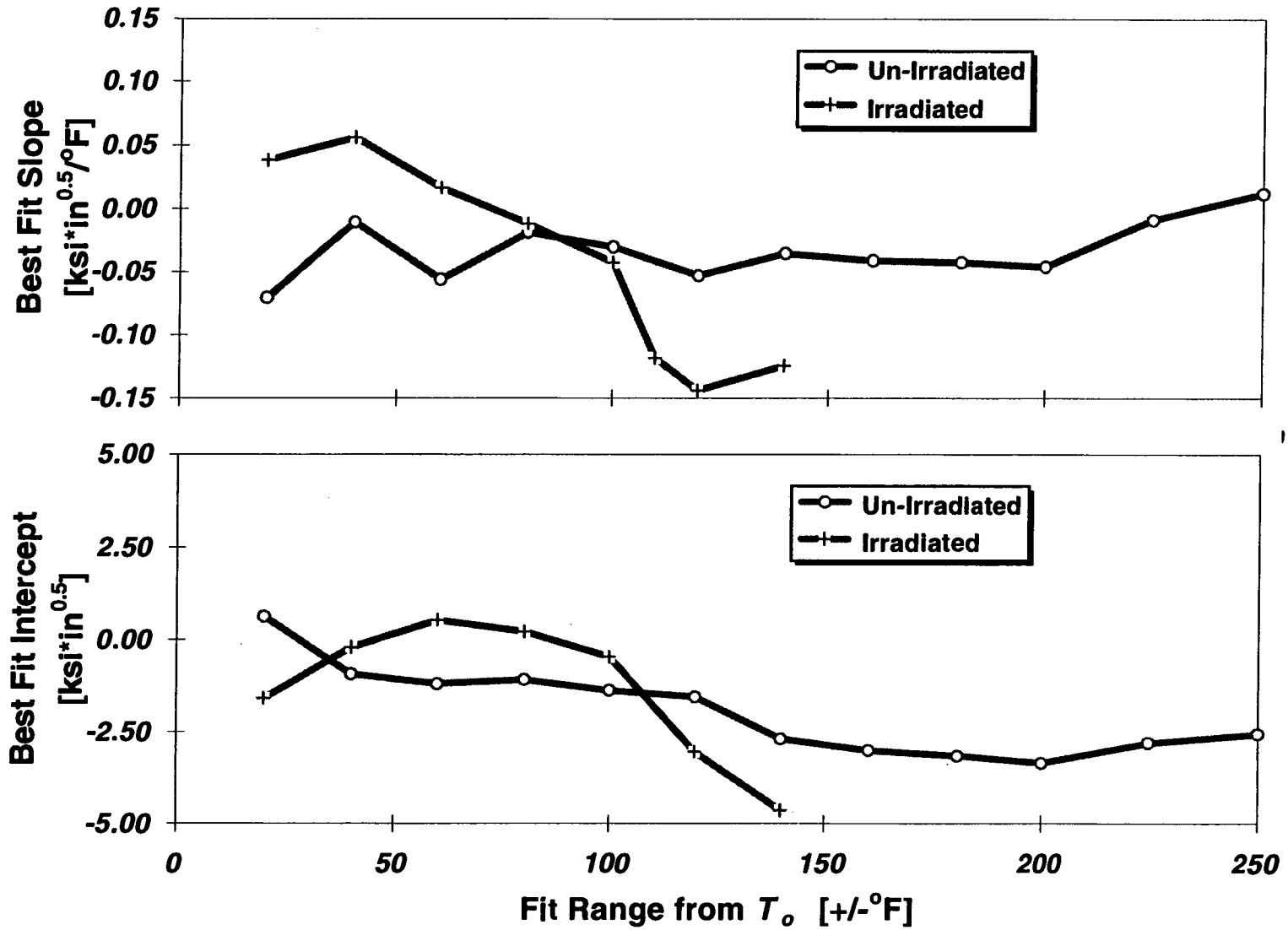


Figure 5-15 Slope (top) and intercept (bottom) values fit to  $K_{Jc}$  residuals over various temperature ranges for un-irradiated and irradiated steels



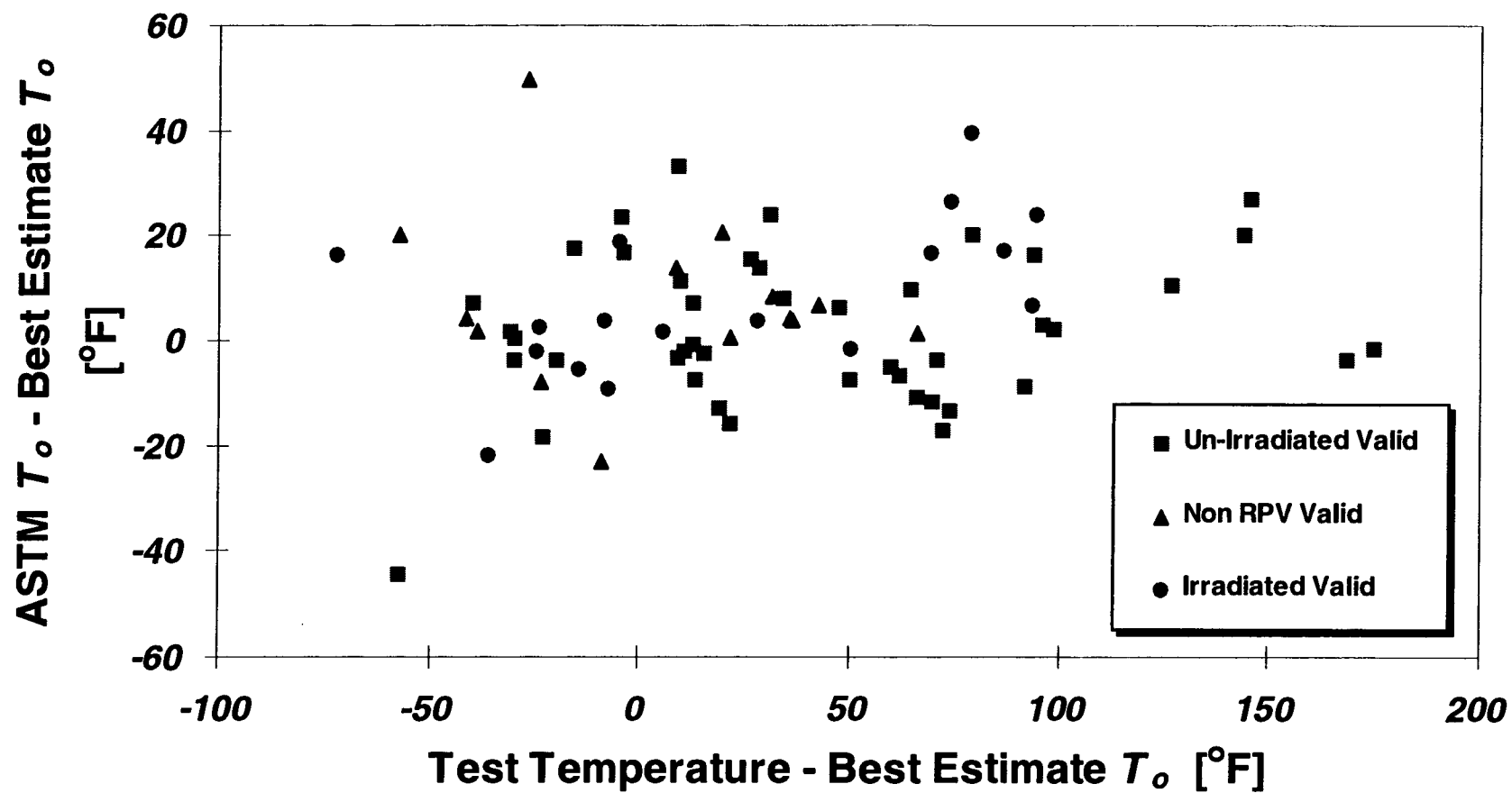


Figure 5-16(a) The influence of test temperature on the difference between ASTM and maximum likelihood estimates of  $T_o$ .

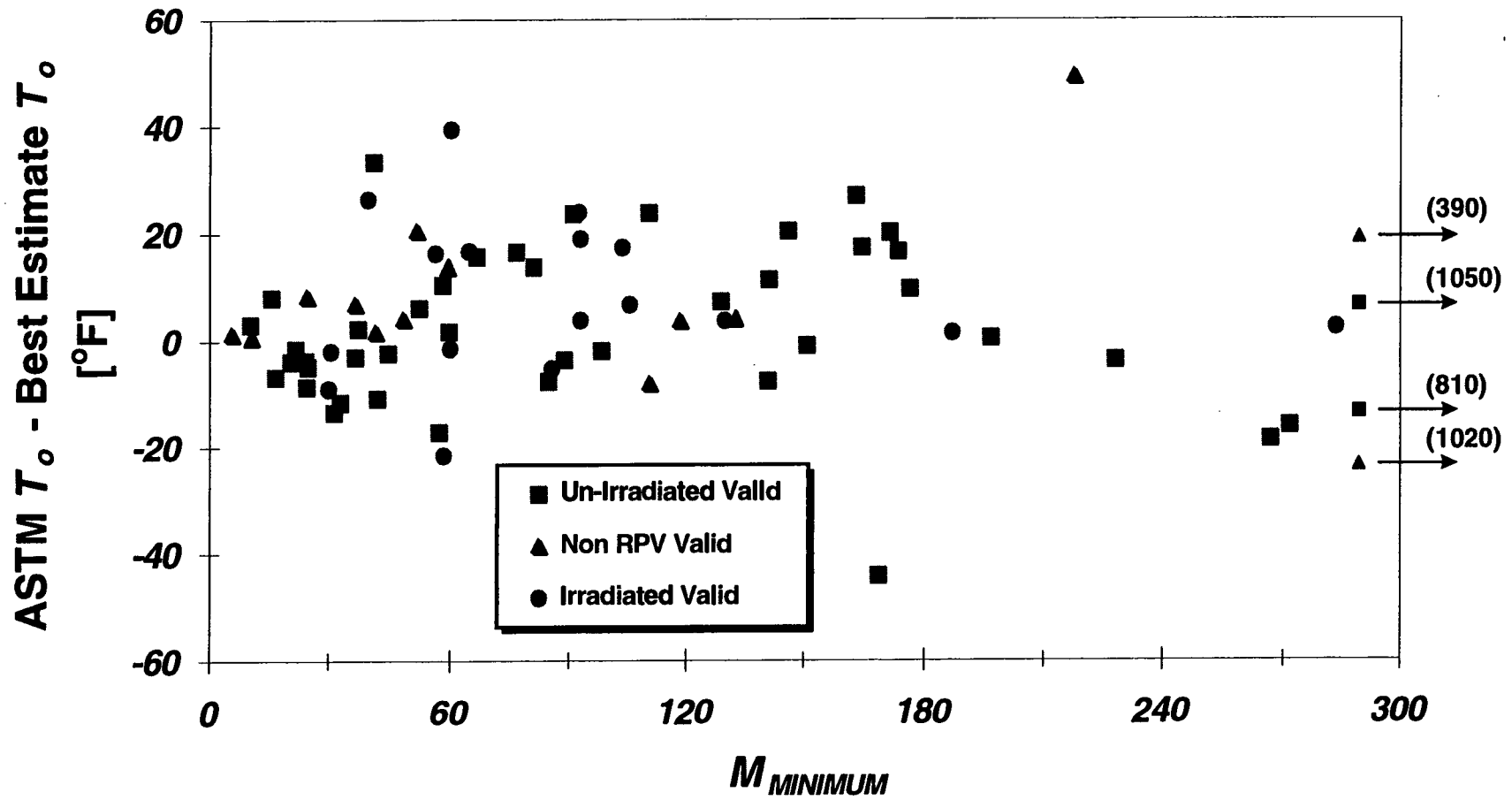


Figure 5-16(b) The influence of specimen deformation before fracture on the difference between ASTM and maximum likelihood estimates of  $T_0$ .

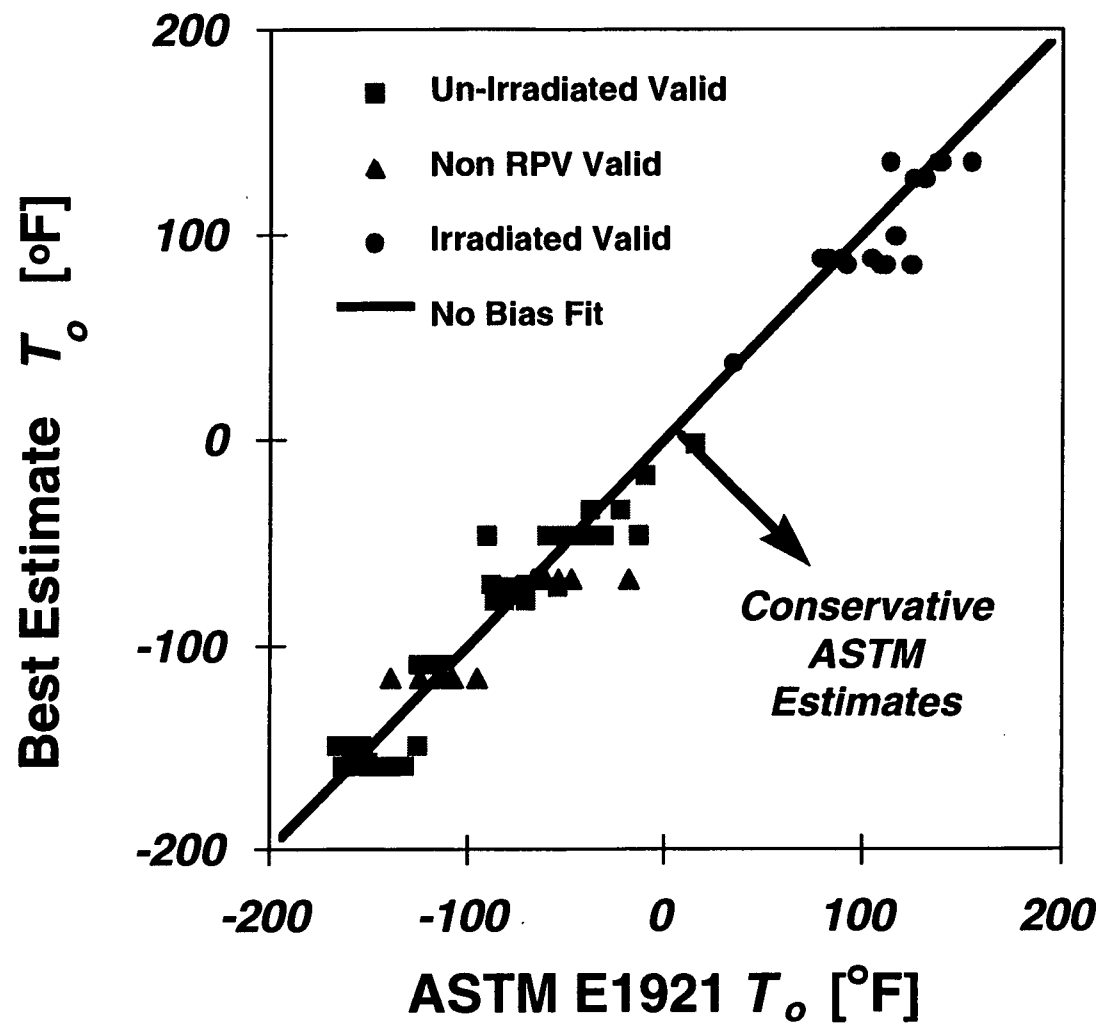


Figure 5-17 Comparison of maximum likelihood (vertical axis) and ASTM E1921 (horizontal axis) estimates of  $T_o$ .

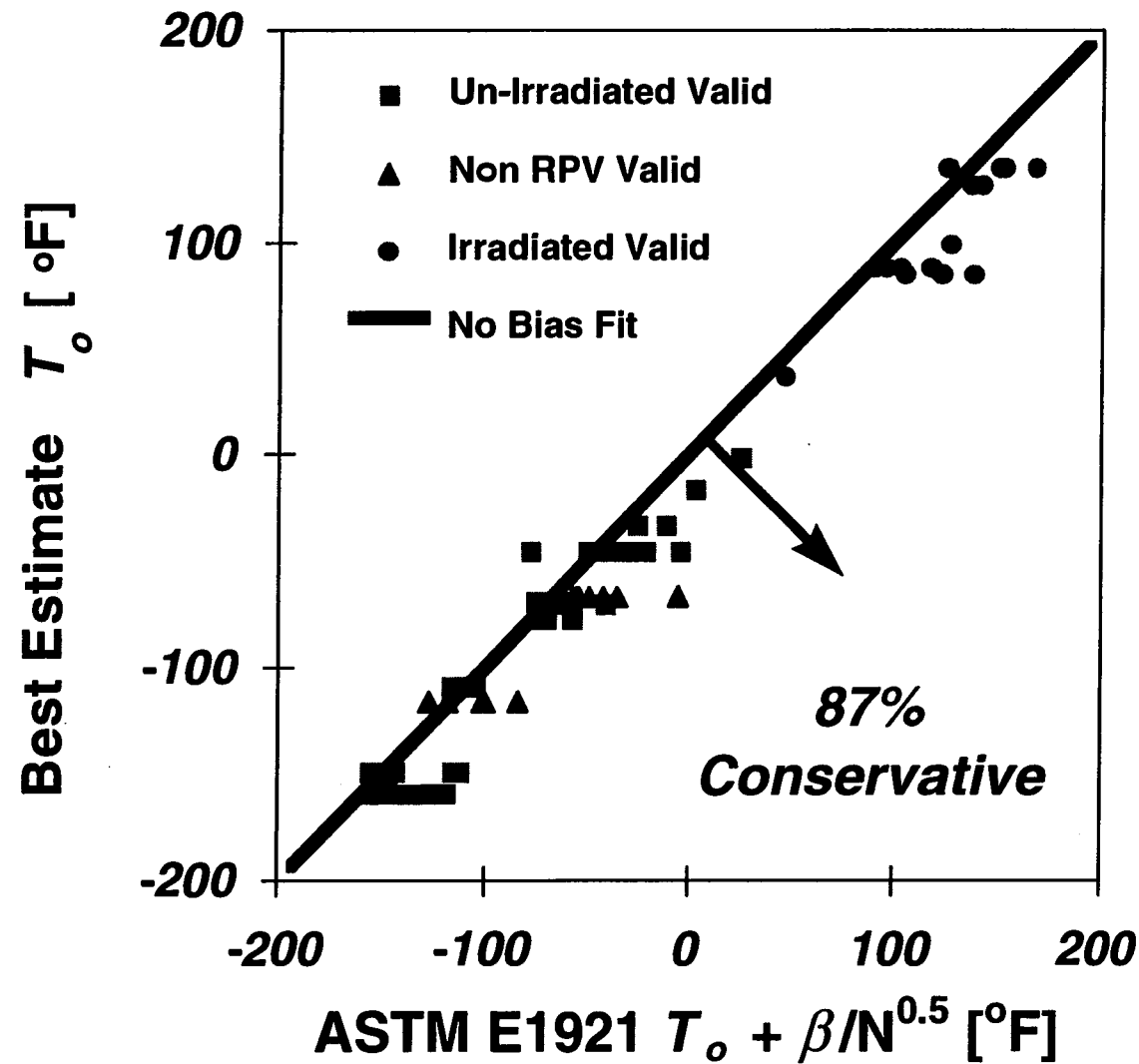


Figure 5-18 Comparison of maximum likelihood (vertical axis) and ASTM E1921 (horizontal axis) estimates of  $T_o$  (ASTM estimate increased by  $\beta/N^{0.5}$  to account for measurement uncertainty)

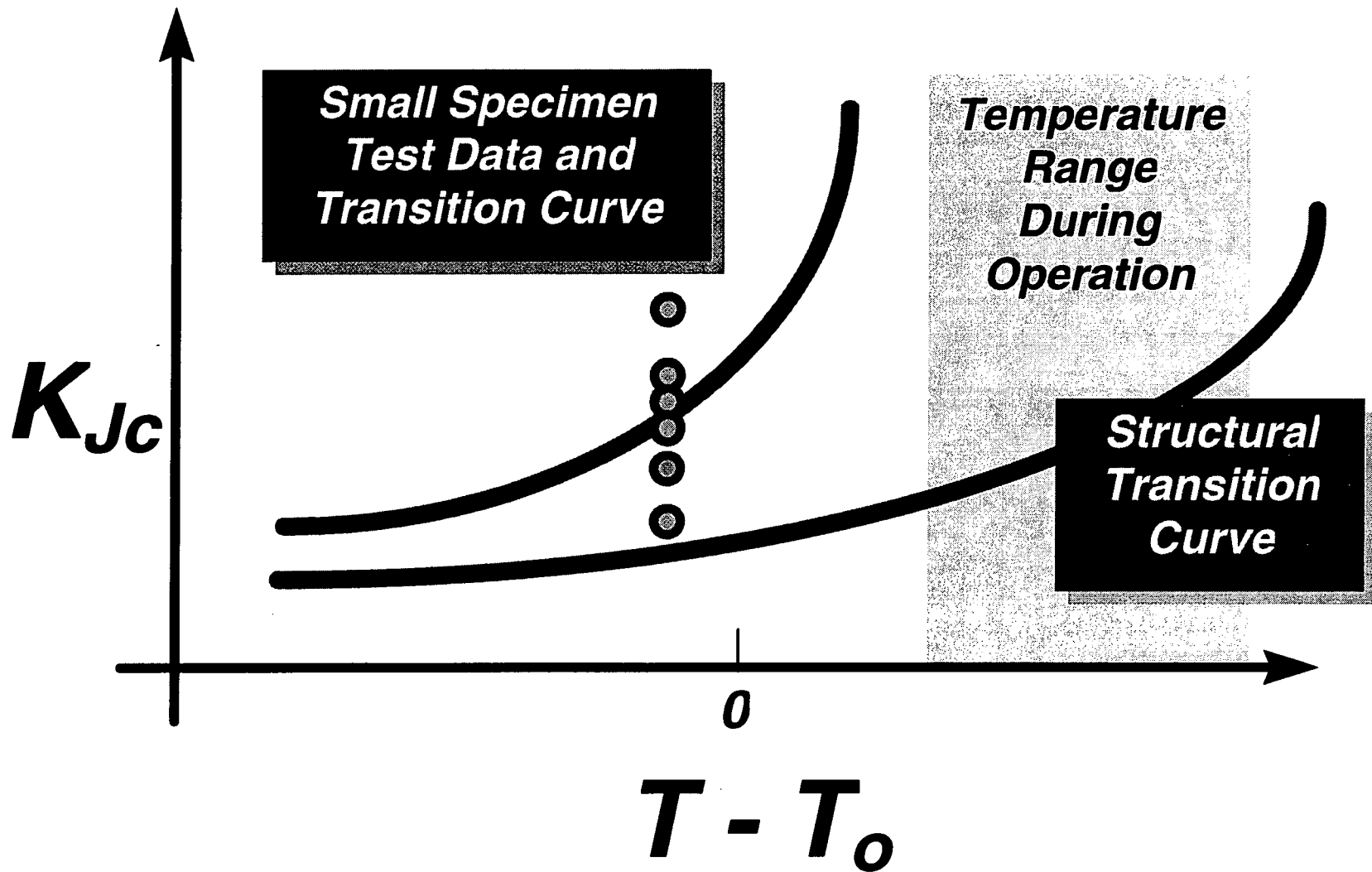


Figure 5-19 Schematic illustration of what the Master Curve may be called upon to do in nuclear RPV applications

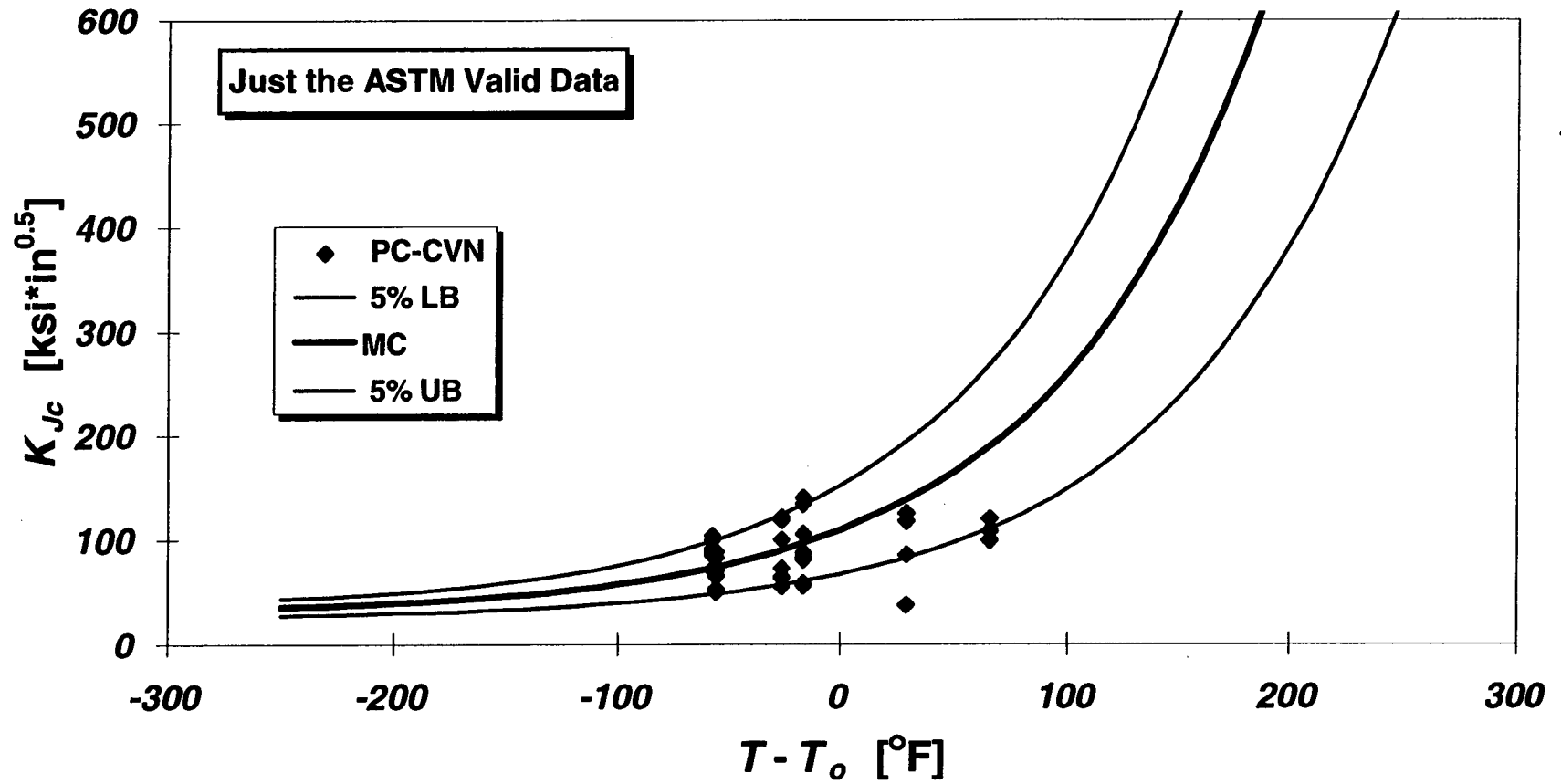


Figure 5-20(a) As-measured precracked CVN  $K_{Jc}$  data for both un-irradiated and irradiated RPV steels compared with Master Curve predictions

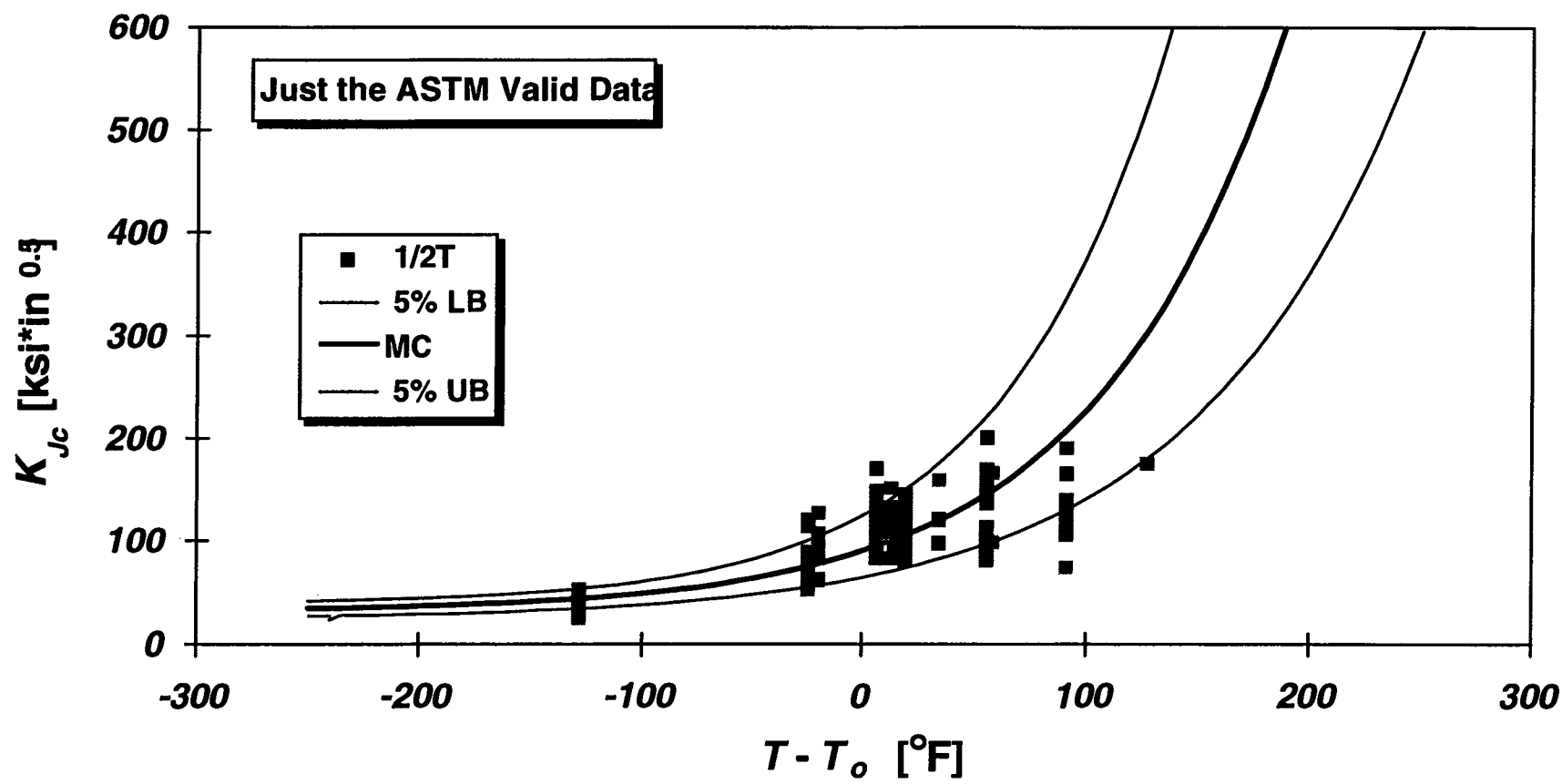


Figure 5-20(b) As-measured 1/2T  $K_{Jc}$  data for both un-irradiated and irradiated RPV steels compared with Master Curve predictions

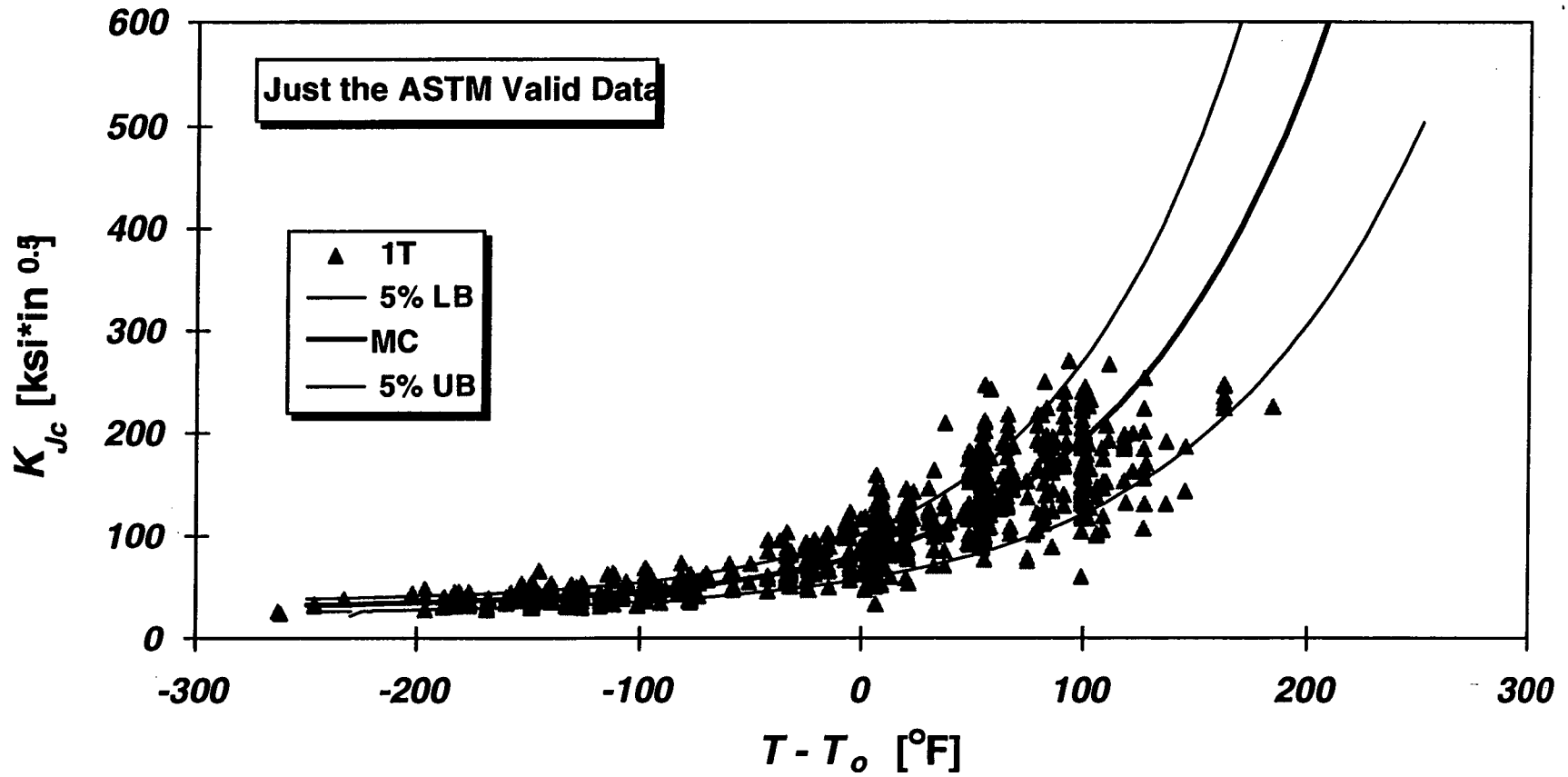


Figure 5-20(c) As-measured 1T  $K_{Jc}$  data for both un-irradiated and irradiated RPV steels compared with Master Curve predictions



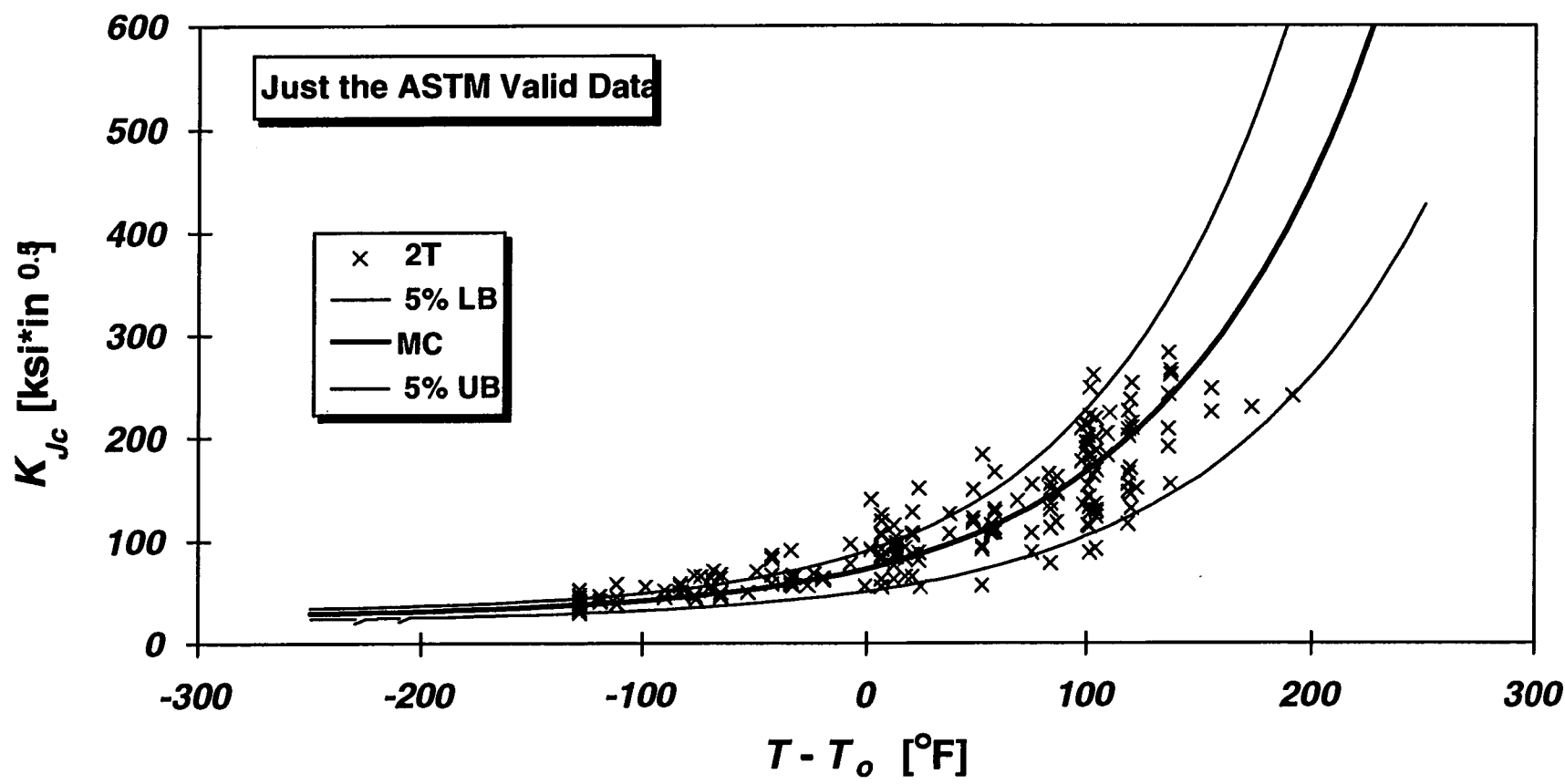


Figure 5-20(d) As-measured 2T  $K_{Jc}$  data for both un-irradiated and irradiated RPV steels compared with Master Curve predictions

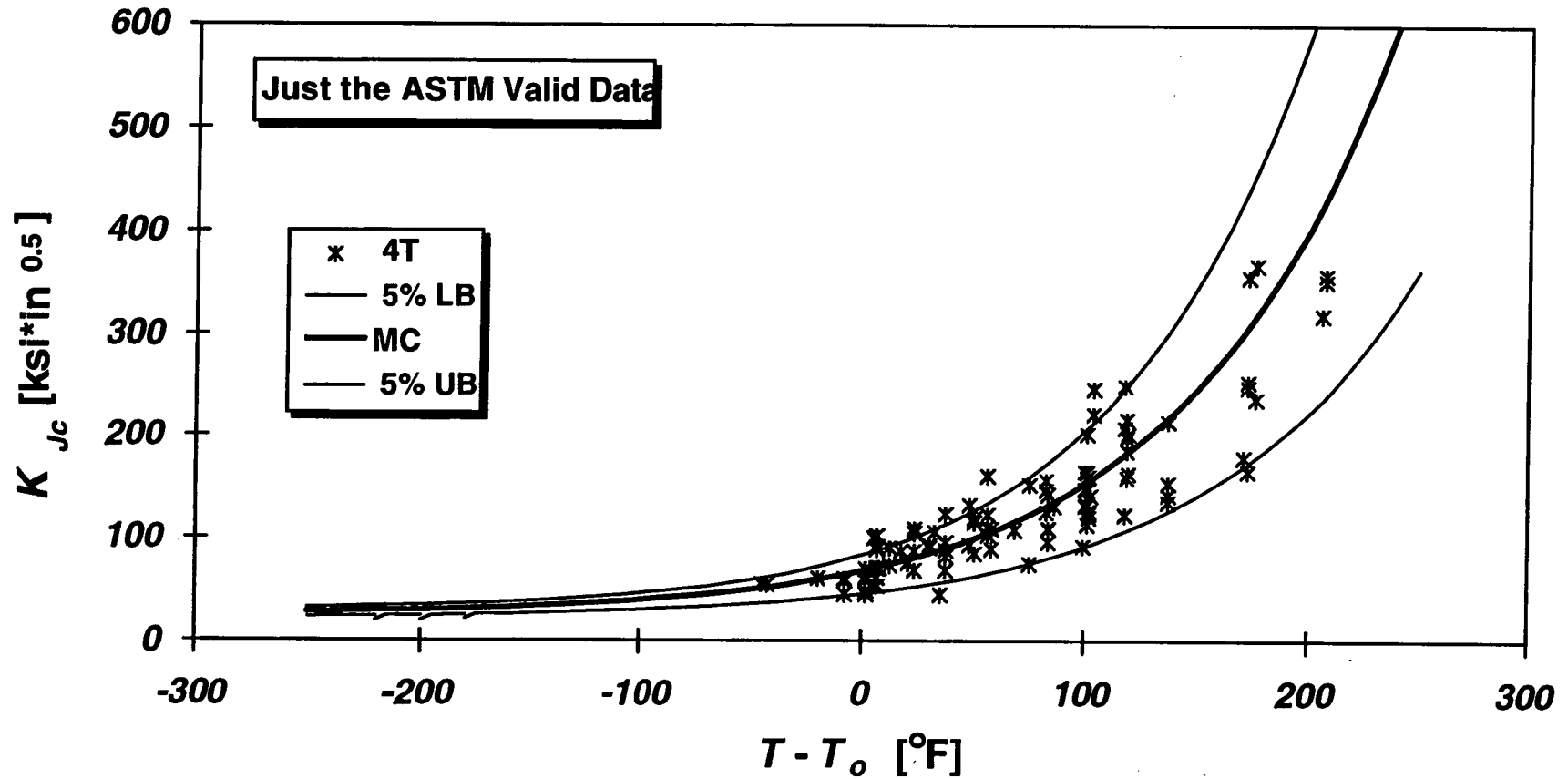


Figure 5-20(e) As-measured 4T  $K_{Jc}$  data for both un-irradiated and irradiated RPV steels compared with Master Curve predictions

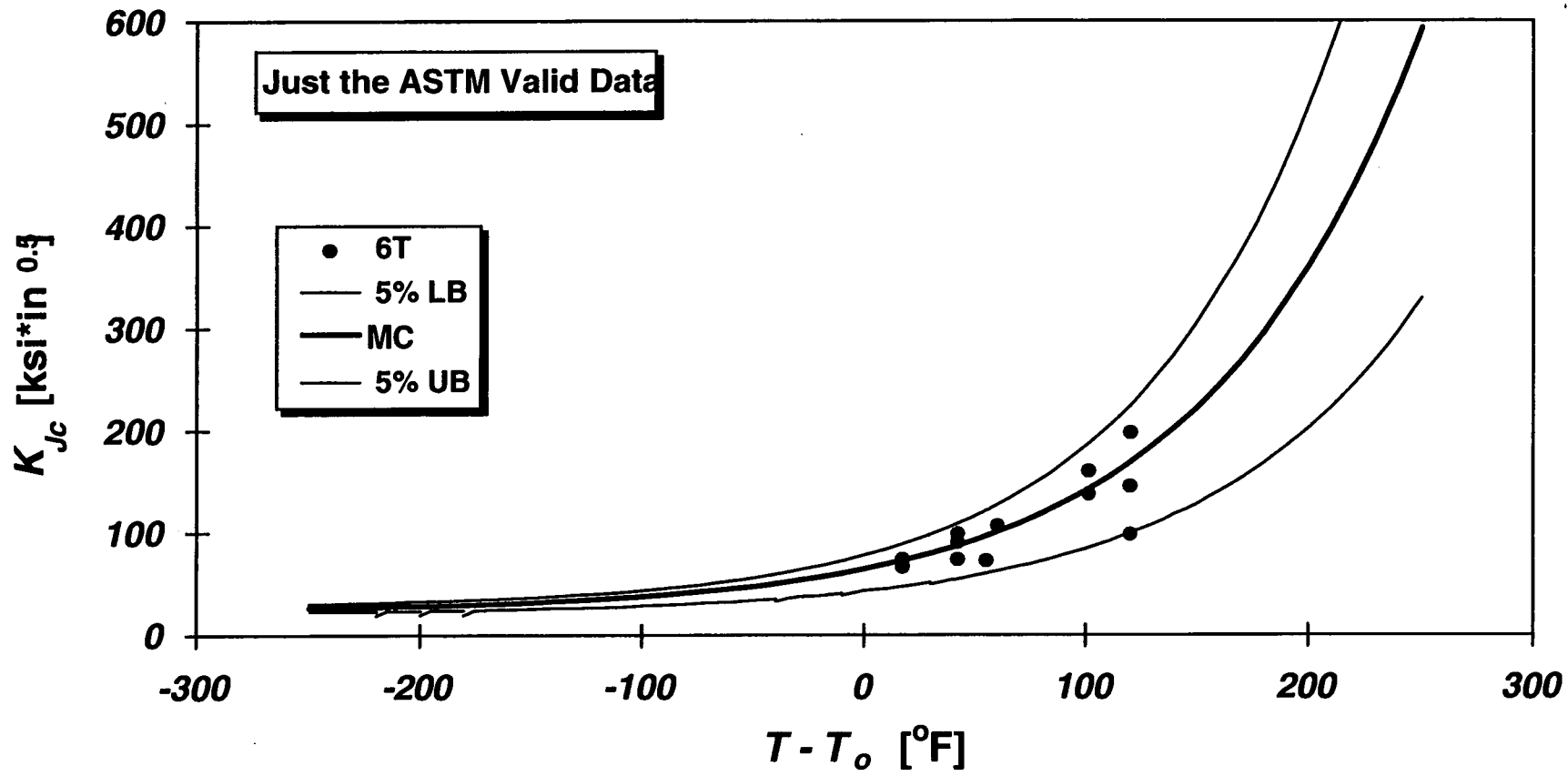


Figure 5-20(f) As-measured 6T  $K_{Jc}$  data for both un-irradiated and irradiated RPV steels compared with Master Curve predictions

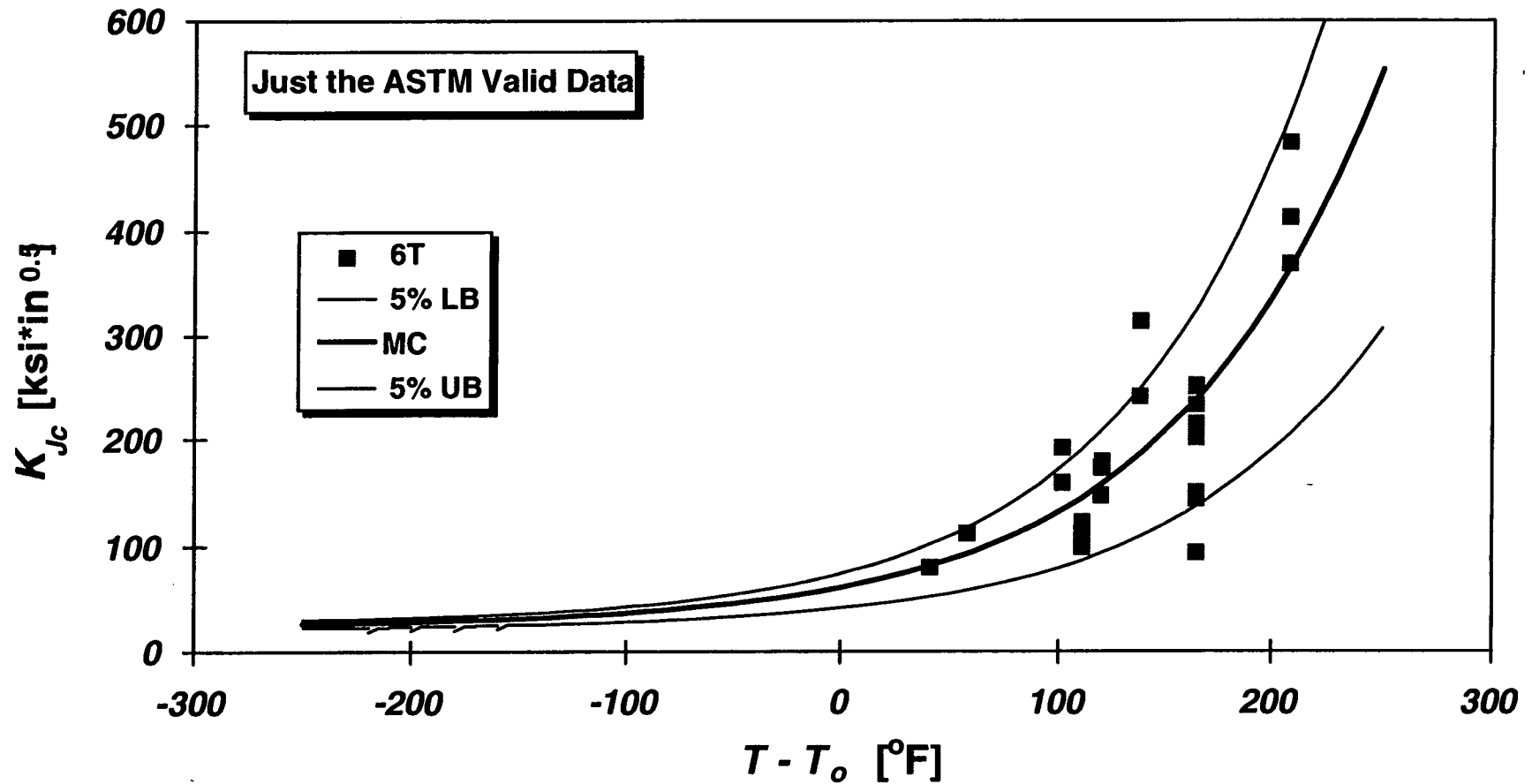


Figure 5-20(g) As-measured 8T  $K_{Jc}$  data for both un-irradiated and irradiated RPV steels compared with Master Curve predictions

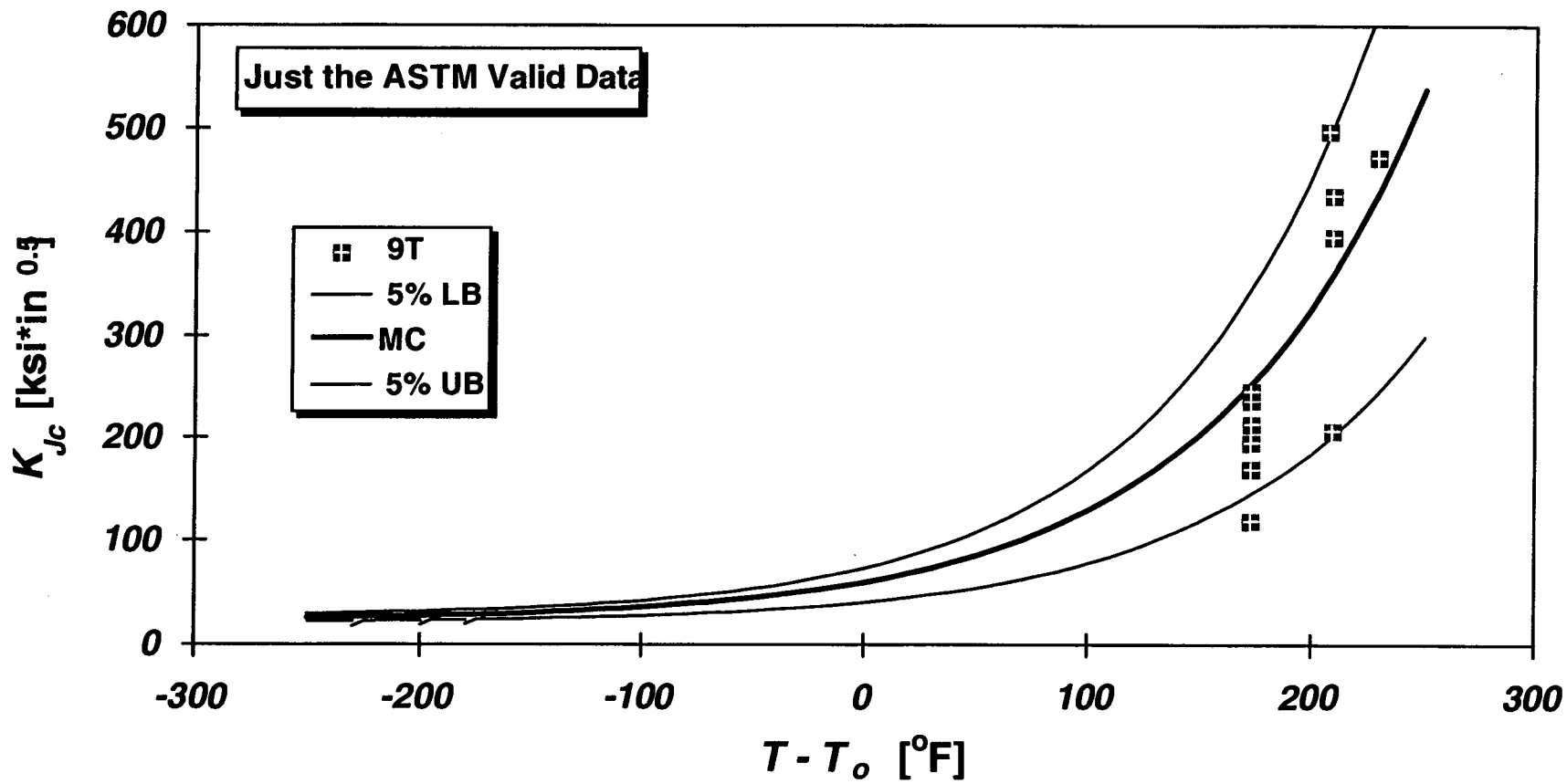


Figure 5-20(h) As-measured 9T  $K_{Jc}$  data for both un-irradiated and irradiated RPV steels compared with Master Curve predictions

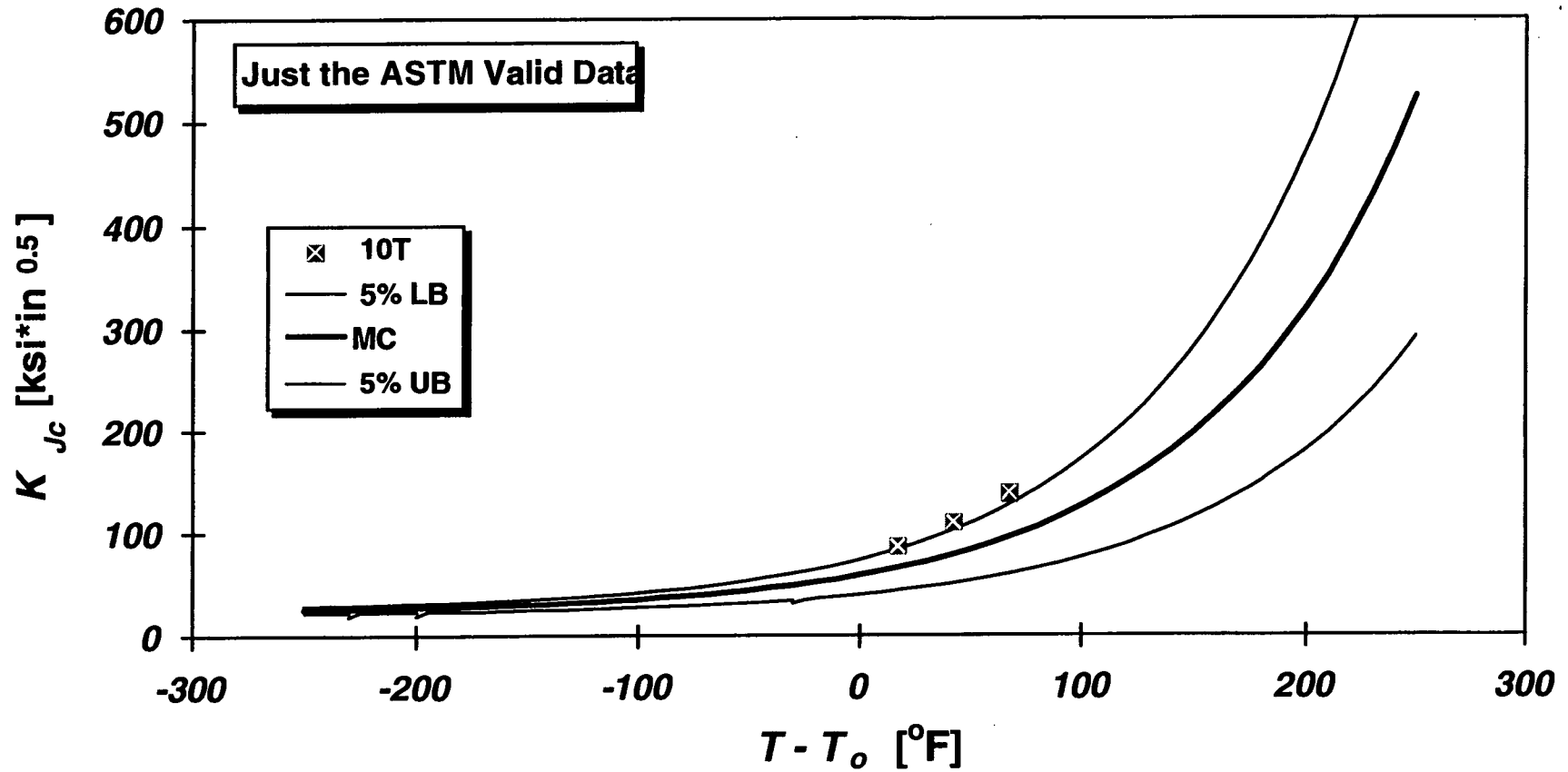


Figure 5-20(i) As-measured 10T  $K_{Jc}$  data for both un-irradiated and irradiated RPV steels compared with Master Curve predictions

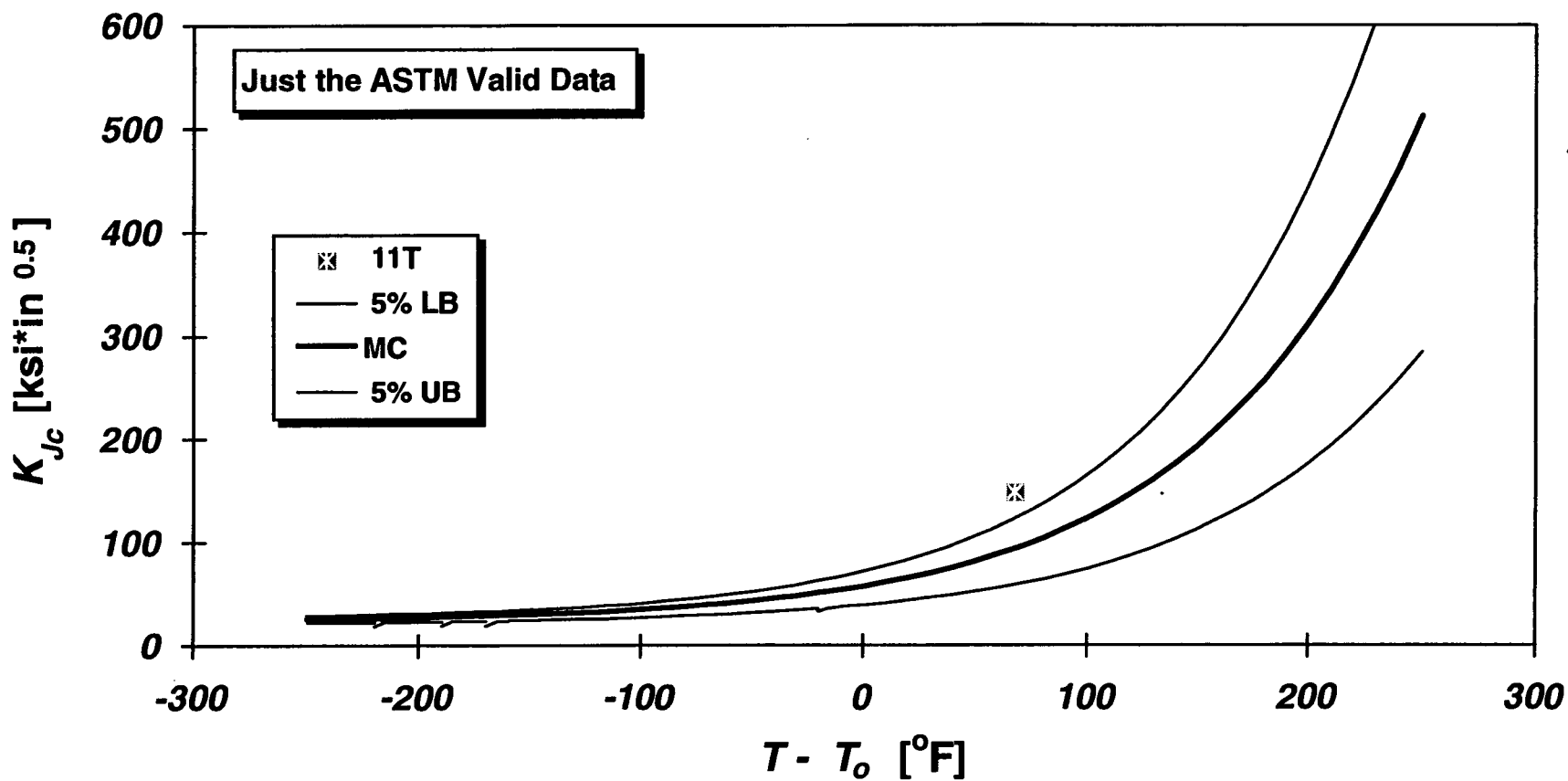


Figure 5-20(j) As-measured 11T  $K_{Jc}$  data for both un-irradiated and irradiated RPV steels compared with Master Curve predictions

## 6.0 PROPOSAL FOR A NEW MEANS OF EVALUATING RPV INTEGRITY

### 6.1 BACKGROUND

The ASME code employs a lower bound fracture toughness transition curve, which is viewed as a structural curve, in the analysis of vessel integrity. The current ASME code supplies a lower bound structural curve for static applications, which is generally termed the  $K_{IC}$  curve. The  $K_{IC}$  curve was determined by constructing an indexing parameter that defined a lower bound curve for all existing fracture toughness data not on the lower shelf. The indexing parameter chosen was  $RT_{NDT}$ , an amalgam of the nil-ductility transition temperature (NDT) and the Charpy V-notch transition temperature. In setting the  $K_{IC}$  curve, it was assumed that the measured values of fracture toughness were size independent, making  $RT_{NDT}$  the only parameter required to determine the bounding structural curve.

Master curve technology provides an alternative means of constructing a complete lower bound structural curve using a single set of fracture toughness measurements from a specific material. The fact that the Master Curve is determined from measurements of the property of interest (fracture toughness) as opposed to the current approach which determines the indexing temperature ( $RT_{NDT}$ ) on the basis of other manifestations of the ductile-to-brittle transition (dynamically loaded specimens with brittle starter notches and blunt notches) makes this new technology extremely attractive. The only value required to establish the Master Curve is  $T_0$ , which can be measured using precracked fracture toughness specimens of Charpy size. The Master Curve offers the additional advantage of allowing direct evaluations of the fracture toughness transition curves in materials with limited availability of archival materials, and in irradiated materials. Measurements of  $RT_{NDT}$  in these cases are impractical or impossible, a fact which necessitates the current correlative approach.

### 6.2 THE ASME AND PVRC APPROACH TO MASTER CURVE IMPLEMENTATION

The current combination of codes and regulations that govern the analysis of reactor vessel integrity with respect to brittle fracture are based on the determination of  $RT_{NDT}$  and the use of the  $K_{IC}$  curve (along with the closely related dynamic  $K_{IR}$  curve). While it is theoretically feasible to replace the  $K_{IC}$  curve with a Master Curve based lower bound, this approach raises many practical obstacles. Among these obstacles are:

1. The current pressurized thermal shock (PTS) evaluation methodology outlined by 10 CFR 50.61 is based on a screening limit for the irradiation shifted value of  $RT_{NDT}$ . This screening limit was based on an analysis using the  $K_{IC}$  and  $K_{IR}$  curves. Adoption of the Master Curve evaluation may require a reevaluation of the screening limit in terms of  $T_0$ .
2. Current procedures for calculating the pressure-temperature operating limits may require revision.



3. Current codes and regulations contain margins which account for uncertainties in both materials properties and analysis procedures. It is difficult to trace the technical justification for these margin terms because they were developed by a consensus building processes in the relevant code committees and regulatory bodies. Revision of the basis of the evaluation may require a lengthy process to reevaluate all of the relevant margin terms.
4. There is not presently a dynamic version of the Master Curve that would be analogous to the  $K_{IR}$  curve. Preliminary studies have provided promising results on using Master Curve analysis for dynamic tests. However, the relationship between the Master Curve and arrest data is more tenuous because the Master Curve analysis is fundamentally a cleavage fracture initiation technology. It is not clear how this technology can be reconciled with the arrest portion of the  $K_{IR}$  database.

The PVRC task group charged with providing the technical basis document for the application of the Master Curve fracture toughness methodology considered these and similar obstacles and adopted the following two stage process for implementation of this technology:

Short Range Objective:

Use the Master Curve indexing temperature,  $T_o$ , as an alternative index for the  $K_{IC}$  curve. The PVRC task group has proposed a new parameter,  $RT_{T_o}$ , which is defined in terms of  $T_o$  and can be used in place of  $RT_{NDT}$  as a reference temperature for the ASME code curves. In effect this would establish  $RT_{T_o}$  as an alternate means for determining  $RT_{NDT}$ .

Long Range Objective:

Adopt the Master Curve, and its associated statistical properties, as the appropriate basis for structural and probabilistic analysis.

The advantage of the two stage process is that it allows limited use of Master Curve technology on an interim basis while the issues associated with full implementation are resolved. The short range plan simplifies the process of implementation because it circumvents many of the practical obstacles associated with changing the ASME code. To achieve the short range objective, the following approach to addressing the list of practical obstacles has been adopted:

1. PTS Evaluation Methodology The short range approach eliminates the need to redefine the PTS screening criteria, because the newly defined reference temperature,  $RT_{T_o}$ , may be used as a direct replacement for  $RT_{NDT}$  in the PTS evaluation methodology.
2. Pressure Temperature Operating Limits Adopting the short range objective also eliminates the need to develop new procedures for calculating pressure-temperature operating limits because  $RT_{T_o}$  can be used as a direct replacement for  $RT_{NDT}$  in the existing procedures.

3. Margin Terms Adoption of the short range objective does require some re-evaluation of the margin terms applied. Many of the current margin terms are preserved because the ASME reference curves and the concept of a referencing temperature are maintained. However the margin terms that relate directly to the uncertainty in the determination of reference temperature must be reevaluated.
4.  $K_{IR}$  Curve The new parameter,  $RT_{To}$ , is based primarily on the equivalence in the resulting  $K_{IC}$  curves. Because a single reference temperature is used to index both the  $K_{IC}$  and  $K_{IR}$  curves, a justification for using this newly defined reference temperature to index the dynamic and arrest data is required.

Sections 6.4 through 6.7 directly address the equivalence between  $RT_{To}$  and  $RT_{NDT}$ , as required by 1 and 2 above. The development of appropriate margin terms for the application of this new reference temperature is presented in Section 7. The use of the Master Curve to define a bound for the dynamic and arrest toughness is described in Section 6.3.

### 6.3 APPROACH TO DYNAMIC AND ARREST TOUGHNESS

$RT_{NDT}$  serves as a reference temperature for both the  $K_{IC}$  curve, which bounds static toughness data and the  $K_{IR}$  curve, which bounds dynamic and arrest toughness data. Implicit in the decision to use the Master Curve technology to estimate  $RT_{To}$  is the assumption that the relationship between the  $K_{IC}$  curve and the  $K_{IR}$  curve will remain the same. The use of a single reference temperature for both curves reflects a long standing belief that the ductile-to-brittle transition temperatures for static and dynamic measurements are correlated. It can be argued that an irradiated material, with an increased yield stress and decreased toughness should exhibit a decreased differential between the static and dynamic transition temperatures. However, the amount of available data is insufficient to positively prove this point. As a practical matter, the dynamic and arrest toughness values have minimal impacts on the reactor vessel integrity. Although the  $K_{IR}$  curve is currently used to set pressure-temperature operating limits, the analysis is based solely on crack initiation and there is no indication of significant dynamic loading events under normal operation of the vessel. The use of the  $K_{IR}$  curve to set pressure-temperature operating limits represents an additional conservatism that has been imposed on the analysis. ASME code committees are currently considering the appropriateness of this extra level of conservatism (there is a Code Case being considered which would allow use of the  $K_{IC}$  curve to establish heatup/cooldown limit curves). However, that consideration is a clearly separate issue, as the proposed  $RT_{To}$  approach maintains the existing level of conservatism by maintaining the relationship between the  $K_{IC}$  and  $K_{IR}$  curves.

### 6.4 OVERVIEW OF APPROACH FOR KEWAUNEE

The objective of the current study is to apply the Master Curve technology to the analysis of vessel integrity for the Kewaunee nuclear reactor vessel. The approach outlined in this study is consistent with the short term objective of the PVRC as outlined in Section 6.2. This short term goal requires a procedure for estimating  $RT_{NDT}$  ( $RT_{To}$ ) and the associated margin terms based on Master Curve analysis. The PVRC and ASME Code task group members have developed a technical basis document to support an ASME Code Case for this alternative procedure applied

to unirradiated materials. The procedures developed for the Kewaunee application are consistent with the principles employed in the draft ASME Code Case, but also apply Master Curve technology to irradiated materials. This approach is supported by the data provided in Section 4 of this report, which demonstrate that the Master Curve technology is applicable to both unirradiated and irradiated reactor pressure vessel steels.

## 6.5 ESTIMATING THE $K_{IC}$ REFERENCE TEMPERATURE ( $RT_{T_0}$ ) FROM $T_0$

The fundamental premise underlying the proposed approach is as follows: if it is possible to define a new indexing temperature ( $RT_{T_0}$ ) for the  $K_{IC}$  curve that assures that the reference  $K_{IC}$  curve will bound the actual material fracture toughness data, then  $RT_{T_0}$  must be the functional equivalent of  $RT_{NDT}$ . Note that because the relationship between  $RT_{NDT}$  and fracture toughness is somewhat tenuous, a one-to-one correspondence between  $RT_{T_0}$  and  $RT_{NDT}$  is not expected. The lack of such an empirical relation between  $RT_{NDT}$  and  $T_0$  has been demonstrated [Sokolov, 1997]. The requirement for functional equivalence eliminates the need for an empirical correlation because it relates directly to intent of the ASME reference curves. It is feasible to define a functionally equivalent indexing temperature because both the  $K_{IC}$  curve and the Master Curve describe the ductile-to brittle transition for static crack initiation tests in pressure vessel steels. However, the Master Curve approach is attractive because it relates the toughness curve to actual toughness measurements rather than the combination of Charpy and drop weight tests used to determine  $RT_{NDT}$ .

A demonstration of functional equivalence requires an examination of both the current technology and the proposed alternative. To provide an objective evaluation of the functional equivalence of the proposed alternative, standards of acceptability must be established. The following sections describe this examination and evaluate the functional equivalency of the draft Code Case. These issues are addressed in two sections as follows:

1. The Master Curve approach is based on a new understanding of the statistics of cleavage fracture that was not available at the time that the ASME code was developed. One important implication of this new understanding is that there is an effect of specimen size on observed fracture toughness values. This size effect is incorporated in the Master Curve, but not in the definition of the  $K_{IC}$  curve. In order to be functionally equivalent,  $RT_{T_0}$  must be based on the same implicit specimen size as  $RT_{NDT}$ . This implicit size is determined in Section 6.5.1 for the  $K_{IC}$  curve.
2. The  $K_{IC}$  curve, as indexed to  $RT_{T_0}$ , must continue to appropriately bound the available fracture toughness data. In order to define a standard of acceptability for the proposed approach, an objective definition of the meaning of the phrase "appropriately bound" is required. Various standards for acceptability are outlined in Section 6.5.2, and their implications for  $RT_{T_0}$  are discussed.

### 6.5.1 Implicit Size Effects in the $K_{IC}$ Curve

The original  $K_{IC}$  curve was drawn to bound data from a variety of specimen sizes. The development of this curve preceded Landes and Schaffer's [1980] observation that measured

values of fracture toughness in the transition region exhibit a size dependence. This size dependence was not apparent in the original data set because the critical specimens were relatively large (making the size correction less obvious) and the number of specimens was limited. The use of  $K_{Ic}$  and Master Curve test procedures expands greatly the available data set. This larger data set contains a wider variety of specimen sizes and tends to emphasize smaller specimens, where the size effect is more obvious.

A unique feature of the Master Curve approach is the explicit treatment of flaw size effects (See Eq. 5-15). Once an acceptable tolerance bound is established, two parameters are required to establish the lower bound curve:  $T_0$  and an appropriate flaw dimension. Increasing crack front length lowers the mean and bounding toughness values. This understanding of the effects of crack front length on toughness represents a significant departure from traditional *LEFM*, where the toughness transition curve is held to be a size invariant material property. However, the  $K_{Ic}$  curve does indeed have a size associated with it because a specific assortment of specimen sizes were tested to establish the bounding curve. The average specimen thickness serves as a characteristic "size" for a data set. Several characteristic sizes are summarized below:

- |                                |              |                     |
|--------------------------------|--------------|---------------------|
| • HSST Plate 02                | 60 values    | Average Size = 2.4T |
| • Original $K_{Ic}$ database   | 163 values   | Average Size = 2.0T |
| • All currently available data | 1,228 values | Average Size = 1.6T |

The particular average flaw size is not important so long as the same data set is used to assess the bounding characteristics of a  $RT_{T_0}$  indexed  $K_{Ic}$  curve relative to a  $RT_{NDT}$  indexed  $K_{Ic}$  curve. However, recognizing that the existing definition of the  $RT_{NDT}$  indexed  $K_{Ic}$  curve has a size inherent to it enables definition of a functionally equivalent  $RT_{T_0}$  indexed  $K_{Ic}$  curve without concern that an "appropriate" size is used in the analysis. This size is defined by the empirical data set used to establish the bounding curve.

While flaw size is implicit to an empirically defined bounding curve, it must be specified explicitly to conduct a structural analysis. In current application, the  $K_{Ic}$  curve is used to assess flaws with different sizes and shapes. Even though this methodology leaves flaw size effects on toughness unaccounted for, it works because the flaw size implicit in the definition of  $RT_{NDT}$  matches the distribution of flaw sizes commonly encountered in RPVs. The flaw size distributions used in PTS analysis provide the best representation of the actual vessel. These flaw size distributions correspond to crack front lengths in the range of 1-2 inches, which match the 1.6-2.5 inch size inherent to the definition of  $RT_{NDT}$ . Conversely, the largest flaw size analyzed in the course of normal vessel integrity analysis is the  $\frac{1}{4}$  T flaw assumed in the determination of the pressure-temperature operating limits. This large flaw size was selected primarily because it assured that the applied-K values calculated for normal loading conditions were large (and therefore conservative). At the time that this reference flaw was selected, it was not anticipated that this large flaw size would produce a penalty in terms of reduced toughness. Therefore, in effect the current practice uses the  $\frac{1}{4}$ -T flaw size to calculate loads, but bases the material toughness curve on more realistic estimates of flaw size (1.6-2.4 inches).

### 6.5.2 Functional Equivalence of $RT_{T_o}$ to $RT_{NDT}$ as an Index Temperature for the $K_{IC}$ Curve

$T_o$  indexes the variation of fracture toughness with temperature. Recently, an ASME task group advocated adoption of a  $T_o$ -based index temperature (termed  $RT_{T_o}$ ) as an alternative to  $RT_{NDT}$  [9] indexing of the ASME  $K_{IC}$  curve. The task group proposed the following relationship:

$$RT_{T_o} \equiv T_o + \Delta \quad (6-1)$$

The task group proposed a  $\Delta$  value of 35°F. The long range objective of the task group is to use a bounding Master Curve as a replacement for the current ASME reference curves. A complete reassessment of the acceptable confidence levels for the ASME reference curves would be consistent with the long range objectives of the task group. However the short range objective of using  $RT_{T_o}$  as an alternative to  $RT_{NDT}$  requires some linkage to historical safety margins. To maintain this linkage,  $\Delta$  must be selected such that the  $K_{IC}$  curve, when indexed to  $RT_{T_o}$ , bounds available fracture toughness data in a manner equivalent to how the  $K_{IC}$  curve indexed to  $RT_{NDT}$  bounds available fracture toughness data. The selection of  $\Delta$  must be based on an understanding of the appropriate relationship between the two index temperatures ( $RT_{NDT}$  and  $RT_{T_o}$ ). The data in Table 5.4 for which both  $T_o$  and  $RT_{NDT}$  values are available are used to examine this relationship.

To perform this evaluation, an objective definition of the term "functionally equivalent" is needed. The purpose of the reference temperature is to set the reference toughness curve ( $K_{IC}$  curve) in a manner that appropriately bounds the data. In order to develop an objective definition of "functional equivalence" a quantitative measure of the bounding nature of the reference curve is required. This quantitative measure may be determined by taking the difference in degrees Fahrenheit between the measured toughness values and the resulting reference curve. This quantity is related to the level of confidence in the bounding curve and provides a measure of the implicit margin on toughness contained in the definition of the reference temperature. As illustrated in Figure 6-1 for two RPV materials, the average temperature differences between the measured toughness data and the reference curve as defined by the current  $RT_{NDT}$  methodology vary considerably from one material to another. In contrast, the statistical nature of the Master Curve technology makes it possible to define this average temperature difference explicitly by controlling the value of  $\Delta$  in equation 6-1 (see Figure 6-2). It is not possible to define  $\Delta$  to maintain the margin implicit to a  $RT_{NDT}$  indexed  $K_{IC}$  curve because no single, unique, margin exists in the current methodology. The ability to define consistent margins is the key advantage of the Master Curve approach and the weakness of the  $RT_{NDT}$  methodology. The selection of an appropriate  $\Delta$  value requires criteria for judging the appropriate spacing between the fracture toughness data and the reference toughness curve. Criteria for judging the functional equivalence of the alternative reference temperature must define both the data set to be analyzed and an appropriate acceptance level. These criteria must encompass the ambiguity in the margin inherent in the existing approach. Three possible criterion are discussed below:

1. When indexed to  $RT_{T_0}$ , the resulting  $K_{IC}$  curve should provide an absolute bound to all data not on the lower shelf.
2. The implicit level of confidence in an  $RT_{T_0}$  indexed  $K_{IC}$  curve should equal or exceed the minimum acceptable level for the limiting material in the current  $RT_{NDT}$  based approach.
3. The implicit level of confidence in the  $RT_{T_0}$  indexed  $K_{IC}$  curve should equal or exceed the average level for the original  $K_{IC}$  database in the current  $RT_{NDT}$  based approach.

In the following discussions, it will be shown that the first criterion imposes a level of conservatism that unnecessarily exceeds currently accepted levels. The remaining two criteria are consistent with the  $\Delta$  value of 35°F selected by the ASME task group.

#### 6.5.2.1 Absolute Bound to All Data

At first inspection, this definition appears consistent with the approach used to establish the  $K_{IC}$  curve. However, this criterion is strongly dependent on the number and type of measurements included in the database and does not provide a rational basis for evaluating functional equivalence.  $\Delta$  can be defined to ensure that a  $K_{IC}$  curve indexed to  $RT_{T_0}$  provides an absolute lower bound to all data not on the lower shelf (i.e. at temperatures exceeding  $T - RT_{NDT} = -100^\circ\text{F}$ ). Analysis of the data in Table 5.4 indicates that a  $\Delta$  value of 105°F would be required to satisfy this criterion. Increases in the amount of toughness data available (163 values when the  $K_{IC}$  curve was established *vs.* 1228 values today) produce a six-fold reduction in the proportion of future data expected to lie below the bounding curve (0.6% historically *vs.* 0.1% now). In order to keep the probability of a single datum falling below the bounding curve constant as the number of data points increases, the value  $\Delta$  of must increase. The adoption of this, or any other, absolute bounding criteria would lead to the irrational situation where obtaining more data on the fracture of pressure vessel steels would increase the margin required of reactor vessel integrity analysis. This increase in margin is neither needed or justified.

#### 6.5.2.2 Implicit Level of Confidence Matches Minimum of Current Approach

The level of margin implicit to the current assessment methodology (i.e., a  $RT_{NDT}$  indexed  $K_{IC}$  curve) varies considerably from material to material (see Figure 6-1). Therefore, in the past one could rely only on a level of implicit margin characteristic of the most limiting material (Plate HSST-02). Consequently, it is the level of confidence in the bounding curve implicit to HSST-02 which the newly proposed  $T_0$ -based methodology must maintain to align with the current licensing basis for commercial nuclear plants. The level of confidence in the bounding curve is directly related to the sum of the squares of the temperature residuals between the bounding curve and the measured toughness values.  $\Delta$  can be defined to ensure that the data set which established the position of the  $K_{IC}$  curve when indexed to  $RT_{NDT}$  (HSST-02) has the same implicit level of confidence (i.e. same proximity of toughness data to the bounding curve) when the  $K_{IC}$  curve is indexed to  $RT_{T_0}$ . This criterion is analogous to the procedure used to establish confidence bounds in regression analysis, and can be accomplished as follows:

1. Calculating the mean sum of squares of temperature residuals between the  $K_{IC}$  curve (indexed to  $RT_{NDT}$ ) and the HSST-02 data set (see Figure 6-3).
2. Varying  $\Delta$  until the mean sum of squares of temperature residuals between the  $K_{IC}$  curve (indexed to  $RT_{T_0}$ ) and the HSST-02 data set becomes equivalent to the value calculated in Step 1.

This value of  $\Delta$  required to maintain the level of conservatism for the HSST 02 data set is 17°F. The proposed value of 35°F exceeds this requirement by 18°F.

### 6.5.2.3 Implicit Level of Confidence for Original $K_{IC}$ Database Maintained

The current ASME reference curve and  $RT_{NDT}$  referencing temperature were based on the analysis of a particular data set. Any judgments about the acceptable levels of confidence in the reference curves for reactor pressure vessel integrity analysis are buried in the relationship between the original fracture toughness data and the reference curve. An equivalent level of confidence for this set of materials can be established using a process similar to that used in Section 6.5.2.2 for the HSST-02 data:

1. Calculate the mean sum of squares of temperature residuals between the  $K_{IC}$  curve (indexed to  $RT_{NDT}$ ) and the original  $K_{IC}$  data set.
2. Vary  $\Delta$  until the mean sum of squares of temperature residuals between the  $K_{IC}$  curve (indexed to  $RT_{T_0}$ ) and the original  $K_{IC}$  data set becomes equivalent to the value calculated in Step 1.

The value of  $\Delta$  required to maintain an equivalent level of confidence for the original  $K_{IC}$  database is 33°F. The proposed value of 35°F exceeds this minimum value.

## 6.6 IMPLICIT MARGINS

In the preceding section the functional equivalence between a  $RT_{T_0}$  and a  $RT_{NDT}$  indexed  $K_{IC}$  curve was evaluated in terms of the level of confidence in the curve as a lower bound to an empirical data set. Had a value of 0°F been selected for  $\Delta$ , the  $K_{IC}$  curve would begin to approach the median Master Curve and the level of confidence that the curve would bound any new measurements would be relatively low. Obviously, the level of confidence that the curve will bound any new data increases as the value of  $\Delta$  increases. As described previously, any procedure for setting the reference temperature contains implicit assumptions about the acceptable level of confidence. Any increase in  $\Delta$  beyond the value required to achieve the minimum acceptable level of confidence may be viewed as the margin implicit in the definition of the reference temperature. This is an implicit margin because it is contained in the definition of the reference temperature as opposed to the explicit margins, which are added on to the reference temperature to cover additional uncertainties or provide an extra degree of conservatism.

The reference toughness curves are meant to provide a lower bound to the measured toughness values. The Master Curve approach provides a lower bound curve with a well defined level of confidence because it keys the reference curve directly to fracture toughness measurements. While the ductile-to-brittle transition is a characteristic attribute of ferritic steels, it is a complex phenomenon. In the traditional approach, the parameter  $RT_{NDT}$  is used to correlate two manifestations of this phenomenon (the Charpy transition temperature and the drop weight nil-ductility temperature) to the manifestation of particular interest (the fracture toughness transition). There is a large material-to-material variability implicit to the traditional correlative approach. This variability has led to inconsistencies in the level of conservatism inherent in the use of  $RT_{NDT}$  as an indexing parameter. These inconsistencies can be eliminated by the use of the Master Curve. The transition portion of the original  $K_{IC}$  curve was determined primarily by one material (HSST Plate 02). However, the degree of conservatism varies greatly from material to material.

As previously described, the implicit margin may be defined as the increase in  $\Delta$  beyond the minimum acceptable level. The only basis for establishing the minimum acceptable level is to analyze what has been historically accepted. The limiting material in the original  $K_{IC}$  database (HSST Plate 02) defines a minimum acceptable level of confidence. Thus the corresponding implicit margin for Plate HSST-02 must be zero. Note that the analysis provided in Section 6.5.2.2 indicates that this level of confidence corresponds to a  $\Delta$  value of 17°F. Because the relationship between a  $T_o$  indexed reference curve and the fracture toughness data is the same for all materials, the use of  $\Delta=17^\circ\text{F}$  would make the confidence level for all materials equivalent to the historically accepted confidence level. This would imply that the implicit margin for the proposed definition  $RT_{T_o}$  (with  $\Delta=35^\circ\text{F}$ ) is 18°F for all materials (including Plate HSST-02).

There is no corresponding fundamental relationship between  $RT_{NDT}$  and the fracture toughness data. Experience subsequent to the establishment of the  $K_{IC}$  curve has indicated that the majority of reactor pressure vessel steels exhibited toughness data well above a  $K_{IC}$  curve indexed to  $RT_{NDT}$ . As previously stated, the work of Sokolov [1997] demonstrates that there is no direct correlation between  $RT_{T_o}$  and  $RT_{NDT}$ . However, there are a number of materials for which  $RT_{NDT}$  and  $T_o$  have been independently measured. In these cases, the implicit margin for the  $RT_{NDT}$  indexed curve can be estimated by taking the difference between the reference temperature calculated with  $\Delta=17^\circ\text{F}$  and  $RT_{NDT}$ . This approach was used to evaluate the implicit margins in  $RT_{NDT}$  values for a variety of materials, as illustrated in Figure 6-4.

The large separation between the  $K_{IC}$  curve and the measured fracture toughness values has led to the general perception that the  $RT_{NDT}$  methodology is highly conservative. This conservatism is evident in the implicit margins illustrated in Figure 6-4. Because HSST-02 sets the acceptable level of confidence on the bounding fracture toughness curve, it has, by definition, an implicit margin of zero. Although many materials have larger implicit margins than Plate HSST-02, there is no rational way to demonstrate that any particular material has a larger implicit margin without making fracture toughness measurements. Master Curve technology uses fracture toughness measurements to set  $RT_{T_o}$ . The use of  $RT_{T_o}$  would increase this implicit margin for all materials exhibiting implicit margins less than 18°F in Figure 6-4. However many materials that now have excessively large implicit margins will have lower values of the reference



temperature ( $RT_{T_0} < RT_{NDT}$ ). The selection of the  $RT_{T_0}$  definition is effectively a determination of the appropriate level of implicit margin. Prior to the development of the Master Curve, there was no rational or consistent basis for the analysis of these margins. The Master Curve provides a basis for estimating margins that is consistent across all materials.

## 6.7 MARGIN TERMS IN THE DETERMINATION OF REFERENCE TEMPERATURES

The ASME  $K_{IC}$  reference curve is a lower bound to measured data. It was constructed by compiling fracture toughness data from multiple materials on a temperature scale referenced to a measured value of  $RT_{NDT}$ . The analysis of the preceding sections indicate that  $RT_{T_0}$  is an indexing parameter for the  $K_{IC}$  curve that is functionally equivalent to current approaches based on  $RT_{NDT}$ . There is an uncertainty associated with the measurement of any value, including  $RT_{NDT}$ . However, it is the relationship between the reference toughness curve and the fracture toughness data that determines the reliability inherent to the overall methodology. Because the  $K_{IC}$  curve was established on an empirical basis using measured values of  $RT_{NDT}$ , the effects of any uncertainty in the determination of the reference temperature are automatically included in the analysis. Therefore, the uncertainty (or explicit margin) applied to measured values of  $RT_{NDT}$  are assumed to be zero (as described in NRC Regulatory Guide 1.99 Rev. 2 and 10CFR50.61). This does not imply that there is no uncertainty in the determination of  $RT_{NDT}$ , but merely that the uncertainty is already reflected in the relationship between  $RT_{NDT}$  and the reference toughness curve. There are also measurement uncertainties in the determination of  $T_0$  (and by association  $RT_{T_0}$ ). ASTM E1921-97 suggests that the uncertainty in the determination of  $T_0$  is described by the Eq. (5-12), which is repeated here for clarity:

$$T_0|_{\text{mod}} = T_0 + \frac{\beta}{\sqrt{N}} \quad (6-2)$$

If the relationship between the  $K_{IC}$  curve and  $RT_{T_0}$  was solely based on consideration of the Master Curve confidence bounds, an uncertainty (or explicit margin) term could be required to assure the appropriate relationship between the measured toughness values and the reference curve. However, the basis for selection of  $\Delta = 35^\circ\text{F}$  in the relationship between  $T_0$  and  $RT_{T_0}$  was empirical. It is interesting to note that the difference between the  $\Delta$  values determined using Plate HSST-02 in Section 6.5.2.2 and the  $\Delta$  value determined using multiple materials in Section 6.5.2.3 is  $15^\circ\text{F}$ . This difference corresponds to typical  $\beta/\sqrt{N}$  values for small data sets. This would seem to indicate that the uncertainty in the  $T_0$  determination is included in the proposed value of  $\Delta=35^\circ\text{F}$ . Therefore, consistent with the current  $RT_{NDT}$  based approach, no explicit margin term should be required when using measured values of  $RT_{T_0}$ . However, for conservatism in the Kewaunee vessel analyses, the uncertainty in  $T_0$  was included as discussed in Section 7.

## 6.8 SUMMARY

The Master Curve provides a superior definition of the fracture toughness transition temperature and facilitates the analysis of margins on a consistent and rational basis. Because

the Master Curve is capable of producing consistent implicit margins, it is feasible to consider what margin is acceptable. The level of margin implicit in the  $RT_{NDT}$  based technology is inconsistent from material to material, rendering general statements about the Master Curve technology increasing or decreasing margins inmeaningless. As a consequence of this variability, in the past one could only rely on a level of confidence consistent with that of the most limiting material. Consequently, it is the historical minimum level of confidence (i.e., that of HSST-02) which the newly proposed  $T_o$ -based methodology must maintain to align with the current licensing basis for commercial nuclear plants.

The ASME code case establishes a  $T_o$ -based index temperature,  $RT_{T_o}$ , in a manner consistent with the intent of current practice. The ASME task group charged with developing the technical basis ASME code case concluded that the functional equivalent of  $RT_{NDT}$  is defined as follows:

$$RT_{T_o} \equiv T_o + 35^\circ F \quad (6-3)$$

This recommendation exceeds the value needed to maintain consistency with the current licensing basis by 18°F. Consequently, this proposal for  $RT_{T_o}$  emerges as an indexing parameter for the  $K_{IC}$  curve that forces every application to exceed the minimum level of confidence inherent in the current procedures. In this sense, the proposed use of  $RT_{T_o}$  as an indexing parameter is more conservative than current approaches based on  $RT_{NDT}$ .

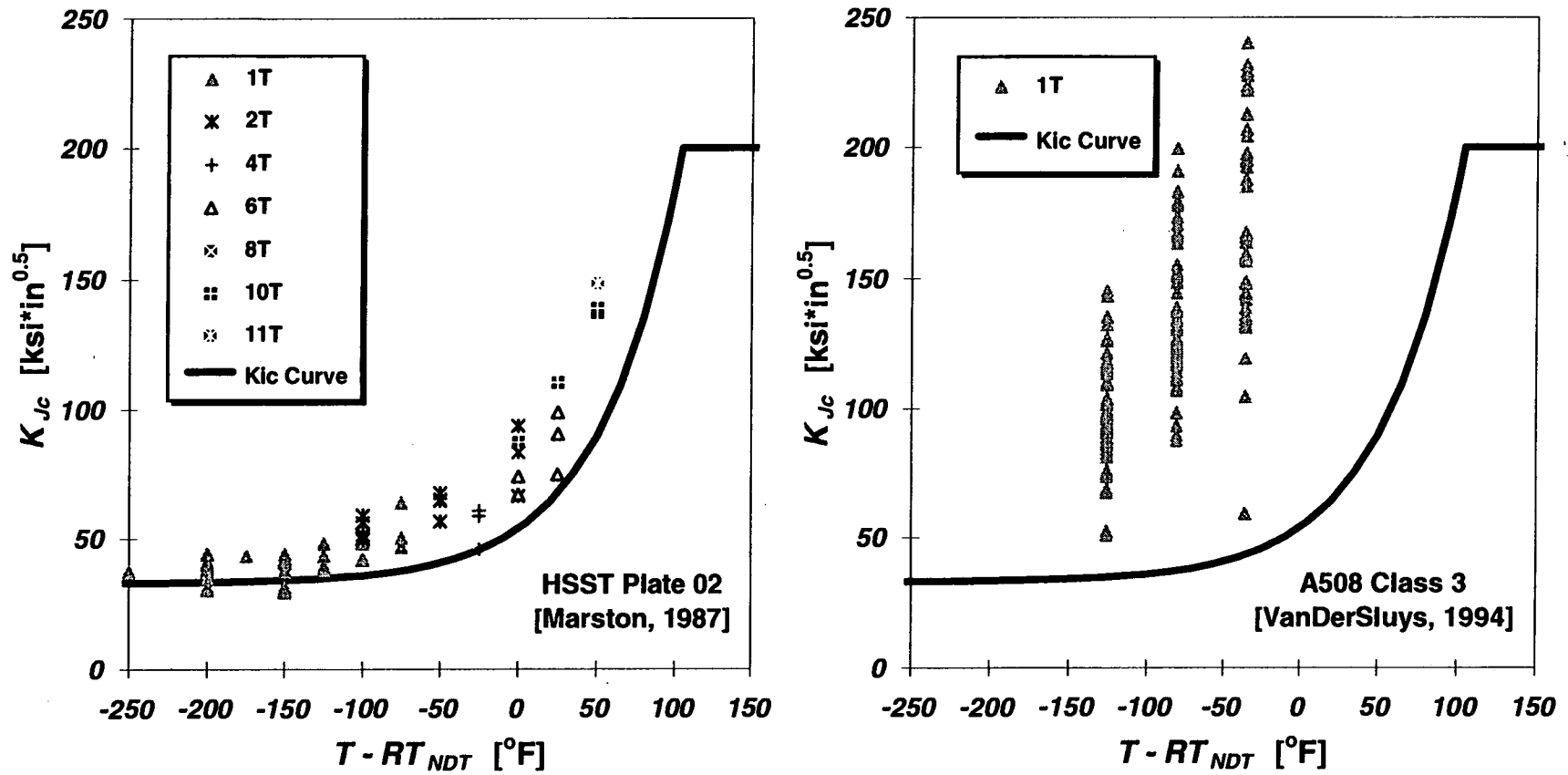


Figure 6-1 Comparison of How  $RT_{NDT}$  Positions Two Different Heats of RPV Steel Relative to the  $K_{Ic}$  Curve

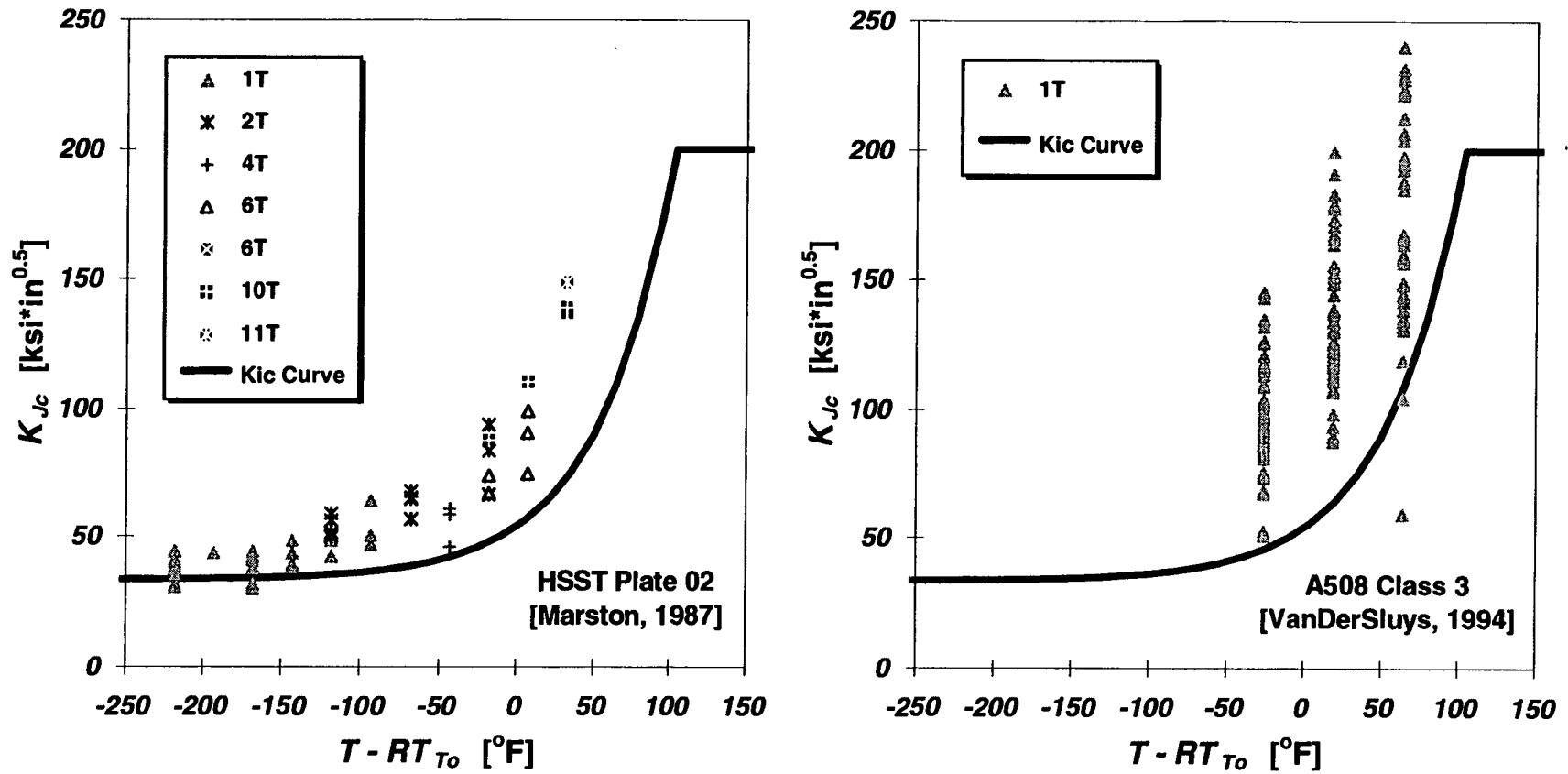


Figure 6-2 Comparison of How  $RT_{To}$  Positions Two Different Heats of RPV Steel Relative to the  $K_{Ic}$  Curve

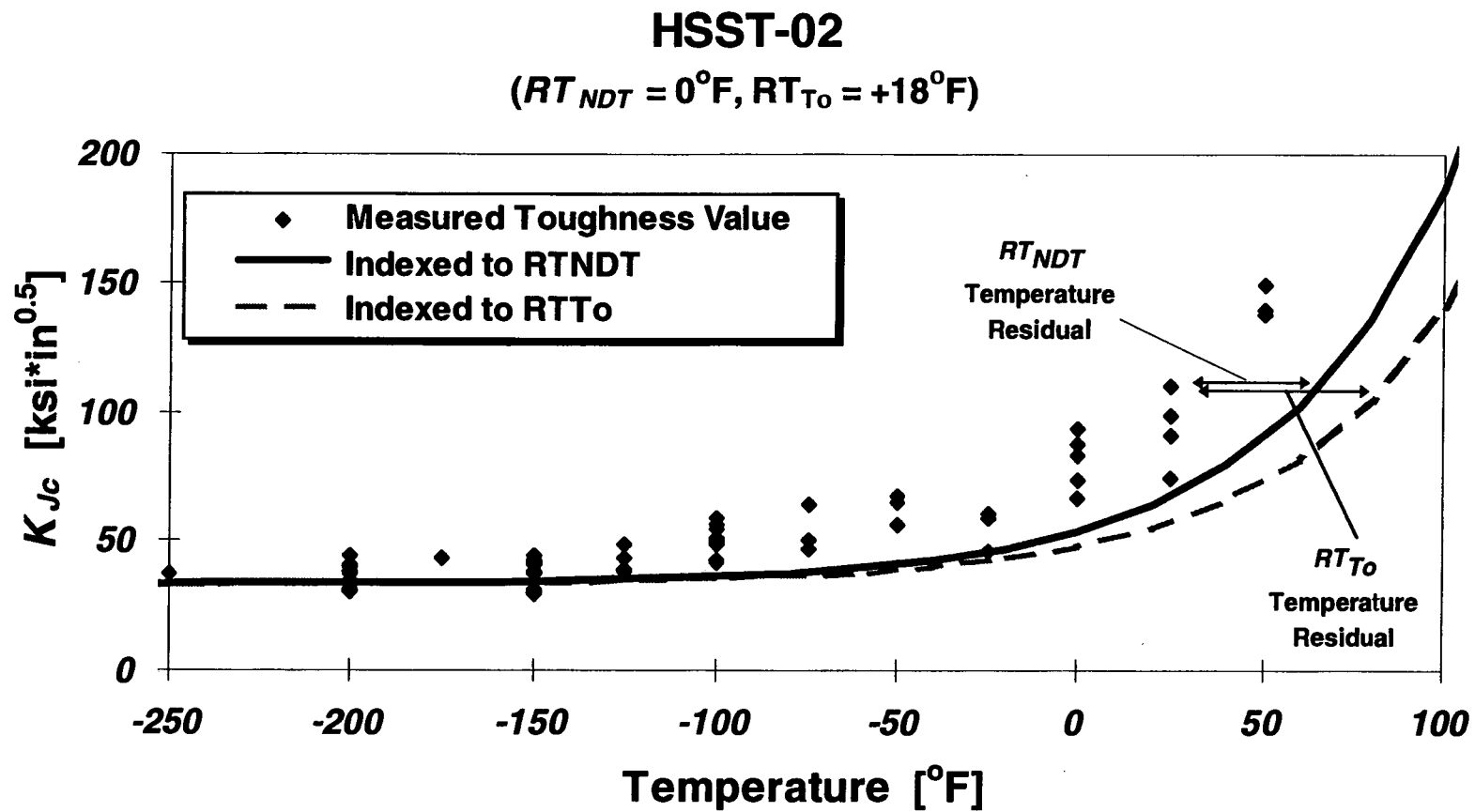


Figure 6-3 HSST-02 Data and the  $K_{Jc}$  Curve Indexed Using  $RT_{NDT}$  (Solid Curve) and  $RT_{T_0}$  (Dashed Curve) Positions

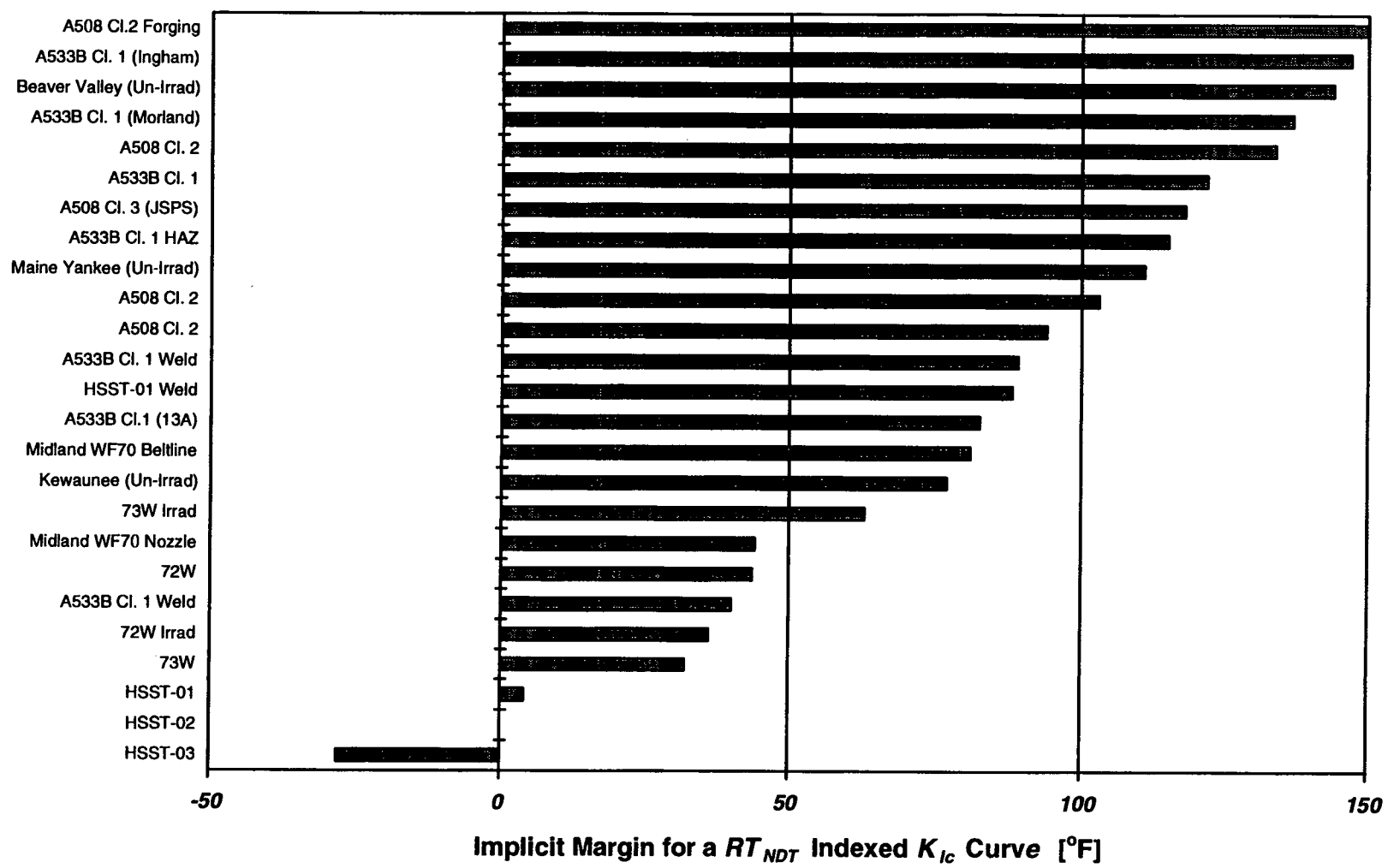


Figure 6-4 Implicit Margin for Various RPV Steels

## 7.0 EVALUATION OF THE KEWAUNEE VESSEL

The objective of this effort is to integrate results obtained using the Master Curve procedure into the existing reactor pressure vessel evaluation methodology. In the preceding sections of this report, it was demonstrated that the  $RT_{70}$  can be used in place of  $RT_{NDT}$  as a reference temperature for the ASME  $K_{IC}$  curve. Although there is no direct correlation between these two parameters, either reference temperature can be used to predict a reliable lower bound toughness curve. In this sense they are functionally equivalent. However within the integrated family of codes and regulations that govern the operation of a nuclear pressure vessel, the value of  $RT_{NDT}$  is often used without direct reference to the  $K_{IC}$  curve. For instance, 10CFR50.61 defines the pressurized thermal shock (PTS) screening criteria in terms of maximum allowed values for the adjusted reference temperature. These screening criteria were based on a probabilistic analysis that described the temperature dependence of fracture toughness in terms of the irradiation adjusted value of  $RT_{NDT}$ . While the relationship between the reference temperature and the fracture toughness data is inherent in this analysis, it is not immediately apparent to the user. The normal pressure-temperature operating limits for the reactor are also directly related to the irradiation adjusted value of  $RT_{NDT}$ . Again, the fracture toughness reference curve (which in this case is the  $K_{IR}$  curve) is inherent in the calculation but not immediately obvious to the user. Implicit in the PVRC short range plan to use  $RT_{70}$  as an alternative means of indexing the fracture toughness reference curve is the assumption that  $RT_{70}$  may also be used as a direct replacement for  $RT_{NDT}$  in reactor pressure vessel integrity analysis.

### 7.1 SUMMARY OF CURRENT APPROACH BASED ON CHARPY TESTING

Reactor pressure vessel integrity analysis requires the evaluation of the fracture toughness of the irradiated material. The determination of  $RT_{NDT}$  in unirradiated material is the first step in this evaluation. The evaluation is then accomplished by calculating the adjusted reference temperature,  $ART$ , as defined in 10 CFR 50.61. The adjusted reference temperature is a conservative estimate of the irradiated value of  $RT_{NDT}$ , which is used as an indexing parameter for the  $K_{IC}$  and  $K_{IR}$  curves.  $ART$  is determined by taking the sum of the unirradiated  $RT_{NDT}$  value ( $IRT$ ), the Charpy transition temperature shift and an explicit margin term,  $M$ :

$$ART = IRT + \Delta RT_{NDT} + M \quad (7-1)$$

The explicit margin term combines the uncertainty in the determination of the unirradiated  $RT_{NDT}$  value,  $\sigma_v$ , with the uncertainty in the determination of the Charpy transition temperature shift,  $\sigma_\Delta$ . As suggested by the notation, the standard deviation of the estimate (or a reasonable approximation of that value) is used as the measure of uncertainty. The explicit margin is defined as two times the root mean square of the unirradiated and irradiated uncertainty values:

$$M \equiv 2\sqrt{\sigma_v^2 + \sigma_\Delta^2} \quad (7-2)$$

Any procedure that uses  $RT_{70}$  as a replacement for  $RT_{NDT}$  in the calculation of the  $ART$  must either account for or maintain the intent and function of the related irradiation shift and margin terms.

Procedures for using  $RT_{70}$  to calculate  $ART$  should parallel current practice. Current practice recognizes several different situations that require different methods of determining the adjusted reference temperature. These methods are illustrated schematically in Figure 7-1. The analysis of the adjusted reference temperature for the Kewaunee vessel is discussed in more detail WCAP 15074. The results of the previous analysis are summarized by methods 1-4 in Table 7-1. These methods accommodate the amount of available data on the vessel materials. In particular the current practice prefers measurements of  $RT_{NDT}$  but allows generic values for classes of materials when measurements are not available, and prefers measurement of Charpy shifts, but allows the use of predictive equations when credible surveillance data is not available. Each method has an associated margin term with a unique combination of uncertainties (see Table 7-1). The margin terms reflect both the uncertainty in the measurement of the transition temperature and the uncertainty associated with use of generic data. In general, the largest penalties are applied to situations where material specific data is not available.

The number of possible permutations has been significantly increased by recent regulatory actions that require the consideration of all sources of data on a material (generally defined as given weld flux and weld wire heat). In Figure 7-1, this effect has been recognized by including an additional material heat evaluation. The material heat evaluation implements the ratio method for adjusting the chemistry factor as described in WCAP 15074. The impact of the material heat evaluation can best be understood by segregating these effects into a separate term,  $\Delta RT_{HT}$ , which includes adjustments made to the calculational procedure based on surveillance data and/or chemistry data on the same heat of material from outside sources. The results of this evaluation for the Kewaunee vessel weld are illustrated in the last two columns of Table 7-1. For the Kewaunee vessel weld, the Maine Yankee weld is the primary source of additional data. The calculation of these  $ART$  values for the Kewaunee nuclear pressure vessel are addressed in a separate report [Server et al., 1998].

The various options for evaluating a reactor pressure vessel weld to determine  $ART$  within the context of Reg. Guide 1.99 (Rev. 2) are outlined below. Similar options exist for reactor vessel plates and forgings. These options are illustrated in the flow chart provided in Figure 7-1.

1. Determine the initial (or un-irradiated) reference temperature (the  $IRT$ ). Use either generic properties or plant specific properties.
  - 1.1 Generic properties
    - 1.1.1  $IRT$  is defined as the industry generic  $RT_{NDT}$  which is specified by the PTS rule as  $-56^{\circ}\text{F}$ .
    - 1.1.2 Include an uncertainty on initial properties in the margin term ( $M$ ) of  $\sigma_1=17^{\circ}\text{F}$ .



- 1.2 Plant specific properties
  - 1.2.1 *IRT* is defined based on measurements for the limiting material in question.
  - 1.2.2 The uncertainty on measured initial properties in the margin term (*M*) is defined as zero.
  
2. Determine the irradiation induced shift ( $\Delta RT_{NDT}$ )
  - 2.1 Credible surveillance program
    - 2.1.1  $\Delta RT_{NDT}$  is defined using the surveillance data based on the fitting procedures detailed in 10 CFR50.61(c)(2)(ii)
    - 2.1.2 The uncertainty on irradiation shift properties in the margin term (*M*) is defined as  $\sigma_{\Delta} = 14^{\circ}\text{F}$ .
  - 2.2 Non-credible surveillance program
    - 2.2.1  $\Delta RT_{NDT}$  is defined using chemistry data based on the fitting procedures detailed in 10 CFR50.61 (c)(1)(iii)
    - 2.2.2 The uncertainty on irradiation shift properties in the margin term (*M*) is defined as  $\sigma_{\Delta} = 28^{\circ}\text{F}$ .
  
3. Determine the heat adjusted reference temperature shift ( $\Delta RT_{HT}$ )
  - 3.1 Credible surveillance program
    - 3.1.1  $\Delta RT_{HT}$  is defined using available surveillance data and the Ratio method detailed in Reg. Guide 1.99 Rev. 2
  - 3.2 Non-credible surveillance program
    - 3.2.1  $\Delta RT_{HT}$  is defined using a heat averaged(best-estimate) chemistry factor
  
4. Calculate the heat adjusted *ART*

$$ART = IRT + \Delta RT_{NDT} + \sqrt{\sigma_i^2 + \sigma_{\Delta}^2} + \Delta ART_{HT} \quad (7-3)$$

## 7.2 ALTERNATIVE APPROACHES BASED ON FRACTURE TOUGHNESS TESTING

### 7.2.1 Structure of Alternative Approaches

Several alternative paths for determining the  $ART$  are illustrated in Figure 7-2. These paths indicate how  $RT_{70}$  measurements on both unirradiated and irradiated materials can be integrated into an  $ART$  evaluation in a way that satisfies the intent of 10CFR50.61. Shifts, uncertainties, and margins are added to measured  $RT_{70}$  values as appropriate, always with the aim of satisfying the intent of 10CFR50.61. A detailed description of the margins adopted in each path, and a basis for these margins, is included in Sections 7.2.2 through 7.2.7

### 7.2.2 Values of $T_0$ Used in these Evaluations

Fracture toughness data for the limiting material in the Kewaunee RPV (Linde 1092 Heat 1P3571) and for this weld in Kewaunee's sister plant, Maine Yankee, are available from the following sources:

- Kewaunee un-irradiated: WCAP-14279, Rev. 1
- Kewaunee irradiated to  $3.36 \times 10^{19}$  n/cm<sup>2</sup>: WCAP-14279, Rev. 1
- Maine Yankee un-irradiated: WPSC(CEOG/RVWG)
- Maine Yankee irradiated to  $6.11 \times 10^{19}$  n/cm<sup>2</sup>: WCAP-14279, Rev. 1

These data are used in this section to calculate  $T_0$  values for the 1P3571 weld by two different techniques.  $T_0$  is calculated as per ASTM E1921-97 (as described in Section 5.2.3.3 of this report) when sufficient replicate testing was performed at one temperature. Also,  $T_0$  is calculated using Wallin's maximum likelihood technique [Wallin, 1995]. This technique permits combination of fracture toughness data obtained at different test temperatures using different specimen sizes. The ASTM E1921-97 procedure for single-size/single-temperature data sets is actually a special case of Wallin's procedure.

$T_0$  is determined iteratively by Wallin's procedure using the following equation and a non-linear root finder:

$$\sum_{i=1}^n \left[ \frac{\delta_i \cdot \exp\{c(T_i - T_0)\}}{a - K_{\min} + b \cdot \exp\{c(T_i - T_0)\}} \right] - \sum_{i=1}^n \left[ \frac{(K_{Jc}^i - K_{\min})^4 \cdot \exp\{c(T_i - T_0)\}}{\|a - K_{\min} + b \cdot \exp\{c(T_i - T_0)\}\|^5} \right] = 0 \quad (7-4)$$

where

$n$  is the number of toughness specimens tested

$T_i$  is the test temperature

$K_{Ic}$  is the measured toughness value, converted to 1T equivalence using Eq. (5-8)

$$a = 28.179 \text{ ksi}\sqrt{\text{in}}$$

$$b = 69.993 \text{ ksi}\sqrt{\text{in}}$$

$$c = 0.0106$$

$$K_{\min} = 18.18 \text{ ksi}\sqrt{\text{in}}$$

$\delta_i$  is 1 if Eq. (7-4) is satisfied

is 0 if Eq. (7-4) is not satisfied

Table 7-2 summarizes the values of  $T_o$  and of measurement uncertainty (Eq. 5-12) for the 1P3571 weld that result from these calculations. Figure 7-3 illustrates that no statistically significant difference exists between the four possible estimates of  $T_o$  for the unirradiated condition. We therefore employ Wallin's technique for  $T_o$  calculation to ensure that no relevant data for the 1P3571 weld is excluded from consideration. The resultant values of  $T_o$  are as follows:

- Kewaunee Weld 1P3571 un-irradiated:  $T_o = -144.2^\circ\text{F}$ ,  $\sigma = 6.5^\circ\text{F}$
- Kewaunee weld 1P3571 irradiated to  $3.36 \times 10^{19} \text{ n/cm}^2$ :  $T_o = 147.7^\circ\text{F}$ ,  $\sigma = 8.2^\circ\text{F}$
- Maine Yankee 1P3571 un-irradiated  $T_o = -158.4^\circ\text{F}$ ,  $\sigma = 12.8^\circ\text{F}$
- Maine Yankee weld 1P3571 irradiated to  $6.11 \times 10^{19} \text{ n/cm}^2$ :  $T_o = 231.6^\circ\text{F}$ ,  $\sigma = 11.5^\circ\text{F}$

### 7.2.3 Verification of $RT_{T_o}$ for Kewaunee Weld 1P3571

$RT_{T_o}$  can be determined for the limiting Kewaunee weld (1P3571) in both the unirradiated and irradiated conditions using Eq. (6-1) and the  $T_o$  data presented in Table 7-2. These values are  $-109^\circ\text{F}$  and  $+183^\circ\text{F}$ , respectively. Figures 7-4 and 7-5 show fracture toughness data for unirradiated and irradiated 1P3571, and plot these data relative to a bounding  $K_{Ic}$  curve indexed to these  $RT_{T_o}$  values. All fracture toughness values on these plots are scaled to 2.4T equivalence using Eq. (5-15). A size of 2.4T is selected to make these 1P3571 data sets equivalent to the average thickness for the HSST-02 data set. Note that these curves still continue to bound all available data.

### 7.2.4 Alternative Measurements of Initial Reference Temperature (Paths 5a & 5b)

Paths 5a and 5b combine unirradiated fracture toughness properties determined by Master Curve testing with irradiation induced Charpy shifts to calculate ART values. The flowcharts for these paths are indicated in Figure 7-2 and the calculations for the Kewaunee are illustrated in Table 7-1. For paths 5a and 5b, the initial reference temperature is the  $RT_{T_o}$  value for the

unirradiated material (-109°F). The margin term associated with this *IRT* is taken as the uncertainty in the determination as defined in ASTM E1921 ( $\sigma_i \equiv \beta/\sqrt{N}$ ). For the unirradiated Kewaunee material, this value is 7°F. Because *IRT* is a measured value, it would be consistent with established practice to set the uncertainty in this value to zero (see Section 6.7). The addition of the extra uncertainty term makes the proposed approach more conservative than the equivalent  $RT_{NDT}$  based approach.

The irradiation induced shift term ( $\Delta RT_{NDT}$ ) in the reference temperature must be evaluated using Charpy data as indicated by paths 5a and 5b. The procedures used to calculate the  $\Delta RT_{NDT}$  term are identical to those used to calculate Charpy shifts in the standard 10CFR50.61 procedures. The calculations for path 5a, follows the same procedures as paths 3 & 4, while path 5b duplicates the calculations of paths 1 & 2. There is, however, one necessary modification. Paths 5a and 5b combine measured fracture toughness values with a Charpy-based irradiation shift, a practice not described in 10CFR50.61. This practice produces an additional uncertainty in the shift term.

Studies conducted at Oak Ridge indicate that, while there is a general correlation between these transition temperatures, significant variability may be expected on a material by material basis [Rosseel, 1998]. For welds, there is a one-to-one correlation between Charpy transition temperature shift and fracture toughness transition temperature shift. However, the 95% confidence bands for this correlation are at  $\pm 54^\circ\text{F}$ . This corresponds to a standard deviation of  $27^\circ\text{F}$ . When using an un-irradiated  $T_0$  and combining it with a Charpy shift, the shift uncertainty ( $\sigma_\Delta$ ) is increased to account for this additional  $27^\circ\text{F}$  according to the following formula:

$$\sigma_\Delta = \sqrt{\sigma_{\Delta CVN}^2 + (27)^2} \quad (7-5)$$

where

$$\sigma_{\Delta CVN} = \begin{array}{l} 14^\circ\text{F for a credible surveillance program, or} \\ 28^\circ\text{F for a non-credible surveillance program (as per Reg. Guide 1.99)} \end{array}$$

The results of calculations performed to determine the adjusted reference temperature at the end of license for the Kewaunee surveillance weld are summarized in Table 7-1. Adjustments for heat uncertainty apply only to the irradiation induced shifts and well established heat-average chemistry and ratioing procedures can be applied to this analysis because there are no alterations in the process of calculating the shift. Table 7-1 accumulates all of these terms for both paths 5a (credible surveillance,  $ART = 242^\circ\text{F}$ ) and 5b (non-credible surveillance,  $ART = 252^\circ\text{F}$ ). Because the fracture toughness determination of *IRT* under ASTM E1921 is much lower than the conventional measurement, the best estimate reference temperature is also much lower. However, the additional uncertainty associated with the process of combining fracture toughness measurements with Charpy shifts consumes a portion of this difference.

### 7.2.5 Direct Measurements of Irradiated Fracture Toughness (Path 6)

Master Curve technology enables direct estimation of a reference temperature ( $RT_{70}$ ) for irradiated materials by testing a set of specimens as per E1921-97. If specimens with appropriate irradiation fluences are available, ART values may be determined directly using the procedure outlined in path 6. This process eliminates both unirradiated testing to determine the  $IRT$  and  $\sigma_I$  (Step 1 in Section 7.2), and the Charpy shift term (Step 2 in Section 7.2). The only contribution to the explicit margin term in this case is the uncertainty in the determination of the irradiated  $T_o$  value. This uncertainty is determined using a procedure outlined in ASTM E1921 ( $\sigma_{70} = \beta/\sqrt{N}$ ). For the irradiated Kewaunee weldment, this value is 8°F. This approach provides a explicit margin for measurement uncertainty in  $T_o$  even though no explicit margin for measurement uncertainty is required under current practice when  $IRT$  values are measured directly. From Table 7-2,  $T_o$  for the irradiated Kewaunee surveillance weld is 148°F. Therefore  $RT_{70}$  in the irradiated condition (i.e., the best estimate of the  $RT_{NDT}$ ) is 183°F ( $T_o + 35^\circ\text{F}$ ). The Kewaunee specific ART value contains an extra 16°F margin term. Adjustments to this procedure for heat uncertainty are discussed separately later.

### 7.2.6 Determination of Fracture Toughness Shift (Path 7)

The determination of the reference temperature for irradiated materials in cases where the neutron fluence for the available specimens does not match the fluence of interest requires an irradiation trend curve. This analysis path is noted as path 7 in Figure 7-2. While this does not apply to the evaluation of the end-of-license evaluation for the Kewaunee vessel, it can be important in considering extended operation. Extended operation of the Kewaunee vessel is considered separately in Section 7.3. The currently accepted curve for predicting the irradiation response of the reference temperature is provided in 10CFR50.61:

$$\Delta RT_{NDT} = (CF)\phi t^{(0.28-0.1\log \phi t)} \quad (7-6)$$

This trend curve predicts irradiation induced shifts in the reference temperature. Although the trend curve is based solely on the analysis of Charpy data, it is routinely used to shift the fracture toughness reference curves. In order to apply this trend curve to the Master Curve measurements, a determination of the irradiation induced shift in the fracture toughness reference temperature ( $T_o$ ) is required. Therefore, measurements of both the unirradiated and irradiated fracture toughness transition temperatures are required. An irradiation induced shift for the measured data,  $\Delta RT$ , can then be calculated. The measured shift in fracture toughness for the Kewaunee surveillance weld was 292°F at  $3.36 \times 10^{19} \text{ n/cm}^2$ . The chemistry factor term in the trend curve can then be recalculated to match the trend curve to the measurement. If more than one measurement is available, a fitting procedure would be required. This chemistry factor may be calculated with a procedure similar to that currently used to determine material specific chemistry factors from surveillance data:

$$CF = \frac{\sum_{i=1}^n \left[ A_i x \phi t_i^{(0.28-0.1 \log \phi t_i)} \right]}{\sum_{i=1}^n \phi t_i^{(0.56-0.2 \log \phi t_i)}} \quad (7-7)$$

where "A<sub>i</sub>" is the measured value of  $\Delta T_0$  and " $\phi t_i$ " is the fluence for each  $\Delta T_0$  determination. The PTS Rule requires a minimum of two  $\Delta RT_{NDT}$  measurements to determine a chemistry factor from Charpy data using this formula. While a similar number of  $T_0$  measurements would be preferable, for the purposes of this analysis, chemistry factors have been calculated on the basis of a single determination. Using this procedure, a chemistry factor of 222°F was calculated for the Kewaunee surveillance weld. A similar analysis for the Maine Yankee surveillance weld derived a chemistry factor of 271°F. These new chemistry factors can then be used to calculate entire trend curves for the reference temperature. The predicted Kewaunee and Maine Yankee trend curve are shown in Figure 7-6.

This procedure keys the prediction to measured fracture toughness data in a manner analogous to the use of Charpy data from a surveillance program to determine  $\Delta RT_{NDT}$ . Therefore, it seems reasonable to select a margin term consistent with the use of the 10CFR50.61 trend curve. Because the prediction is based on measured values rather than a generic trend curve, the uncertainty term from paths 3&4 ( $\sigma_\Delta = 14^\circ\text{F}$ ) was assumed for path 7. Note that if the point of analysis is the point of measurement, this methodology will reduce to the same best estimate value as method 6. In this case, there would be a margin penalty for selecting path 7 over path 6. However, as the distance between the point of analysis and the point of measurement grows, the amount of extrapolation required increases and the use of the larger uncertainty term seems more reasonable. This distinction may become important in situations where estimates of fracture toughness are required for neutron fluences lower than the fluence at the point of measurement. One example of this situation would be evaluations of the attenuation of fracture toughness through the vessel wall when a determination of the fracture toughness at the vessel ID fluence is available. In this case, margin terms consistent with the calculations in path 6 should be applied to the trend curve predictions.

### 7.2.7 Heat to Heat Uncertainty (Surrogate Materials)

Within the regulatory process, significant questions about the effects of material variability on the predicted fracture toughness transition temperature have been raised. Welds fabricated with identical weld wire heats and fluxes have exhibited varying sensitivities to irradiation. This situation exists for the Kewaunee and Maine Yankee surveillance welds. Both surveillance programs contain Linde 1092 welds fabricated from weld wire heat 1P3571. However, the Maine Yankee material has demonstrated a higher sensitivity to irradiation. Metallurgical studies [Server, 1998] indicate clear differences in these two materials. Most significantly, the Maine Yankee weld appears to have a higher Cu content than the Kewaunee weld. Given the clear differences in these materials, the obvious question is as follows: is the Kewaunee surveillance weld an appropriate surrogate for the structural welds in the Kewaunee reactor vessel? In order to assure that the predicted transition temperatures are representative of the

## 7.5 RECOMMENDATION FOR ART VALUES

On the basis of these results, it is recommended that the following values of the adjusted reference temperature,  $ART$ , be used for assessment of the structural integrity of the Kewaunee Nuclear Power Plant reactor pressure vessel at the EOL fluence of  $3.34 \times 10^{19}$  n/cm<sup>2</sup>.

$$ART = 199^{\circ}\text{F} \quad (\text{Kewaunee Data Only})$$

$$ART_{HT} = 234^{\circ}\text{F} \quad (\text{Adjusted for Maine Yankee Data})$$

The fracture toughness data required for a direct determination of the  $ART$  value for the Kewaunee surveillance weld at the extended operation fluence of  $5.06 \times 10^{19}$  n/cm<sup>2</sup> is not currently available. The utility plans are to obtain this data and complete the evaluation as the surveillance specimens become available. In the interim, the value of  $ART$  determined on the basis of the Maine Yankee fracture toughness data is recommended:

$$ART_{HT} = 249^{\circ}\text{F} \quad (\text{Includes Heat Adjustment}).$$

Table 7-1 ART Determination for the Kewaunee Weld and Vessel

Method	Best Estimate of Initial RT <sub>NDT</sub> Value (IRT), °F	Standard Deviation for IRT ( $\sigma$ ), °F	Kewaunee Surveillance Estimate of Shift ( $\Delta$ RT), °F	Standard Deviation for $\Delta$ RT ( $\sigma_D$ ), °F	Best Estimate of Irradiated Value, °F	Total Margin (M) °F	Adjusted Reference Temperature (ART) °F	Additional Adjustment for Heat Uncertainty ( $\Delta$ RT <sub>HT</sub> ) °F	Heat Adjusted Reference Temperature (ART <sub>HT</sub> ) °F
1.) Current Technology Measured IRT; No Credible CVN Data	Measured Value, RT <sub>NDT</sub> = -50	"Assumed" 0	RG1.99R2, CF Table 246	RG1.99R2 28	IRT+ $\Delta$ RT 196	$2(\sigma_1^2 + \sigma_\Delta^2)^{1/2}$ 56	IRT+ $\Delta$ RT+M 252	Ind. Mean Chemistry 36	288
2.) Current Technology; Generic IRT; No Credible CVN Data	PTS Rule RT <sub>NDT</sub> = -56	PTS Rule 17	RG1.99R2, CF Table 246	RG1.99R2 28	IRT+ $\Delta$ RT 190	$2(\sigma_1^2 + \sigma_\Delta^2)^{1/2}$ 66	IRT+ $\Delta$ RT+M 256	Ind. Mean Chemistry 36	292
3.) Current Technology; Measured IRT; Credible CVN Data	Measured Value, RT <sub>NDT</sub> = -50	"Assumed" 0	RG1.99R2, Data Fit 253	RG1.99R2 14	IRT+ $\Delta$ RT 203	$2(\sigma_1^2 + \sigma_\Delta^2)^{1/2}$ 28	IRT+ $\Delta$ RT+M 231	Ratio Adj. 36	267
4.) Current Technology ; Generic IRT; Credible CVN Data	PTS Rule RT <sub>NDT</sub> = -56	PTS Rule 17	RG1.99R2, Data Fit 253	RG1.99R2 14	IRT+ $\Delta$ RT 197	$2(\sigma_1^2 + \sigma_\Delta^2)^{1/2}$ 44	IRT+ $\Delta$ RT+M 241	Ratio Adj. 36	277
5a.) Master Curve ; Unirradiated To ; Credible CVN Data	Unirradiated To +35°F RT <sub>To</sub> = -109	ASTM $\beta/\sqrt{n}$ 7	RG1.99R2, Data Fit 253	RG1.99R2 & To to CVN 30	RT <sub>NDT(U)</sub> + $\Delta$ RT <sub>NDT</sub> 144	$2(\sigma_1^2 + \sigma_\Delta^2)^{1/2}$ 62	IRT <sub>To</sub> + $\Delta$ RT <sub>NDT</sub> +M 206	Ratio Adj. 36	242
5b.) Master Curve; Unirradiated To ; No Credible CVN Data	Unirradiated To +35°F RT <sub>To</sub> = -109	ASTM $\beta/\sqrt{n}$ 7	RG1.99R2, CF Table 246	RG1.99R2 & To to CVN 39	RT <sub>NDT(U)</sub> + $\Delta$ RT <sub>NDT</sub> 137	$2(\sigma_1^2 + \sigma_\Delta^2)^{1/2}$ 79	IRT <sub>To</sub> + $\Delta$ RT <sub>NDT</sub> +M 216	Ind. Mean Chemistry 36	252
6.) Master Curve; Irradiated To	NA	NA	NA	ASTM $\sigma_{To} = \beta/\sqrt{n}$ 8	Irradiated To +35°F 183	$2\sigma_{To}$ 16	RT <sub>To(irr)}</sub> + M 199	MY meas. w/ Ratio Adj. 35	234
7.) Master Curve Shift; Measured RT <sub>NDT(U)</sub> ; Irr. To-Unirr. To	Unirradiated To +35°F RT <sub>To</sub> = -109	ASTM $\beta/\sqrt{n}$ 7	Data Fit, CF = 222 292	Similar to RG1.99R2 14	RT <sub>To</sub> + $\Delta$ RT <sub>To</sub> 183	$2(\sigma_1^2 + \sigma_\Delta^2)^{1/2}$ 31	IRT + $\Delta$ RT <sub>To</sub> +M 214	MY meas. w/ Ratio Adj. 35	249



vessel materials, the NRC has required additional adjustments to the predictions. These adjustments require use of industry mean chemistry values, and/or of the ratio procedure.

For the Kewaunee vessel, adjustments to the *ART* to account for heat uncertainty require analysis of the Maine Yankee surveillance weld. The analysis of the heat uncertainty in the Charpy data was described by Server [1998] and is summarized in Table 7-1. For the Charpy data, the adjustment applied depends on the availability of credible surveillance data. If credible data surveillance data is not available, the heat adjustment is based on an industry mean chemistry approach. If credible surveillance data is available, the results are adjusted using the ratio procedure. Both the industry mean chemistry approach and the ratio procedure produce additional adjustments for heat chemistry of 36°F. This adjustment applies to all of the Charpy based methods for determining *ART*, including paths 5a and 5b, which combine unirradiated  $T_0$  measurements with Charpy transition temperature shifts.

An alternative method of determining the heat uncertainty is required for paths 6 and 7, which use irradiated  $T_0$  measurements in lieu of Charpy shifts. The heat uncertainty can be estimated from a knowledge of the Maine Yankee fracture toughness data. The higher radiation sensitivity of the Maine Yankee surveillance weld is evident in the higher chemistry factor calculated in Section 7.2.6 (271°F for Maine Yankee versus 222°F for Kewaunee). The industry average composition for weld heat 1P3571 is intermediate to the two surveillance welds (chemistry factor ratio = 0.536). It would therefore be expected that the heat adjusted trend curve should fall between the two surveillance welds. This intermediate trend curve can be constructed by applying the ratio procedure to the respective chemistry factors. The chemistry factor determined for weld 1P3571 by applying this ratioing technique is 248°F. The trend curve produced corresponding to this heat average (or ratioed) chemistry factor is also illustrated in Figure 7-6. At the projected Kewaunee EOL fluence of  $3.34 \times 10^{19}$  n/cm<sup>2</sup>, the difference between the Kewaunee surveillance weld and the 1P3571 industry average trend curve is 35°F. This difference corresponds closely to the 36°F value found by applying a similar analysis to the Charpy data. This agreement indicates the concerns about material variability and surrogate materials are independent of the Master Curve. Therefore it is possible to use the technically superior Master Curve approach and maintain the desired level of margin to accommodate the desired margin for material uncertainty. The 35°F material heat adjustment has been added to both cases 6 and 7 to obtain appropriate end-of-license *ART* values for the material in the Kewaunee beltline circumferential weld. These values are: 234°F for path 6 and 249°F for path 7. The higher value for path 7 can be attributed to the higher margins imposed to accommodate the use of the trend curve.

### 7.3 CALCULATIONS FOR EXTENDED OPERATION

The response of the Kewaunee reactor pressure vessel to extended operation has also been evaluated. The calculation *ART* values for a target extended operation fluence of  $5.06 \times 10^{19}$  n/cm<sup>2</sup> are indicated in Table 7-3. For paths 1 through 5b and for path 7, these calculations are simple extensions of the procedures outlined for Table 7-2. In these cases, the calculations have been repeated using the higher fluence values. However, path 6 requires additional consideration, which is also summarized in Table 7-3.

The application of path 6 requires a measurement of fracture toughness at the fluence of interest. For Kewaunee, the extended end-of-license fluence is significantly higher than the available plant-specific surveillance data. However,  $T_0$  data from the Maine Yankee 1P3751 surveillance weld was determined at a fluence that slightly exceeds the target for extended operation of the Kewaunee vessel. The determined  $RT_{T_0}$  value for the Maine Yankee surveillance weld at a fluence of  $6.1 \times 10^{19}$  n/cm<sup>2</sup> is 267°F. The trend curve provided in Figure 7-3 can be used to determine that the  $RT_{T_0}$  value for the Maine Yankee surveillance weld at  $5.06 \times 10^{19}$  n/cm<sup>2</sup> should be 257°F. Applying a measurement uncertainty of 12°F to the  $RT_{T_0}$  value produces an ART value of 281°F for the Maine Yankee surveillance weld. This value must then be adjusted to provide a response appropriate to the industry mean chemistry. This can be accomplished by applying the ratio procedure described in Section 7.2.7. In this case, the industry mean response is expected to have a lower radiation sensitivity than the Maine Yankee surveillance weld. Therefore, the adjustment to the Maine Yankee ART for heat uncertainty is negative (-32°F). The heat adjusted ART value for extended operation of the Kewaunee reactor vessel calculated using the procedures outlined under path 6 is 249°F.

#### 7.4 COMPARISON OF METHODS

Table 7-1 and Figure 7-7 compare the eight different methods for estimating the irradiated fracture toughness transition temperature for the Kewaunee surveillance weld. The most interesting comparisons between methods is in the best estimate of the ART (sixth column in Table 7-1), and the best estimate of the ART adjusted for uncertainties in initial properties, in shift value, and in heat variability (last column in Table 7-1).

Methods 1 through 4 are analyses based on  $RT_{NDT}$  and Charpy data. Methods 1 through 4 are 10CFR 50.61 assessments of the Kewaunee reactor pressure vessel. These methods produce best estimates of the reference temperature that only vary over a limited range (from 190°F to 203°F). However, when the margin terms and heat adjustment terms are included, the corresponding ART values are approximately 80°F higher and the range of values increases significantly (from 267°F to 292°F).

The Master Curve test procedure is employed in Methods 5a, 5b, 6 and 7. In all four cases, the best estimate of the irradiated reference temperature is lower than estimates based on  $RT_{NDT}$  and Charpy. The lowest estimates of irradiated reference temperature were obtained in methods 5a (144°F) and 5b (137°F), which combined the unirradiated  $RT_{T_0}$  measurements with shifts based on Charpy data. The unirradiated  $RT_{T_0}$  value for the Kewaunee weld (-109°F) was significantly lower than the unirradiated  $RT_{NDT}$  value (-50°F). Conversely, direct measurement of the ART Method 6 produces a higher value (183°F). However, when the margins are added in, the ART value for the direct measurement is the lowest. This reversal occurs because a large margin must be applied in paths 5a and 5b to account for the uncertainty that arises when Charpy data is used to shift unirradiated  $T_0$  values. As direct measurements of fracture toughness at the fluence of interest are available, it is recommended that Method 6 be adopted for analysis of the Kewaunee vessel.

Table 7-2 Summary of Kewaunee and Maine Yankee Weld  $T_0$  Values

Data Set ID	$T_0$ Calculation Method	# of Valid Tests	Invalid Tests ?	Test Temperature [°F]	$T_0$ [°F]	$\sigma = \beta/N^{0.5}$ [°F]
Kewaunee Unirradiated 1/2T	E1921-97	7	None	-187	-129.0	12.8
Kewaunee Unirradiated PC-CVN	E1921-97	8	2 with bad precrack	-200	-148.5	12.0
Kewaunee Unirradiated PC-CVN (ReCon)	E1921-97	7	None	-200	-154.3	12.8
Kewaunee Unirradiated All	Wallin 97	22	None	various	-144.2	6.5
Kewaunee Irradiated PC-CVN (ReCon)	E1921-97	8	1 above $K_{Ic}$ Limit & 1 with bad precrack	136	135.9	10.8
Kewaunee Irradiated PC-CVN (ReCon)	N/A	3	None	59	N/A	N/A
Kewaunee Irradiated 1XWOL	N/A	2	None	136	N/A	N/A
Kewaunee Irradiated ALL	Wallin 97	13	1 above $K_{Ic}$ Limit	various	147.7	8.2
Maine Yankee Unirradiated PC-CVN	E1921-97	7	None	-200	-158.4	12.8
Maine Yankee Irradiated PC-CVN (ReCon)	E1921-97	7	1 above $K_{Ic}$ Limit	210	231.6	11.5

Table 7-3 ART Determination for the Kewaunee Weld and Vessel ( $5.06 \times 10^{19}$  n/cm<sup>2</sup> version)

Method	Best Estimate of Initial RT <sub>NDT</sub> Value (IRT), °F	Standard Deviation for IRT ( $\sigma_i$ ), °F	Kewaunee Surveillance Estimate of Shift ( $\Delta$ RT), °F	Standard Deviation for $\Delta$ RT ( $\sigma_\Delta$ ), °F	Best Estimate of Irradiated Value, °F	Total Margin (M) °F	Adjusted Reference Temperature (ART) °F	Additional Adjustment for Heat Uncertainty ( $\Delta$ RT <sub>HT</sub> ) °F	Heat Adjusted Reference Temperature (ART <sub>HT</sub> ) °F
1.) Current Technology Measured IRT; No Credible CVN Data	Measured Value, RT <sub>NDT</sub> = -50	"Assumed" 0	RG1.99R2, CF Table 263	RG1.99R2 28	IRT+ $\Delta$ RT 213	$2(\sigma_i^2 + \sigma_\Delta^2)^{1/2}$ 56	IRT+ $\Delta$ RT+M 269	Ind. Mean Chemistry 39	308
2.) Current Technology; Generic IRT; No Credible CVN Data	PTS Rule RT <sub>NDT</sub> = -56	PTS Rule 17	RG1.99R2, CF Table 263	RG1.99R2 28	IRT+ $\Delta$ RT 207	$2(\sigma_i^2 + \sigma_\Delta^2)^{1/2}$ 66	IRT+ $\Delta$ RT+M 273	Ind. Mean Chemistry 39	312
3.) Current Technology; Measured IRT; Credible CVN Data	Measured Value, RT <sub>NDT</sub> = -50	"Assumed" 0	RG1.99R2, Data Fit 270	RG1.99R2 14	IRT+ $\Delta$ RT 220	$2(\sigma_i^2 + \sigma_\Delta^2)^{1/2}$ 28	IRT+ $\Delta$ RT+M 248	Ratio Adj. 39	287
4.) Current Technology; Generic IRT; Credible CVN Data	PTS Rule RT <sub>NDT</sub> = -56	PTS Rule 17	RG1.99R2, Data Fit 270	RG1.99R2 14	IRT+ $\Delta$ RT 214	$2(\sigma_i^2 + \sigma_\Delta^2)^{1/2}$ 44	IRT+ $\Delta$ RT+M 258	Ratio Adj. 39	297
5a.) Master Curve; Unirradiated To; Credible CVN Data	Unirradiated To +35°F RT <sub>To</sub> = -109	ASTM $\beta/\sqrt{n}$ 7	RG1.99R2, Data Fit 270	RG1.99R2 & To to CVN 30	RT <sub>To</sub> + $\Delta$ RT <sub>NDT</sub> 161	$2(\sigma_i^2 + \sigma_\Delta^2)^{1/2}$ 62	IRT <sub>To</sub> + $\Delta$ RT <sub>NDT</sub> +M 223	Ratio Adj. 39	262
5b.) Master Curve; Unirradiated To; No Credible CVN Data	Unirradiated To +35°F RT <sub>To</sub> = -109	ASTM $\beta/\sqrt{n}$ 7	RG1.99R2, CF Table 263	RG1.99R2 & To to CVN 39	RT <sub>To</sub> + $\Delta$ RT <sub>NDT</sub> 154	$2(\sigma_i^2 + \sigma_\Delta^2)^{1/2}$ 79	IRT <sub>To</sub> + $\Delta$ RT <sub>NDT</sub> +M 233	Ind. Mean Chemistry 39	272
6.) Master Curve; Irradiated To  <i>See Note</i> <i>M.Y. Fluence</i> <i>Kewaunee Ext. EOL</i>	NA	NA	NA	ASTM $\sigma_{To} = \beta/\sqrt{n}$ 12	To +35°F Meas. 267 Est. 257	$2\sigma_{To}$ 24	RT <sub>To(Irr.)</sub> + M 291 281	Kew. meas. w/ Ratio Adj. -32	$6.1 \times 10^{19}$ 259 $5.1 \times 10^{19}$ 249
7.) Master Curve Shift; Measured RT <sub>NDT(U)</sub> ; Irr. To-Unirr. To	Unirradiated To +35°F RT <sub>To</sub> = -109	ASTM $\beta/\sqrt{n}$ 7	Data Fit, CF = 222 311	Similar to RG1.99R2 14	RT <sub>To</sub> + $\Delta$ RT <sub>To</sub> 202	$2(\sigma_i^2 + \sigma_\Delta^2)^{1/2}$ 31	IRT <sub>To</sub> + $\Delta$ RT <sub>To</sub> +M 233	MY meas. w/ Ratio Adj. 37	270

Note: Case 6 based on the Maine Yankee Measurement at  $6.1 \times 10^{19}$  n/cm<sup>2</sup>. The result was then ratioed back to the Kewaunee vessel chemistry.

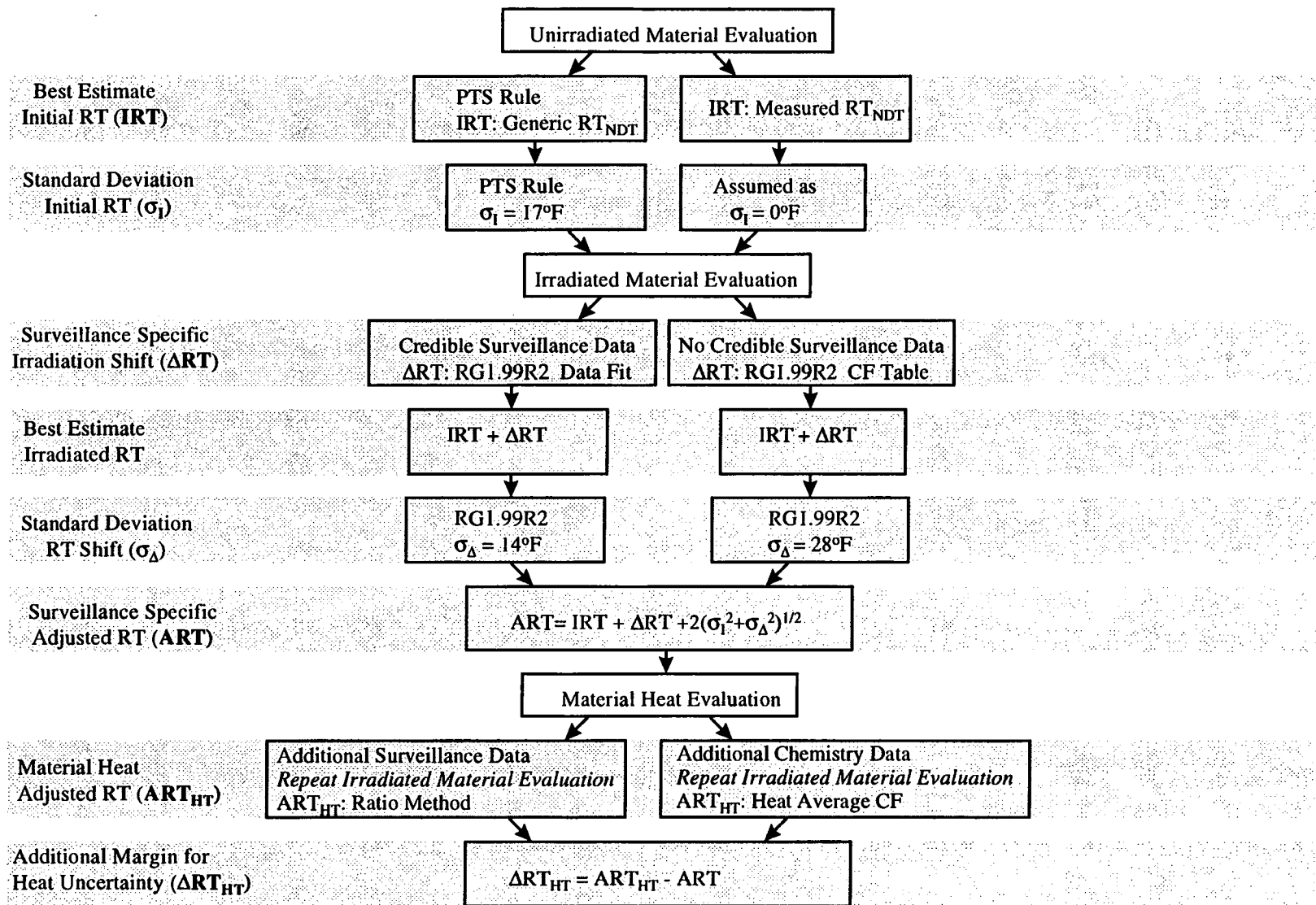


Figure 7-1 Paths for Estimation of the ART Using Current Technology

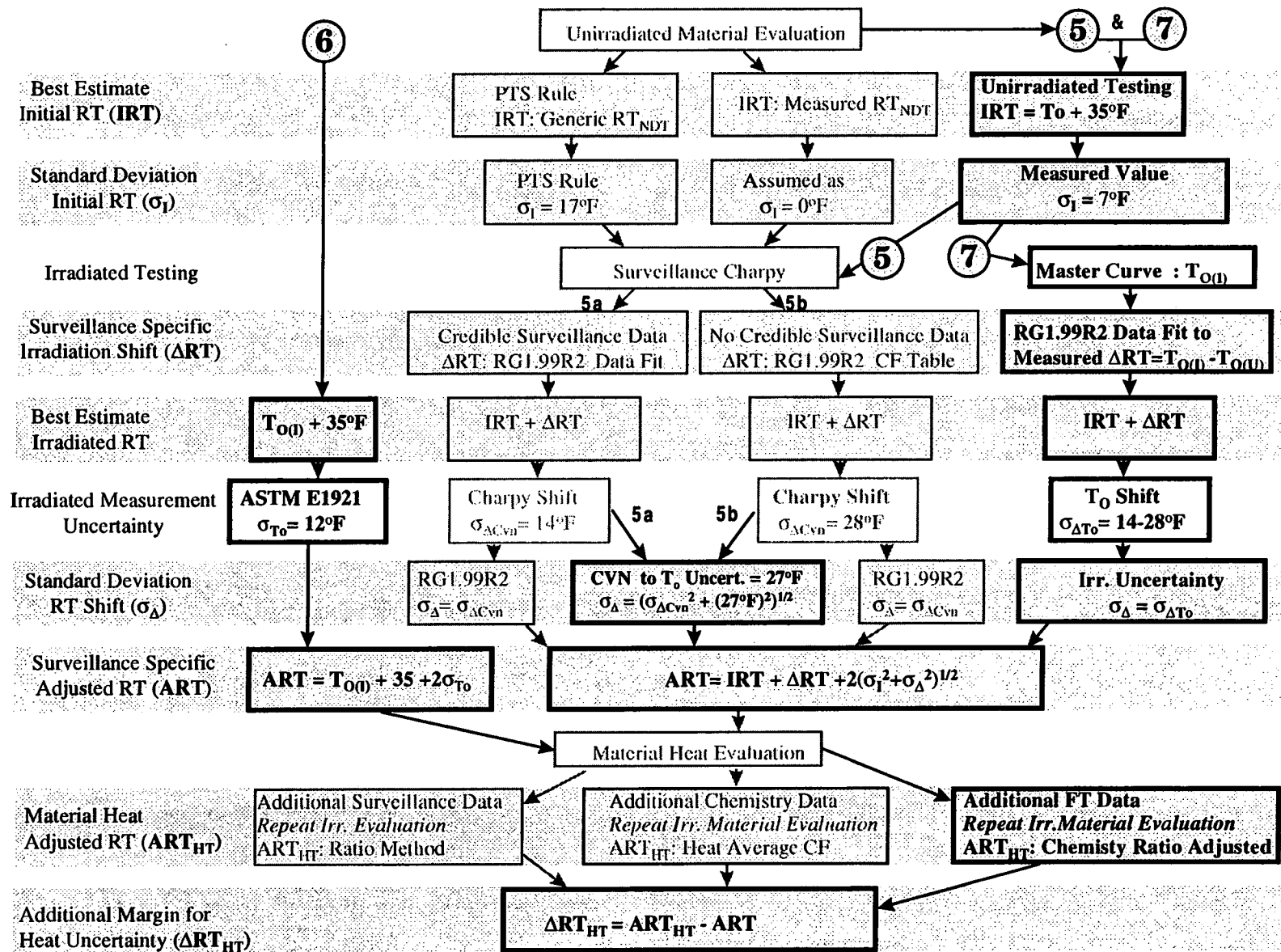


Figure 7-2 Paths for Implementation of Master Curve Estimation of the ART Compared with Current Technology (specific numbers represents the case for 51 EFPY)

Mean Square Distance to Bounding  
Toughness Curve [°F]

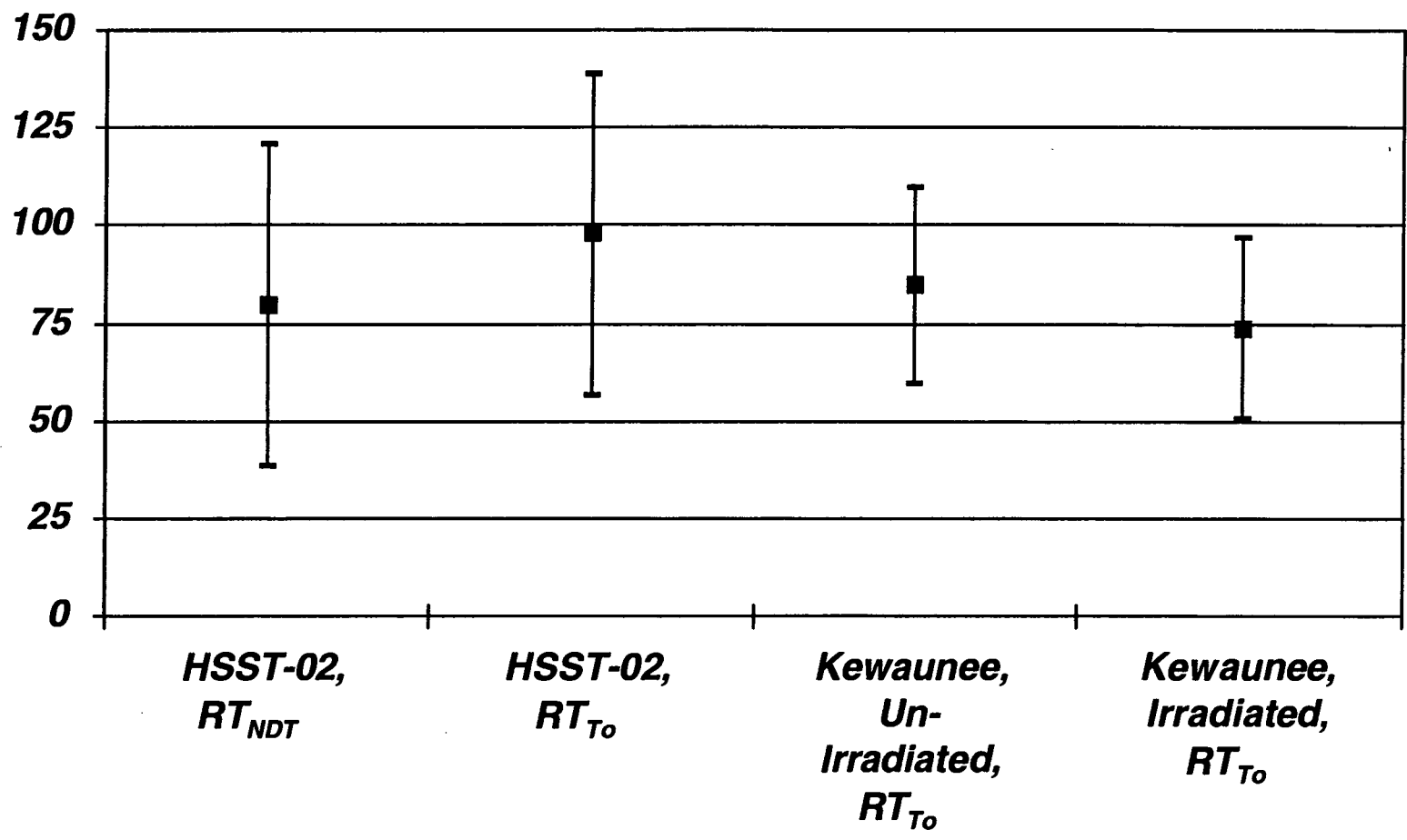


Figure 7-3 Comparison of mean square distance between fracture toughness data and bounding toughness curves between Kewaunee and HSST Plate 02.

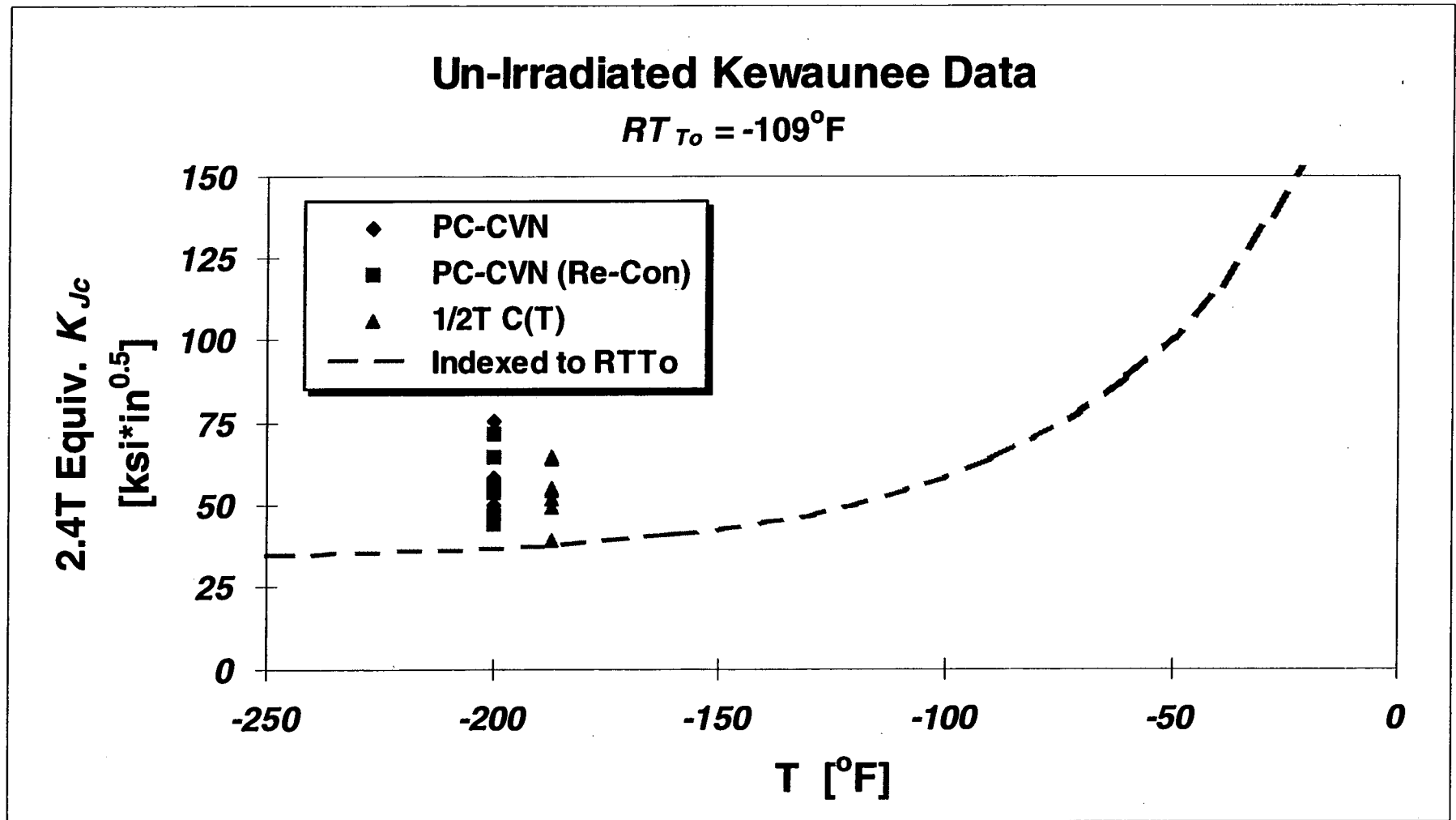


Figure 7-4 Comparison of un-irradiated Kewaunee fracture toughness data and bounding  $K_{Jc}$  curve based on  $RT_{T_0}$ .



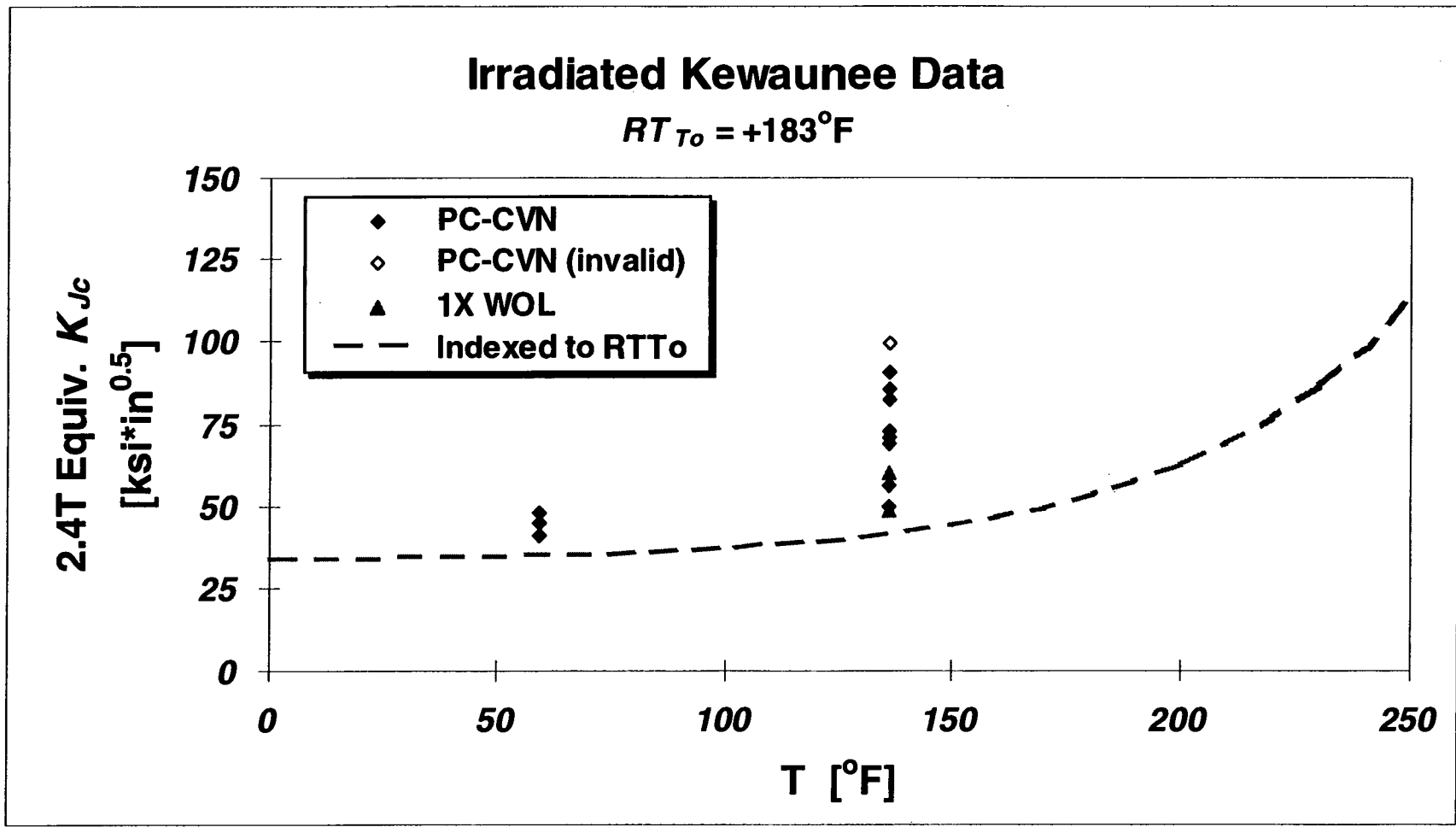


Figure 7-5 Comparison of irradiated Kewaunee fracture toughness data and bounding  $K_{Jc}$  curve based on  $RT_{T_0}$

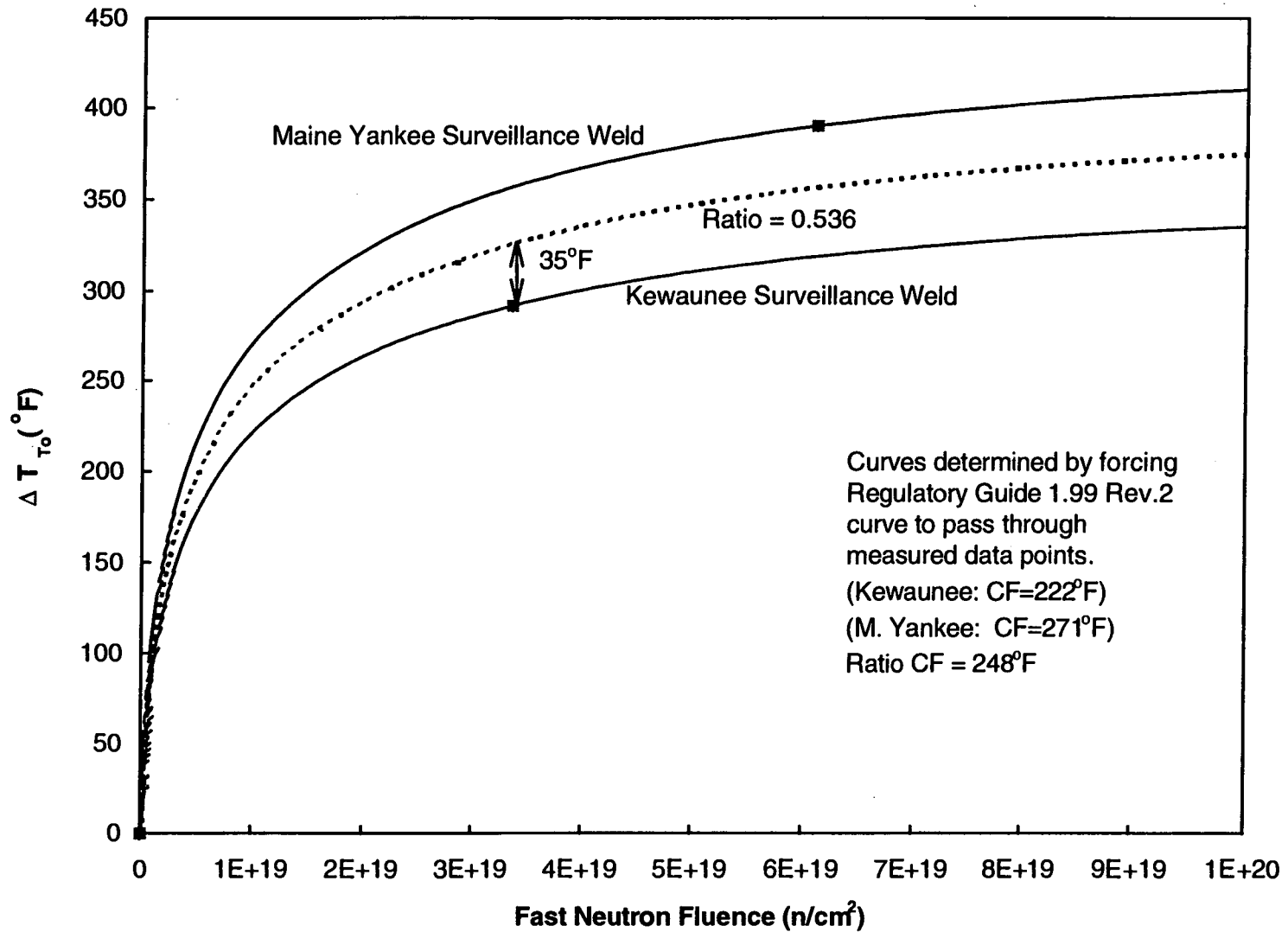


Figure 7-6 Variation of  $RT_{T_0}$  with Neutron Fluence for Kewaunee and Maine Yankee Materials

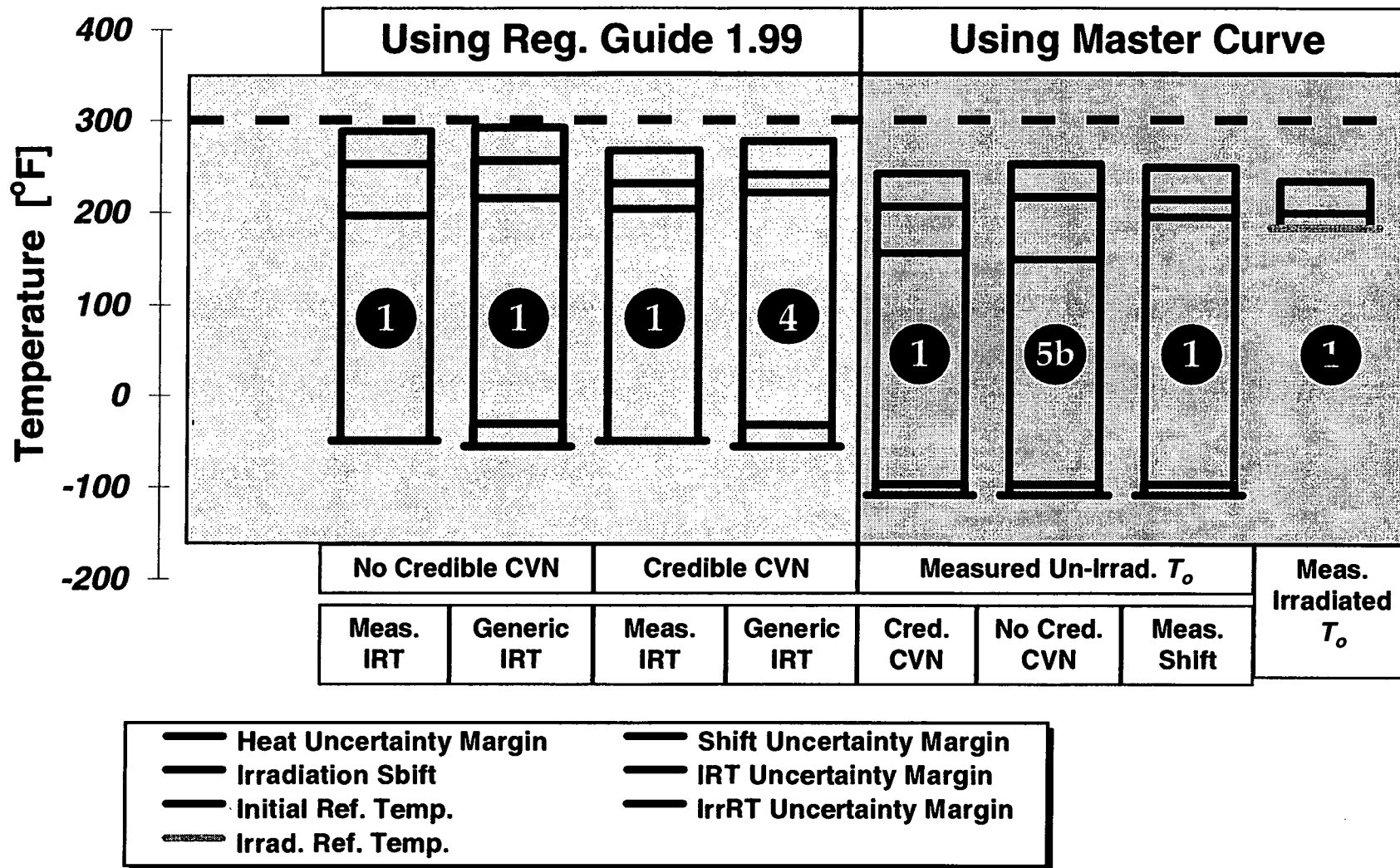


Figure 7-7 Comparison of ART Values Calculated by Various Techniques

5b

## 8.0 SUMMARY AND CONCLUSIONS

This investigation provides a technical basis for, and empirical support of, use of the Master Curve index temperature ( $T_o$ ) as a means to directly measure the adjusted reference temperature for an irradiated RPV steel. The investigation focuses in the following four areas:

1. The technical basis for application of the Master Curve to RPV steels,
2. The bias and accuracy of  $T_o$  values measured using ASTM E1921,
3. Determination of an  $T_o$ -based index temperature ( $RT_{T_o}$ ) for the  $K_{Ic}$  curve, and
4. A margins strategy for  $RT_{T_o}$  that matched the intent of 10CFR 50.61 procedures.

A database of fracture toughness values for reactor pressure vessel steels (both irradiated and unirradiated) was developed to address items 1 through 3. This database includes over 1,600 E1921 valid fracture toughness values from plates, welds, and forgings. The conclusions of this investigation are as follows:

1. The three premises of the Wallin Master Curve are supported by the great preponderance (>90%) of the empirical database for RPV steels. The Master Curve applies with equal accuracy to irradiated and unirradiated steels.
2. When  $T_o$  is estimated in accord with the requirements of E1921, the resultant values are unbiased with regard to test temperature, level of deformation at fracture, and number of tests conducted. The standard deviation of E1921  $T_o$  estimates relative to  $T_o$  estimates determined using considerably larger data sets is 14°F for the RPV steels considered.
3. A proposed ASME code case advocates addition of 35°F to  $T_o$  (determined by E1921) to establish a temperature to index the ASME  $K_{Ic}$  curve. This temperature is called  $RT_{T_o}$ . The value of 35°F exceeds that needed to maintain an equivalent level of safety to current  $RT_{NDT}$  based by 18°F. Consequently, use of  $RT_{T_o}$  as an indexing parameter for the  $K_{Ic}$  curve is more conservative than use of  $RT_{NDT}$ . Furthermore, the  $T_o$ -based toughness estimation methodology reduces considerably the degree of scatter in fracture toughness data, and contains implicit margins of 18°F on toughness which are consistent for every steel considered.  $RT_{T_o}$  is therefore superior to  $RT_{NDT}$  as an index temperature for the  $K_{Ic}$  curve.
4. Measurements of  $T_o$  are made in both the irradiated and unirradiated conditions for the limiting weld in the Kewaunee RPV (Linde 1092 Heat 1P3571) and for this weld in Kewaunee's sister plant, Maine Yankee. These values are used to develop  $RT_{T_o}$  estimates, along with associated margins that satisfy the intent of 10 CFR 50.61. Based on these analyses, ART values of 234°F and 249°F are determined at EOL and extended EOL for the Kewaunee. These values, which are based on irradiated  $T_o$  measurements, reflect conservative assumptions about the effects of neutron damage on fracture

on fracture toughness. The recommended procedure contains a level of confidence that is higher than the minimum requirements of the current technology, with a corresponding implicit margin of 18°F. The recommended *ART* values also contain explicit margins of 16-24°F to account for measurement uncertainty and a heat uncertainty adjustment of approximately 35°F.

5b

1

## 9.0 REFERENCES

- 10 CFR 50 Nuclear Regulatory Commission 10 CFR Part 50, "Fracture Toughness Requirements for Light Water Reactor Pressure Vessels."
- Alexander and Cheverton, 1993 Alexander, D.J., and Cheverton, R.D., "Fracture Properties of Specially Heat Treated ASTM A508 Cl. 2 Pressure Vessel Steel," Fracture Mechanics 23rd Symposium, ASTM STP 1189, Ravinder Chona, Ed., American Society for Testing and Materials, pp. 365-380, 1993.
- ASTM E399-90 "Test Method for Plane-Strain Fracture Toughness Testing of Metallic Materials," ASTM, 1998.
- ASTM E1921-97 "Test Method for Determination of Reference Temperature,  $T_{\sigma}$ , for Ferritic Steels in the Transition Range," ASTM, 1997.
- Curry and Knott, 1978 Metal Science, 12, pp. 511-514, 1978.
- Curry and Knott, 1979 Metal Science, 13, pp. 341-345, 1979.
- Dodds, et al., 1991 Dodds, R.H., Anderson, T.L., and Kirk, M.T., "A Framework to Correlate a/W Ratio Effects on Elastic-Plastic Fracture Toughness ( $J_c$ )," International Journal of Fracture, Vol. 48, pp. 1-22, 1991.
- Griffith, 1920 "The Phenomena of Rupture and Flow in Solids," Philosophical Transactions, Series A, Vol. 221, pp. 163-198, 1920.
- Hiser, 1990 Hiser, A.L., "Correlation of Irradiation-Induced Transition Temperature Increases from CV and  $K_{Ic}/K_{Ic}$  Data," NUREG/CR-5494, United States Nuclear Regulatory Commission, march 1990.
- Hutchinson, 1968 Hutchinson, J.W., "Singular Behavior at the End of a Tensile Crack in a Hardening Material," Journal of Mechanics and Physics of Solids, 16, pp. 13-31, 1968.
- Ingham, et al., 1989 Ingham, T., et al., "Fracture Toughness in the Transition Regime for A533B Steel: Prediction of Large Specimen Results from Small Specimen Tests," *Fracture Mechanics:*

- Perspectives and Directions (20<sup>th</sup> Symposium)*, ASTM STP 1020, R.P. Wei and R.P. Gangloff, Eds., American Society for Testing and Materials, pp. 369-389, 1989.
- Iwadate, et al., 1983  
Iwadate, T., Tanaka, Y., Ono, S., and Watanabe, J., "An Analysis of Elastic Plastic Fracture Toughness Behavior for  $J_{IC}$  Measurement in the Transition Region", Elastic-Plastic Fracture: Second Symposium, Volume II-Fracture Resistance Curves and Engineering Applications, ASTM STP 803, C.F. Shih and J.P. Gudas, Eds., American Society for Testing and Materials, 1983, pp. II-531-II-561.
- Koppenhoefer, et al., 1995  
Koppenhoefer, K.C., Kirk, M.T., and Dodds, R.H., "Requirements for Determining Small Scale Yielding Fracture Toughness Values from Bend Specimens," Constraint Effects in Fracture, Theory and Applications: Second Volume, ASTM STP 1244, Mark Kirk and Ad Bakker Eds., American Society for Testing and Materials, Philadelphia, 1995, pp. 445-460.
- Landes and Shaffer, 1980  
Landes, J.D. and Shaffer, D.H., "Statistical Characterization of Fracture in the Transition Region," Fracture Mechanics, 12th Conference, ASTM STP 700, American Society for Testing and Materials, pp. 368-382, 1980.
- Lidbury and Moskovic, 1993  
Lidbury, D. and Moskovic, R., "Assessment of the Ductile-to-Brittle Transition Toughness Behavior of an A508 Cl. 3 PWR Pressure Vessel Steel by a Statistical Approach," American Society of Mechanical Engineers Pressure Vessel and Piping Conference Proceedings, Vol. 250: Pressure Vessel Integrity, pp. 283-294, 1993.
- Marston, 1978  
Marston, T.U., "Flaw Evaluation Procedures, Background and Application of ASME Section XI Appendix A," EPRI Report NP-719-SR, Electric Power Research Institute, 1978.
- Mayfield, et al., 1997  
Mayfield, M.E., et al., "Application of Revised Fracture Toughness Curves in Pressure Vessel Integrity Analysis," Paper #106, SMIRT Conference, Lyon, France, August, 1997.
- McCabe, 1993  
McCabe, D.E., "A Comparison of Weibull and  $\beta_{IC}$  Analysis of Transition Range Data," Fracture Mechanics, 23rd Symposium, ASTM STP 1189, Ravinder Chona, Ed., American Society for Testing and Materials, Philadelphia, PA, pp. 80-94, 1984.

- McCabe, et al., 1994  
McCabe, D.E., et al., "Unirradiated Material Properties of Midland Weld WF-70," NUREG/CR-6249, U.S. Nuclear Regulatory Commission, 1994.
- McGowan, et al., 1988  
McGowan, et al., "Characterization of Irradiated Current-Practice Welds and A533 Grade B Class 1 Plate for Nuclear Pressure Vessel Service," NUREG/CR-4880, U.S. Nuclear Regulatory Commission, 1988.
- Morland, 1990  
Morland, E., "Fracture Toughness in the Transition Regime for A533B-1 Steel: The Effect of Specimen Sidegrooving," Fracture Mechanics 21st Symposium, ASTM STP 1074, J.P. Gudas, J.A. Joyce, and E.M. Hackett, Eds., American Society for Testing and Materials, pp. 215-237, 1990.
- Moskovic, 1993  
Moskovic, R., "Statistical Analysis of Censored Fracture Toughness Data in the Ductile to Brittle Transition Temperature Region," Engineering Fracture Mechanics, Vol. 44, No. 1, pp. 21-41, 1993.
- Nanstad, et al., 1992  
Nanstad, R.K., et al., "Irradiation Effects on Fracture Toughness of Two High-Copper Submerged-Arc Welds, HSSI Series 5., NUREG/CR-5913, U.S. Nuclear Regulatory Commission, 1992.
- Nanstad, 1997  
Personal communication.
- Nevalainen and Dodds, 1995  
Nevalainen, M., and Dodds, R.H., "Numerical Investigation of 3D Constraint Effects on Brittle Fracture in SE(B) and C(T) Specimens," Int. J. Fract., 74, 131-161, 1995.
- Oak Ridge National Laboratory  
Rosseel, T.M., "Heavy-Section Steel Irradiation Program, Semiannual Progress Report for October 1996 - March 1997," NUREG/CR-5591, U.S. Nuclear Regulatory Commission, 1997.
- Orowan, 1948  
Orowan, E., Transactions of the Institute of Engineers and Shipbuilders in Scotland, 89, p. 165, 1945.
- Pellini and Puzak, 1963  
Pellini, W. S. and Puzak, P. P., "Fracture Analysis Diagram Procedures for the Fracture-Safe Engineering Design of Steel Structures," Welding Research Council Bulletin No. 88, May 1963.
- Rice and Rosengren, 1968  
Rice, J.R., and Rosengren, G.F., "Plane Strain Deformation Near a Crack Tip in a Power-Law Hardening Material," Journal of Mechanics and Physics of Solids, 16, pp. 1-12, 1968.



- Rice and Johnson, 1970  
Rice, J.R., and Johnson, M.A. in *Inelastic Behavior of Solids*, M.F. Kanninen, et al., Eds., pp. 641-672, McGraw Hill, New York, New York, 1970.
- Ritchie, Knott, and Rice, 1973  
Ritchie, Knott, and Rice, "On the Relationship Between Critical Tensile Stress and Fracture Stress in Mild Steels, *J. Mech Phys Sol.*, 21, pp. 395-410, 1973.
- Rolfe and Novack, 1964  
Rolfe, S., and Novack, S., ASTM STP 410, American Society for Testing and Materials, p. 126, 1964
- Ruggieri, et al., 1998  
Ruggieri, C., Dodds, R.H., and Wallin, K., "Constraint Effects on Reference Temperature,  $T_r$ , for Ferritic Steels in the Transition Region," *Engineering Fracture Mechanics*, to appear.
- Scrawley and Brown, 1963  
Scrawley and Brown, ASTM STP 381, American Society for Testing and Materials, p. 123, 1963.
- Server, 1998  
WCAP 15074, "Evaluation of the 1P3571 Weld Metal from the Surveillance Programs for Kewaunee and Main Yankee"
- Smith, 1966  
Smith, E., *Physical Basis of Yield and Fracture*, Conference Proceedings, Institute of Physics and the Physical Society, London, p. 36, 1966.
- Smith, 1968  
Smith, E., *International Journal of Fracture Mechanics*, 4, p. 131.
- Sokolov, et al., 1997  
Sokolov, M.A., Wallin, K., and McCabe, D.E., "Application of Small Specimens to Fracture Mechanics Characterization of Irradiated Pressure Vessel Steels," *Fatigue and Fracture Mechanics: 28th Volume*, ASTM STP 1321, J.H. Underwood, B.D. MacDonald, and M.R. Mitchell, Eds., American Society for Testing and Materials, 1997.
- Sokolov, 1998  
Sokolov, M.A., "Statistical Analysis of the ASME  $K_{Ic}$  Database," *Journal of Pressure Vessel Technology*, Vol. 120, February 1998.
- VanDerSluys and Miglin, 1994  
VanDerSluys, W.A. and Miglin, M.T., "Results of MPC/JSPS Cooperative Testing Program in the Ductile-to-Brittle Transition Region," *Fracture Mechanics: 24th Volume*, ASTM STP 1207, J.D. Landes, D.E. McCabe, and J.A.M. Boulet, Eds., American Society for Testing and Materials, pp. 308-324, 1994.
- Wallin, Saario, and Törrönen, 1984  
Wallin, Saario, and Törrönen, "Statistical Model for Carbide Induced Brittle Fracture in Steel," *Metal Science*, 18, pp. 13-16, 1984.

- Wallin 1984 · Wallin, K., "The Scatter in  $K_{Ic}$  Results," Engineering Fracture Mechanics, 19(6), pp. 1085-1093, 1984.
- Wallin 1985 Wallin, K., "The Size Effect in  $K_{Ic}$  Results," Engineering Fracture Mechanics, 22, pp. 149-163, 1985.
- Wallin 1993 Wallin, K., "Irradiation Damage Effects on the Fracture Toughness Transition Curve Shape for Reactor Vessel Steels," Int. J. Pres. Ves. & Piping, 55, pp. 61-79, 1993.
- Wallin, 1995 Wallin, K., "Re-Evaluation of the TSE Results Based on the Statistical Size Effect," VTT Manufacturing Technology, Report VALB97, 1995.
- Williams, 1998 Williams, J.F., "Determination of Reference Temperature,  $T_r$ , for Nuclear Pressure Vessel Steels in both the Irradiated and Unirradiated Conditions," Westinghouse STC Report 98-9TC5-WOGFT-R1, March 1998.
- WRC-175, 1972 PVRC Ad Hoc Group on Toughness Requirements, "PVRC Recommendations on Toughness Requirements for Ferritic Materials." Welding Research Council Bulletin No. 175, August 1972.
- Yoon, 1997 Yoon, K.K., "A Direct Fracture Toughness Model for Irradiated Reactor Vessel Weld Material Based on Reference Temperature," ASME PVP Proceedings, Vol. 346, pp. 121-126, 1997